

Open-System Virus Particle Physics: A Non-Self-Adjoint, Stochastic PDE, and Fock-Space Framework for Many-Lattice Viral Dynamics

L. St. Kleess

Baruch College, Department of Natural Sciences, Manhattan, USA

February 17, 2025

Abstract

We develop a theoretical biophysics model, grounded in a mathematical framework that integrates ideas from virophysics and advanced PDE analysis to model complex, damped viral phonon dynamics in the presence of multiplicative noise. Our framework describes systems with rich internal arrangement states and accommodates an unbounded number of viral lattices by lifting a non-self-adjoint single-lattice operator—assumed to be m -sectorial (or maximally dissipative) and subject to external forcing or operator-valued noise—to a second-quantized setting on bosonic or fermionic Fock spaces. In this way, we construct a many-lattice evolution governed by a non-unitary semigroup that admits both equilibrium and non-equilibrium steady states, thereby enabling detailed flux and cycle analyses under broken detailed balance. Moreover, by incorporating a multiplicative-noise extension into the PDE layer, we show that the overall system remains well-posed and preserves its m -sectorial structure, which is essential for capturing the resource-limited and stochastic dynamics observed in real viral systems.

In previous work, four axioms were introduced to ground viral lattice theory in fundamental physical principles: Metabolic Inertia, Deterministic Physical Interactions, Self-Organization into Periodic Lattices, and Conservation of Energy. In the present analysis, which adopts a non-equilibrium viewpoint and leverages topological flux interpretations from infinite-dimensional geometry, we show how persistent probability-current loops and cohomologically nontrivial flow fields arise whenever detailed balance is broken by sustained resource input. These loop integrals reflect irreducible flux around closed paths in configuration space, indicating that no global scalar potential can capture the viral lattice evolution when subjected to energy transfer from a host or external environment. The theory extends to stochastic settings where sub-cellular randomness or thermal fluctuations are represented by operator-valued noise, and it applies to both continuum PDE manifolds and piecewise-smooth hybrid systems in which Markov jumps and Fock-space replication processes are present.

Motivated by these observations, we propose two additional axioms. First, the Axiom of Non-Equilibrium Flux Persistence states that, in the presence of sustained energy input, viral lattice configurations may sustain persistent probability-current loops in state space, revealing a topological obstruction to detailed balance. Second, the Axiom of Stochastic Continuity of Lattice Evolution stipulates that, under realistic stochastic perturbations, the continuum mechanics of virions is governed by m -sectorial PDEs coupled to operator-valued noise, ensuring well-posedness of the associated semigroups and reproducing the sub-cellular variability observed *in vivo*. These refinements underscore the importance of a cohomological perspective on flux loops, highlighting the relevance of resource-driven irreversibility and the potential for viral capsids to remain actively reconfiguring at steady state.

This document presents a step-by-step derivation of the non-self-adjoint operator constructions, develops proofs of well-posedness under the Lumer–Phillips and Hille–Yosida theorems, and demonstrates how Markov jumps, replication–annihilation events, and PDEs with complex damping can be unified in a single framework. The resulting theory provides a mathematically rigorous description of viral lattice dynamics far from equilibrium, clarifies the topological nature of flux loops that encode persistent capsid rearrangements, and lays the groundwork for future operator-theoretic and geometric investigations in open-system virology and virophysics.

Contents

1	Introduction: Motivation for a Multi-Lattice Formalism in Viral Modeling	3
1.0.1	Expanded Axioms of Viral Lattice Theory	3
1.0.2	Why Does Fock Space Resolve the “Many-Body Problem” in Viral Modeling?	5
1.1	Mass Bands in Biophysical and Experimental Virological Settings	7
1.1.1	The Total Mass Operator	13
1.1.2	Virological and Biophysical Applications and Interpretations.	16
1.2	Unified Macro-Arrangement and Continuum-Field Description of a Viral Lattice . .	19
2	Second Quantization: Many-Lattice Operator on $\mathcal{F}_{\pm}(\mathcal{H}_{\text{lat}})$	30
2.1	Purely Formal Model vs. Resource Constraints: An Operator-Theoretic Resolution .	35
2.2	Hybrid PDE–Markov–Noise Model with Second Quantization	42
2.2.1	Multiplicative Noise and Host Fluctuations.	43
3	Flux Integrals, Cycle Summations, and Markovian Jumps in Finite and Infinite Dimensions	48
3.0.1	Markovian Jumps in Fock Space	49
3.0.2	Implications for Virus Particle Motion and Non-Equilibrium Biology	52
4	Homology, Cohomology, and Flux Classification	56
4.1	Homology Loops and Their Virological Significance	57
4.1.1	Loop Classifications and Hierarchies	57
4.2	Cohomological Currents and Dynamical Phenotypes	58
4.3	Connecting Homology & Cohomology to Viral Open-System Dynamics	58
4.4	Theoretical Implications for Viral Fitness and Pathogenesis	59

1 Introduction: Motivation for a Multi-Lattice Formalism in Viral Modeling

Viral Lattice Theory was originally developed to describe the *internal*, continuum-mechanical dynamics of a *single* virion’s capsid—including vibrational modes, elastic deformations, and conformational shifts [1]. While this mechanistic viewpoint provides valuable insight into individual capsid behavior, *real-world infections* often involve extremely large virion populations, frequently on the order of 10^9 – 10^{11} particles within a single host [2]. Modeling merely $N \approx 100$ virions (sufficient for minimal infective-dose studies [3]) does not encompass the vast complexity observed in high-load infections such as those in SARS-CoV-2 cases [4].

To bridge the gap between individual-lattice mechanics and large-population dynamics, we propose an *extended* multi-lattice formalism. This extension retains the core physical underpinnings of single-virion theory (elastic PDE models, local Markov transitions, *etc.*) but couples them with population-level effects such as replication, resource constraints, and open-system interactions. In doing so, we generalize the foundational axioms of *Viral Lattice Theory* to accommodate non-equilibrium processes, operator-valued noise, and second-quantized replication or annihilation. Consequently, both *deterministic* and *stochastic* aspects of large virion ensembles can be rigorously analyzed within a unified operator-theoretic setting. After reviewing the single-lattice PDE approach, we introduce new axioms (Axioms 5 and 6) to anchor non-equilibrium and stochastic extensions. We then incorporate multi-lattice effects, highlighting how *Markovian jumps* (discrete arrangement transitions) and *creation–annihilation operators* (replication, clearance) combine in an m -sectorial framework. Finally, we explore saturable resource constraints, ensuring that *infinite replication* does not occur in a realistic host environment. This operator-algebraic paradigm leverages PDE drift, finite-state transitions, second quantization, and stochastic forcing to capture the genuine complexity of viral replication *in vivo*.

1.0.1 Expanded Axioms of Viral Lattice Theory

Axiom 1 (Metabolic Inertia). In their extracellular form, virions are metabolically inert: they neither synthesize nor consume chemical energy (e.g., ATP), and they remain in a quiescent, stable state outside of host cells. *Extracellular virions lack the enzymatic machinery required for metabolism and energy production, a fact well established in virological studies [2, 5]. This inertness underpins their ability to persist in diverse environments until encountering a suitable host.*

Axiom 2 (Deterministic Physical Interactions). The motion and collisions of extracellular virions are dictated by physical forces and can be modeled deterministically by classical mechanics, with negligible influence from biological feedback mechanisms in the extracellular milieu. *Virions in extracellular fluids mainly experience classical forces such as hydrodynamic drag and electrostatic interactions, which dominate over biochemical feedback processes at that stage [5, 7]. This justifies deterministic modeling approaches for extracellular viral motion.*

Axiom 3 (Self-Organization into Periodic Lattices). When provided sufficient energy input and appropriate initial conditions, virions can spontaneously organize into periodic (or quasi-periodic) lattice structures that represent local or global minima of the free-energy landscape. *Experimental observations have demonstrated that viral capsids can self-assemble into highly symmetric, periodic structures [8]. This self-organization is driven by inter-subunit interactions and is fundamental to capsid stability.*

Axiom 4 (Conservation of Energy). In the absence of external dissipation or forcing, the total mechanical energy of the viral lattice system—including vibrational quanta (“viral phonons”)—remains

constant. This reflects an underlying Hamiltonian structure in which excitations introduced into the lattice do not spontaneously dissipate or emerge without an external energy source. *Although real systems invariably include some degree of damping or external input, the premise of energy conservation in an idealized, closed viral assembly system offers a baseline for understanding the energetics of virion formation and vibration. In this model, “viral phonons” act as quantized vibrational modes that conserve the energy imparted to them, reinforcing the Hamiltonian nature of the system’s core [5].*

Axiom 5 (Non-Equilibrium Flux Persistence). In settings where sustained energy or resource input is available, viral lattice configurations may sustain persistent probability-current loops in their state space, indicating a breach of detailed balance and signifying active, non-equilibrium dynamics. *Many viral processes (capsid assembly, morphological transitions) operate under continuous resource inflows (host ATP, etc.) and do not settle into static equilibria. Instead, steady-state flux loops manifest as ongoing rearrangements or replication cycles, consistent with resource-driven, open-system thermodynamics.*

Axiom 6 (Stochastic Continuity of Lattice Evolution). In the presence of environmental fluctuations (e.g., thermal noise, varying host resources), the continuum mechanics of virions is governed by m -sectorial PDEs coupled to operator-valued noise, guaranteeing well-posedness and robust modeling of subcellular randomness. *In vivo, viral processes are inherently stochastic due to fluctuating host conditions and thermal effects. Modeling these dynamics with m -sectorial PDEs that include stochastic terms captures the randomness observed in single-virus tracking experiments and biochemical assays [8, 10]*

Together, these expanded axioms define an operator-theoretic scaffold for *multi-lattice* viral modeling. The first four axioms (Metabolic Inertia, Deterministic Interactions, Self-Organization, Energy Conservation) reflect the core principles established in early *Viral Lattice Theory*. The two additional axioms (Non-Equilibrium Flux Persistence and Stochastic Continuity) address open-system and noisy dynamics, aligning the theory with non-equilibrium statistical mechanics and real biological observations of large viral populations. They provide a unifying conceptual platform from which to develop mathematically consistent PDE–Markov–Fock formalisms capable of describing both single-virion mechanics and population-scale replication in resource-limited, stochastic environments.

Gaps in Current Experimental and Theoretical Approaches.

- *Indirect Assays for Viral Load:* Many traditional virological methods measure infections indirectly. Plaque assays, for example, focus on the *consequences* of viral replication (lysed cell patches in tissue culture) rather than the spatiotemporal motion or conformational states of individual virions [2, 11]. Such assays, though crucial for clinical diagnostics, offer limited insight into how virus particles move, interact, or structurally evolve in real time.
- *Scale Complexity:* Monitoring the paths or shapes of billions of virions *in vivo* is experimentally difficult. Electron microscopy or single-particle fluorescence studies provide high-resolution images [12], but scaling up to statistically representative numbers (millions to billions of virions) quickly becomes infeasible.
- *Need for Robust Mathematical Frameworks:* From a physics standpoint, the naive route to modeling $N \gg 1$ virions is to form an N -fold tensor product of single-lattice Hilbert spaces. However, this approach grows combinatorially and cannot readily handle the ongoing *creation* (replication) and *annihilation* (degradation) of virions that define real infection dynamics.

The present work addresses these gaps by extending *viral lattice theory* to describe *arbitrarily large* virion populations, leveraging a *second-quantization* (Fock-space) formalism reminiscent of quantum many-body systems [13]. While we adopt operator-theoretic methods from quantum mechanics (creation/annihilation operators, m -sectorial semigroup theory [14]), the system here is *not* quantum in the strict physical sense. Rather, the entire viral lattice plays the role of ‘particles’ within an abstract Fock space, enabling:

1. **Exponential Particle Growth:** Viral replication leads to rapid expansion from tens to billions of particles. The Fock space’s direct-sum construction naturally accommodates new “lattice factors” without forcing a redefinition of the entire state space.
2. **Creation & Annihilation Operators:** Viral replication emerges as creation operators $\hat{a}^\dagger(\varphi)$, while capsid degradation or immune clearance corresponds to annihilation operators $\hat{a}(\varphi)$. These processes mimic real infection dynamics [15, 16].
3. **Phonon and Mass-Band Extensions:** Single-capsid modes, including partial/complete genome packaging and vibrational (phonon) states, straightforwardly lift to the multi-capsid setting. Thus, the structure of each lattice remains preserved even as the total population evolves.
4. **Mathematical Tractability:** Standard theorems (e.g. Hille–Yosida, Lumer–Phillips) guarantee well-defined semigroup evolution for an m -sectorial single-lattice generator, thereby ensuring a rigorous basis for PDE or Markov chain models of infection [10].

Although clinical and immunological research often emphasizes infection outcomes (pathology, immune response, plaque formation), there is growing interest in understanding the *microscopic* dynamics of virion motion [12, 17]. By coupling operator theory methods with biophysical insights, we aim to offer a framework that virologists could use to:

1. Simulate and predict how large populations of virions collectively navigate host environments.
2. Identify critical transitions (e.g. capsid rearrangements, genome packaging) that might serve as therapeutic targets.
3. Bridge continuum-level assays (e.g. plaque counts, viral titers) with the underlying discrete interactions and motions of individual virus particles.

In summary, the second-quantized, many-lattice approach presented here builds upon earlier single-lattice treatments to address *realistic* viral loads and the ensuing population-level complexities. The formalism is designed not merely as an abstract extension, but as a practicable tool that leverages standard mathematical physics techniques (Fock-space theory, m -sectorial operators) to illuminate the micro-to-macro connection in virology.

1.0.2 Why Does Fock Space Resolve the “Many-Body Problem” in Viral Modeling?

Real-world infections regularly involve virion populations on the order of 10^9 – 10^{11} particles within a single host (as observed, for instance, in severe SARS-CoV-2 infections [4]). Modeling such expansive populations introduces a classic *many-body problem*, as the sheer number of interacting particles (each potentially following stochastic or dynamical rules) rapidly produces intractable complexity. In *quantum* many-body settings, even comparatively modest system sizes yield wavefunctions too

elaborate to handle exactly, reflecting intricate correlations and entanglement [18,19]. Though virions themselves are not quantum objects in the strict sense, the combinatorial explosion of possible replication states and their chaotic host environment parallels the challenges of high-dimensional, multi-particle systems. To meet these challenges, we adopt a *Fock-space* (“many-lattice”) framework:

1. *No Fixed N*: Unlike traditional models that require a fixed number N of particles or virions, Fock space incorporates a *direct sum* over all $N = 0, 1, 2, \dots$. This inherently allows for indefinite replication (creation) and degradation (annihilation) events [13,14].
2. *Regular Structure & Sectoriality*: The infinite-dimensional direct-sum layout remains sufficiently *regular* for advanced functional-analytic theorems (e.g. m -sectorial semigroup results). One may embed dissipative or non-self-adjoint terms that capture viral clearance, immune responses, or resource-limited replication [10].

From a computational viewpoint, this is vastly more efficient than periodically redefining a finite- N framework whenever N changes. Biologically, it aligns with the reality of viral load fluctuations, which can surge or crash due to replication bursts or immune-mediated elimination. An appealing feature is that the *single-lattice* state space for each virion—containing details such as capsid conformation, partial genome packaging, vibrational (phonon) modes [1]—remains intact:

- *Mass-Band Diversity*: By labeling creation/annihilation operators with band or subtype indices, one can incorporate multiple strains, mutational variants, or distinct capsid compositions without losing track of the underlying physics.
- *Conformational Spectrum*: The same operator approach that modeled each virion’s internal structure (e.g. protein subunit rearrangements) straightforwardly extends to an unbounded population of capsids.
- *Resource/Environment Coupling*: Since the single-lattice generator can incorporate external energy input or noisy boundary conditions, the multi-lattice extension inherits these features seamlessly.

Hence, large-scale phenomena, such as exponential population growth, competition among viral sub-populations, or abrupt extinction events can be described in a single, coherent framework. Similar to quantum many-body physics, where each additional particle inflates the state-space dimension [18,19], a large viral population poses a combinatorial explosion of possible configurations. The Fock-space method mitigates this, because states of the entire population are built from tensor products of single-lattice spaces, then symmetrized (or antisymmetrized) if required. This blocks the naive exponential blow-up into a tractable direct-sum of multi-virion sectors. Creation/annihilation operators form a closed algebra of simple transformations (adding/removing one virion-lattice), making it straightforward to code or analyze repeated processes (e.g. replication cycles). The m -sectorial approach ensures we can incorporate random forcing, gain/loss processes, and boundary effects, retaining well-posedness of the PDE or Markov model [10].

Furthermore, the formalism allows coupling each capsid-lattice sector to host variables (e.g. resource concentrations), enabling system-level PDEs or semigroups that unify viral replication with intracellular or extracellular dynamics. By including *labels* for genome sequences, one can embed mutation pathways into creation/annihilation processes, opening a path to model both population growth and genetic drift in one operator framework [15]. Fock-space expansions handle both discrete (e.g. distinct conformational states) and continuous (e.g. vibrational modes) degrees of freedom,

reflecting the multi-scale nature of viral dynamics. In sum, the many-lattice Fock-space approach elegantly accommodates unbounded viral replication, compositional diversity, and environmental chaos. It leverages established results in functional analysis and second quantization [13, 14] to ensure mathematical rigor, while preserving the essential mechanics of single-capsid physics. By providing a unifying framework, it paves the way for more accurate simulations and theoretical predictions of how large viral populations evolve, move, and adapt within a complex biological milieu.

1.1 Mass Bands in Biophysical and Experimental Virological Settings

Definition 1.1 (Single-Lattice Hilbert Space). Let \mathcal{H}_{arr} be a Hilbert space encoding the *arrangement states* of a viral capsid lattice. Such arrangement states may include:

1. **Structural conformations** (e.g. closed, partially open, etc.),
2. **Occupancy or genome-packing states** (e.g. bound vs. unbound, partial vs. full genome),
3. **Markovian microstates** (e.g. binding-site accessibility or chemical modifications).

Additionally, let \mathcal{H}_{ph} be a separable Hilbert space representing *phonon* (vibrational) degrees of freedom, often arising from an L^2 -type setting or a bosonic Fock space describing lattice vibrations [20].

We then define the **single-lattice Hilbert space**

$$\mathcal{H}_{\text{lat}} := \mathcal{H}_{\text{arr}} \otimes \mathcal{H}_{\text{ph}}, \quad (1.1)$$

thereby capturing both arrangement-level and phonon-level dynamics of an *individual* viral lattice (capsid). The arrangement space \mathcal{H}_{arr} encodes discrete or Markovian states (chemical binding, conformational states, *etc.*), while \mathcal{H}_{ph} encapsulates continuum or vibrational degrees of freedom, ensuring that both structural configurations and wave-like (phonon) modes are represented in a unified Hilbert-theoretic framework.

Remark 1.2 (Mass Bands in Biophysical and Virological Settings). In more advanced treatments, one may incorporate multiple *mass bands* reflecting variations in genome loading, capsid protein stoichiometry, or other molecular factors. Concretely, \mathcal{H}_{arr} is expanded into a direct sum of subspaces, each corresponding to a distinct “mass band.” This concept is analogous to *mass gaps* in quantum mechanics or quantum field theory, where different particle species (or quasi-particles) carry distinct intrinsic quantum numbers (mass, spin, *etc.*).

Empirically, viral populations often exhibit a practical range of masses or diameters (e.g. 80–100 nm) conducive to infectivity and structural stability, while outliers—though possible due to viral mutations—tend to be rare. Modeling these possible masses or sizes as discrete *bands* (labeled m_k) maintains biophysical plausibility by restricting to experimentally observed values. In second-quantized formulations, creation/annihilation operators labeled by m_k reflect “mass-resolved” occupancy or replication events, paralleling how quantum systems distinguish multiple particle species via distinct mass or charge eigenvalues. This approach integrates the elegance of operator algebra with realistic virological constraints on virion size and assembly [2, 5, 21].

Theorem 1.3 (Direct Sum Decomposition for Mass Bands). *Suppose the arrangement Hilbert space \mathcal{H}_{arr} is refined into a direct sum of subspaces*

$$\mathcal{H}_{\text{arr}} = \bigoplus_{k \in \mathcal{I}} \mathcal{H}_{\text{arr}}^{(m_k)}, \quad (1.2)$$

where each $\mathcal{H}_{\text{arr}}^{(m_k)}$ corresponds to a distinct “mass band” labeled by m_k . Then the single-lattice Hilbert space (1.1) admits a decomposition

$$\mathcal{H}_{\text{lat}} = \left(\bigoplus_{k \in \mathcal{I}} \mathcal{H}_{\text{arr}}^{(m_k)} \right) \otimes \mathcal{H}_{\text{ph}} \cong \bigoplus_{k \in \mathcal{I}} \left(\mathcal{H}_{\text{arr}}^{(m_k)} \otimes \mathcal{H}_{\text{ph}} \right), \quad (1.3)$$

so that the mass-band information is embedded directly into the arrangement component of each lattice mode. This structure generalizes the notion of distinct particle species in quantum systems, ensuring that only physically realizable virion masses (or size classes) are included in the viral lattice model.

Proof. Because direct sums and tensor products commute up to canonical isomorphisms, we have

$$\left(\bigoplus_{k \in \mathcal{I}} \mathcal{H}_{\text{arr}}^{(m_k)} \right) \otimes \mathcal{H}_{\text{ph}} \cong \bigoplus_{k \in \mathcal{I}} \left(\mathcal{H}_{\text{arr}}^{(m_k)} \otimes \mathcal{H}_{\text{ph}} \right) \quad (1.4)$$

by standard results in Hilbert space theory [22, 23]. Labeling each direct-summand by m_k ensures that each “mass band” m_k corresponds to a subspace $\mathcal{H}_{\text{arr}}^{(m_k)}$, yielding the desired decomposition of the total arrangement-phonon space. \square

Virological Interpretation. In second-quantized formalisms, one then introduces creation and annihilation operators

$$\hat{b}_{m_k}^\dagger, \quad \hat{b}_{m_k}, \quad (1.5)$$

each labeled by the band index m_k , to encode mass-resolved replication or clearance processes. Hence, if \hat{N}_{m_k} is the number operator for virions of mass m_k , resource-limited or stochastic PDE terms can couple distinct mass bands to reflect real biological phenomena (e.g. transitions among partially packaged vs. fully packaged genomes). By restricting to m_k that lie in an empirically observed set, the framework preserves fidelity to experimental data while leveraging quantum-inspired operator methods [2, 5].

Tracking Virion Occupancy and Mass-Resolved Operators. The operator $\hat{n}_{\mathbf{R}_i}(t)$ measures how many virions occupy a given site \mathbf{R}_i at time t . Summing across all sites yields the total virion count in the lattice model. By further decomposing states according to the discrete mass bands $\{m_i\}$, one can stratify the population by mass (or size). Introducing mass-specific creation and annihilation operators $\hat{b}_{m_i}^\dagger$ and \hat{b}_{m_i} enables the definition of a total mass operator

$$\hat{M}_{\text{total}} = \sum_i m_i \hat{b}_{m_i}^\dagger \hat{b}_{m_i}, \quad (1.6)$$

acting on the arrangement-level Hilbert space

$$\mathcal{H}_{\text{arr}} = \bigoplus_i \mathcal{H}_{\text{arr}}^{(m_i)}, \quad (1.7)$$

where each $\mathcal{H}_{\text{arr}}^{(m_i)}$ corresponds to a particular mass band m_i . From a virological standpoint, \hat{M}_{total} encodes how the mechanical or inertial properties of the viral lattice evolve amid replication, genome packaging, or partial capsid degradation. By adopting bosonic commutation relations (or an appropriate generalization), these operators embed into a Fock space $\mathcal{F}(\mathcal{H}_{\text{arr}})$, allowing one to compute expectation values $\langle \hat{n}_{\mathbf{R}_i} \rangle$ or $\langle \hat{M}_{\text{total}} \rangle$ that capture real-time assembly/disassembly events, resource-driven replication bursts, or host-induced perturbations. This yields a “quantum-inspired” perspective on viral population dynamics subject to both structural constraints and mass distributions [2, 5].

Definition 1.4 (Discrete Mass Spectrum and Projection Operators). Let $\mathcal{I} \subset \mathbb{N}$ be an index set labeling permissible mass values $\{m_k\}_{k \in \mathcal{I}}$, with

$$\mathcal{H}_{\text{arr}} = \bigoplus_{k \in \mathcal{I}} \mathcal{H}_{\text{arr}}^{(m_k)}. \quad (1.8)$$

For each m_k , let $P^{(m_k)} : \mathcal{H}_{\text{arr}} \rightarrow \mathcal{H}_{\text{arr}}^{(m_k)}$ be the orthogonal projection satisfying $P^{(m_k)}\psi \in \mathcal{H}_{\text{arr}}^{(m_k)}$ for all $\psi \in \mathcal{H}_{\text{arr}}$, and

$$\sum_{k \in \mathcal{I}} P^{(m_k)} = I, \quad (1.9)$$

the identity operator. This family of projections partitions the arrangement space according to mass band subspaces.

Theorem 1.5 (Self-Adjointness of the Total Mass Operator). *Assume that $\{m_k\}_{k \in \mathcal{I}}$ is a (possibly infinite) discrete subset of \mathbb{R} . Define the operator*

$$\hat{M}_{\text{total}} = \sum_{k \in \mathcal{I}} m_k P^{(m_k)}, \quad (1.10)$$

where each $P^{(m_k)}$ is the orthogonal projection of Definition 1.4. Then \hat{M}_{total} is self-adjoint (essentially self-adjoint on its natural domain $\mathcal{D}(\hat{M}_{\text{total}}) \subset \mathcal{H}_{\text{arr}}$) and has a purely point spectrum

$$\sigma(\hat{M}_{\text{total}}) = \{m_k\}_{k \in \mathcal{I}}. \quad (1.11)$$

Equivalently, one may interpret each m_k as an eigenvalue of \hat{M}_{total} with corresponding eigenspace $\mathcal{H}_{\text{arr}}^{(m_k)}$.

Proof. Since each $P^{(m_k)}$ is an orthogonal projection onto $\mathcal{H}_{\text{arr}}^{(m_k)}$, the operator $m_k P^{(m_k)}$ is symmetric and bounded, and thus trivially self-adjoint on its restricted domain. The sum (1.10) is well-defined because $\sum_{k \in \mathcal{I}} P^{(m_k)} = I$ and each mass m_k is finite by assumption. The resulting operator is diagonal with respect to the decomposition $\mathcal{H}_{\text{arr}} = \bigoplus_{k \in \mathcal{I}} \mathcal{H}_{\text{arr}}^{(m_k)}$; its domain comprises all vectors ψ such that ψ lies in a finite or countably infinite direct sum of these eigenspaces (depending on whether \mathcal{I} is finite or countably infinite). Hence, the spectrum is purely discrete, and each m_k is an eigenvalue with eigenspace $\mathcal{H}_{\text{arr}}^{(m_k)}$. This construction is a standard example of a *direct sum of bounded self-adjoint operators* [22, 23]. \square

Continuum Limit and Density Operators. *In a continuum setting, one may replace site-based operators $\hat{n}_{\mathbf{R}_i}$ by a density operator $\hat{\rho}(\mathbf{r}, t)$, whose expectation values yield spatial density distributions of virions in real time. Correlating $\hat{\rho}$ with displacement or stress operators illuminates how local mass variations (arising from partial genome packaging or selective degradation) alter mechanical stiffness or shift normal modes [24]. Consequently, occupancy and mechanical degrees of freedom coexist in a single operator-theoretic framework, bridging quantum-like treatments of viral populations with advanced models in quantum fluids or soft matter physics.*

Biophysical Context and Perspectives. *The self-adjoint total mass operator \hat{M}_{total} tracks how replication or degradation modifies the lattice's inertial properties. Empirically, virions can exhibit size/mass heterogeneity (e.g., due to partial genome encapsidation or conformational differences), and labeling each band by m_k encodes these physically observed categories. In resource-limited replication scenarios, creation and annihilation processes may selectively populate or deplete specific*

bands, reflecting differential fitness or stability [2, 5]. Meanwhile, embedding such mass-resolved operators in Fock space, with the appropriate commutation relations, permits advanced semigroup or nonself-adjoint PDE analyses that unify continuum elastic modes, Markov jumps, and operator valued noise, consistent with the broader viral lattice framework.

Definition 1.6 (Fock Space over a Hilbert Space). Let \mathcal{H} be a separable Hilbert space. The **bosonic Fock space** over \mathcal{H} is defined by

$$\mathcal{F}_+(\mathcal{H}) := \bigoplus_{n=0}^{\infty} (\mathcal{H}^{\otimes n})_+, \quad (1.12)$$

where $(\cdot)_+$ denotes the symmetrized subspace of the n -fold tensor product $\mathcal{H}^{\otimes n}$, and the direct sum includes the *vacuum* sector (corresponding to $n = 0$). Similarly, the **fermionic Fock space** over \mathcal{H} is given by

$$\mathcal{F}_-(\mathcal{H}) := \bigoplus_{n=0}^{\infty} (\mathcal{H}^{\otimes n})_-, \quad (1.13)$$

where $(\cdot)_-$ denotes the antisymmetrized subspace. We often write

$$\mathcal{F}_{\pm}(\mathcal{H}) = \bigoplus_{n=0}^{\infty} (\mathcal{H}^{\otimes n})_{\pm}, \quad (1.14)$$

with “+” or “−” indicating bosonic or fermionic statistics, respectively [23, 25, 26].

In the context of *viral lattice theory*, we typically adopt a bosonic construction:

1. Viral “particles” (virions or capsid subunits) can be regarded as *indistinguishable* quasi-particles under many experimental settings [2, 21].
2. Symmetrized tensor products naturally model situations where ordering of virions is irrelevant (e.g., assembling identical capsids in an infected cell).
3. Creation and annihilation operators (\hat{a}^\dagger , \hat{a}) in $\mathcal{F}_+(\mathcal{H})$ capture replication (increasing virion count) or degradation (decreasing virion count), with appropriate resource-limited or saturable terms.

Specifically, if \mathcal{H}_{lat} is the *single-lattice* Hilbert space from Definition 1.1 (including arrangement states, phonon modes, and mass-band considerations), its Fock space

$$\mathcal{F}_+(\mathcal{H}_{\text{lat}}) = \bigoplus_{n=0}^{\infty} (\mathcal{H}_{\text{lat}}^{\otimes n})_+ \quad (1.15)$$

encodes all possible n -particle configurations in a symmetric fashion. This multi-layered approach:

1. Respects empirical mass constraints (“mass bands”) by restricting \mathcal{H}_{lat} to physically plausible virion masses,
2. Accommodates discrete conformational states (\mathcal{H}_{arr}) and continuum or discrete vibrational modes (\mathcal{H}_{ph}),
3. Employs second-quantized creation/annihilation processes to describe population-level replication, ensuring a rigorous operator-theoretic foundation for studying viral assembly and adaptation under host/environmental stresses.

Thus, the bosonic Fock space formalism provides a powerful framework for modeling an *unbounded* number of virions or capsid units, while naturally integrating resource-limited or noise-driven dynamics into the PDE and Markov jump processes that govern capsid evolution.

Definition 1.7 (Arrangement Space with Mass Bands). Let \mathcal{I} be an indexing set (finite or countably infinite), and let $\{m_k\}_{k \in \mathcal{I}} \subset \mathbb{R}$ be a (discrete) collection of physically admissible mass values for virions or capsid assemblies. For each $k \in \mathcal{I}$, let $\mathcal{H}_{\text{arr}}^{(m_k)}$ be a (possibly infinite-dimensional) Hilbert space describing *arrangements* of entities of mass m_k . The *total arrangement space* is the direct sum

$$\mathcal{H}_{\text{arr}} = \bigoplus_{k \in \mathcal{I}} \mathcal{H}_{\text{arr}}^{(m_k)}. \quad (1.16)$$

A generic vector in \mathcal{H}_{arr} is then a formal sum

$$\Psi = \sum_{k \in \mathcal{I}} \Psi^{(m_k)}, \quad \Psi^{(m_k)} \in \mathcal{H}_{\text{arr}}^{(m_k)}, \quad (1.17)$$

with only finitely or countably many nonzero components, depending on the chosen norm topology. In standard quantum mechanical or virological analogies, each subspace $\mathcal{H}_{\text{arr}}^{(m_k)}$ represents configurations of a *fixed* mass m_k . One could further refine these subspaces to account for other quantum numbers (e.g. spin, charge) or, in a biophysical setting, for conformational states linked to different biomarkers or chemical modifications. By labeling the arrangement spaces according to discrete mass values m_k (which may be informed by empirical capsid size distributions), the theory ensures that:

1. Only physically plausible virion (capsid) masses contribute to the model, mirroring observed mass spectra or typical infective diameters [5].
2. Each subspace $\mathcal{H}_{\text{arr}}^{(m_k)}$ captures the detailed arrangement or conformational features associated with that mass range, allowing for partial folding, binding states, or genome insertion relevant to real viruses [2].
3. The second-quantized Fock construction over \mathcal{H}_{arr} then incorporates creation/annihilation operators that respect these mass labels, so that newly created capsids (particles) automatically fall into an appropriate mass band, preserving biophysical realism.

In this way, the arrangement space with mass bands seamlessly integrates into the bosonic (or fermionic) Fock framework (Definition 1.6), providing a unified operator-theoretic platform for analyzing viral replication, capsid assembly/disassembly, and vibrational or PDE-driven dynamics [2, 21].

Definition 1.8 (Orthogonal Projection Operators). Let $\{m_k\}_{k \in \mathcal{I}}$ be the discrete set of permissible mass values from Definition 1.7, and recall that

$$\mathcal{H}_{\text{arr}} = \bigoplus_{k \in \mathcal{I}} \mathcal{H}_{\text{arr}}^{(m_k)}. \quad (1.18)$$

For each $m_k \in \{m_k\}_{k \in \mathcal{I}}$, define the map

$$P^{(m_k)} : \mathcal{H}_{\text{arr}} \rightarrow \mathcal{H}_{\text{arr}}, \quad (1.19)$$

by setting

$$P^{(m_k)} \left(\sum_{j \in \mathcal{I}} \Psi^{(m_j)} \right) = \Psi^{(m_k)}, \quad (1.20)$$

where each $\Psi^{(m_j)} \in \mathcal{H}_{\text{arr}}^{(m_j)}$. In other words, $P^{(m_k)}$ selects the component of a vector in \mathcal{H}_{arr} that lies in the subspace $\mathcal{H}_{\text{arr}}^{(m_k)}$.

Lemma 1.9 (Properties of $P^{(m_k)}$). *Each operator $P^{(m_k)}$ in Definition 1.8 is an orthogonal projection. Moreover,*

$$P^{(m_k)}P^{(m_\ell)} = \delta_{k,\ell}P^{(m_k)}, \quad \text{and} \quad \sum_{k \in \mathcal{I}} P^{(m_k)} = I_{\mathcal{H}_{\text{arr}}}, \quad (1.21)$$

the identity operator on \mathcal{H}_{arr} . Furthermore,

$$P^{(m_k)} \circ P^{(m_k)} = P^{(m_k)}, \quad \langle P^{(m_k)}\Phi, \Psi \rangle = \langle \Phi, P^{(m_k)}\Psi \rangle, \quad (1.22)$$

showing that $P^{(m_k)}$ is idempotent and self-adjoint, hence an orthogonal projection.

Proof. By construction, $P^{(m_k)}$ annihilates components in any $\mathcal{H}_{\text{arr}}^{(m_j)}$ with $j \neq k$, and it leaves vectors in $\mathcal{H}_{\text{arr}}^{(m_k)}$ unchanged. The direct sum $\mathcal{H}_{\text{arr}} = \bigoplus_{j \in \mathcal{I}} \mathcal{H}_{\text{arr}}^{(m_j)}$ admits a unique decomposition of any vector $\sum_j \Psi^{(m_j)}$. It follows that $P^{(m_k)}$ is idempotent and self-adjoint in the natural inner product, yielding $P^{(m_k)}P^{(m_\ell)} = \delta_{k,\ell}P^{(m_k)}$. Summing over $k \in \mathcal{I}$ gives $\sum_k P^{(m_k)} = I_{\mathcal{H}_{\text{arr}}}$. \square

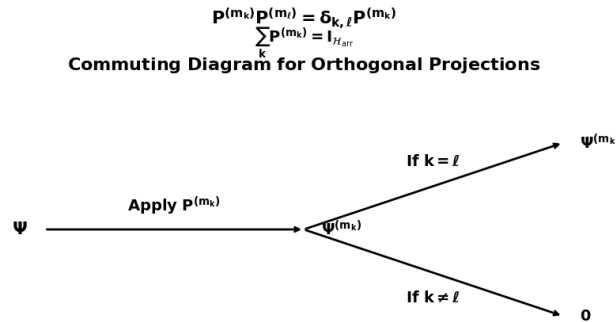


Figure 1: **Commuting Diagram for Orthogonal Projections.** A schematic illustrating how each orthogonal projection $p^{(m_k)}$ acts on a state Ψ in the arrangement Hilbert space \mathcal{H}_{arr} . If $p^{(m_k)}$ matches the label m_ℓ in Ψ , the projected state $\Psi^{(m_k)}$ persists (*i.e.*, $\Psi^{(m_k)} \neq 0$), whereas projections onto other labels yield 0. Collectively, these orthogonal projections satisfy $p^{(m_k)}p^{(m_\ell)} = \delta_{k,\ell}p^{(m_k)}$ and $\sum_k p^{(m_k)} = I_{\mathcal{H}_{\text{arr}}}$, reflecting the block-diagonal (direct sum) structure of the arrangement space. Such commuting diagrams underlie the spectral decomposition of number- or mass-band labels in Fock-space formulations of viral lattice models.

Remark 1.10 (Biological Interpretation of Projection Operators.). From a *virological* viewpoint, each projection $P^{(m_k)}$ “filters out” the component of a viral arrangement state corresponding to mass m_k . If one imagines a distribution of virions or capsids across multiple *mass bands*, then $P^{(m_k)}$ effectively says: “Focus only on capsids (or assemblies) that weigh m_k .” In reality, certain assemblies might incorporate partial genomes or slightly different stoichiometries, producing distinct mass classes. The projection operators thus mirror the laboratory practice of segregating viral particles by mass/density (e.g., via ultracentrifugation or gradient separation), each $P^{(m_k)}$ representing a theoretical analog of *isolation* of the mass- m_k fraction.

Definition 1.11 (Total Mass Operator). Using the projection operators from Definition 1.8, we define the *total mass operator* \hat{M}_{total} on \mathcal{H}_{arr} by

$$\hat{M}_{\text{total}} = \sum_{k \in \mathcal{I}} m_k P^{(m_k)}. \quad (1.23)$$

This operator acts diagonally with respect to the decomposition $\mathcal{H}_{\text{arr}} = \bigoplus_{k \in \mathcal{I}} \mathcal{H}_{\text{arr}}^{(m_k)}$, assigning the eigenvalue m_k to vectors in the subspace $\mathcal{H}_{\text{arr}}^{(m_k)}$. In a physical sense, \hat{M}_{total} tracks how the viral population’s *overall mass* (or mass distribution) evolves when virions replicate, degrade, or shift their genome/capsid contents. Thus far, we have described how \mathcal{H}_{arr} (arrangement-level states) may be partitioned into discrete mass bands. We may also consider \mathcal{H}_{lat} (a *single-lattice* Hilbert space, including vibrational/phonon degrees of freedom; see Definition 1.1), and then form a *multi-lattice* Fock space [23, 25, 26]:

$$\mathcal{F}_+(\mathcal{H}_{\text{lat}}) = \bigoplus_{n=0}^{\infty} \left(\mathcal{H}_{\text{lat}}^{\otimes n} \right)_+, \quad (1.24)$$

where each copy of \mathcal{H}_{lat} corresponds to one lattice (or one virion/capsid). In scenarios where *multiple distinct* lattice types (e.g. different strains or significantly different protein stoichiometries) coexist, one may form:

$$\mathcal{H}_{\text{lat}}^{(1)} \oplus \mathcal{H}_{\text{lat}}^{(2)} \oplus \dots \quad (1.25)$$

and then build a *graded* or *multi-type* Fock space, potentially reminiscent of grand canonical ensembles in quantum many-body physics [27].

Whereas a single lattice \mathcal{H}_{lat} describes *one* lattice’s arrangement states + phonons + mass, the multi-lattice Fock space $\mathcal{F}_+(\mathcal{H}_{\text{lat}})$ accommodates an *unbounded* number of such lattices—potentially representing an entire viral population in one host cell. The creation and annihilation operators

$$\hat{a}^\dagger(\varphi), \quad \hat{a}(\varphi), \quad (1.26)$$

for $\varphi \in \mathcal{H}_{\text{lat}}$, allow modeling of replication events (increasing capsid count) or degradation events (reducing capsid count). In a resource-limited regime, the net flux of creation/annihilation can display nontrivial *circulation* in configuration space, signaling broken detailed balance and active viral replication cycles [2, 5].

Remark 1.12 (Projection Operators in Fock Space.). Given a decomposition of \mathcal{H}_{lat} into mass bands or arrangement modes, one naturally extends each projection $P^{(m_k)}$ to operate on \mathcal{H}_{lat} and then lifts it to the n -particle subspace $(\mathcal{H}_{\text{lat}}^{\otimes n})_+$ by taking tensor products. At the Fock level, such extended projections identify “which fraction” of n -particle states lie in a given mass subspace. This is analogous to selecting a subset of n virions that each weigh m_k . Biologically, we might interpret this as focusing on the portion of the viral population occupying a certain mass range, or subunits adopting specific stoichiometry. Mathematically, it clarifies how mass-resolved selection in \mathcal{H}_{arr} translates to n -particle states in the Fock space [23, 26].

1.1.1 The Total Mass Operator

We next establish that the *mass operator* \hat{M}_{total} admits a self-adjoint realization and possesses a purely discrete spectrum, corresponding to the eigenvalues $\{m_k\}_{k \in \mathcal{I}}$. From the viewpoint of *viral lattice theory*, each m_k may be interpreted as a distinct “mass band” or arrangement sector describing, for instance, different capsid conformations, subunit stoichiometries, or other internal viral parameters [2, 5]. This result underpins subsequent analyses of spectral decompositions and

dynamical properties (e.g. PDE or Fock-space extensions) relevant to viral phonon modes and resource-driven replication processes.

Theorem 1.13 (Self-Adjointness of \hat{M}_{total}). *Let $\{m_k\}_{k \in \mathcal{I}}$ be real numbers, and define the operator \hat{M}_{total} as in Definition 1.11. Then \hat{M}_{total} is self-adjoint (essentially self-adjoint on its natural domain), and its spectrum is*

$$\sigma(\hat{M}_{\text{total}}) = \{m_k : k \in \mathcal{I}\}. \quad (1.27)$$

Each m_k is an eigenvalue, with corresponding eigenspace $\mathcal{H}_{\text{arr}}^{(m_k)}$.

Proof. For any $\Phi, \Psi \in \mathcal{H}_{\text{arr}}$, decompose

$$\Phi = \sum_j \Phi^{(m_j)} \quad \text{and} \quad \Psi = \sum_\ell \Psi^{(m_\ell)}, \quad (1.28)$$

where $\Phi^{(m_j)}$ and $\Psi^{(m_\ell)}$ lie in the subspaces associated with each m_j and m_ℓ , respectively. By definition, we have

$$\langle \Phi, \hat{M}_{\text{total}} \Psi \rangle = \left\langle \sum_j \Phi^{(m_j)}, \sum_\ell m_\ell P^{(m_\ell)} \Psi \right\rangle = \sum_\ell m_\ell \langle \Phi, P^{(m_\ell)} \Psi \rangle, \quad (1.29)$$

where $P^{(m_\ell)}$ is the orthogonal projection onto $\mathcal{H}_{\text{arr}}^{(m_\ell)}$. Note that $P^{(m_\ell)} \Phi^{(m_j)} = 0$ when $j \neq \ell$, and $P^{(m_j)}$ is an orthogonal projection for each j . Thus,

$$\langle \Phi, \hat{M}_{\text{total}} \Psi \rangle = \sum_\ell m_\ell \langle \Phi^{(m_\ell)}, \Psi^{(m_\ell)} \rangle = \sum_j m_j \langle \Phi^{(m_j)}, \Psi^{(m_j)} \rangle. \quad (1.30)$$

By the symmetry of the inner product,

$$\langle \hat{M}_{\text{total}} \Phi, \Psi \rangle = \sum_j m_j \langle \Phi^{(m_j)}, \Psi^{(m_j)} \rangle = \langle \Phi, \hat{M}_{\text{total}} \Psi \rangle. \quad (1.31)$$

Hence, \hat{M}_{total} is symmetric (Hermitian). Next, consider the domain

$$\mathcal{D}(\hat{M}_{\text{total}}) = \left\{ \Psi = \sum_{k \in \mathcal{I}} \Psi^{(m_k)} \mid \sum_{k \in \mathcal{I}} m_k^2 \|\Psi^{(m_k)}\|^2 < \infty \right\}. \quad (1.32)$$

Since each m_k is real, \hat{M}_{total} is *essentially self-adjoint* on this maximal domain, and the spectral theorem for block-diagonal (direct sum) operators implies that the eigenvalue set is precisely $\{m_k\}_{k \in \mathcal{I}}$. Specifically, for any $\Psi^{(m_k)} \in \mathcal{H}_{\text{arr}}^{(m_k)}$,

$$\hat{M}_{\text{total}} \Psi^{(m_k)} = m_k \Psi^{(m_k)}, \quad (1.33)$$

so m_k is an eigenvalue with eigenspace $\mathcal{H}_{\text{arr}}^{(m_k)}$. Consequently, the point spectrum coincides with $\{m_k : k \in \mathcal{I}\}$, and there are no other eigenvalues. In operator-theoretic terms, \hat{M}_{total} is the orthogonal direct sum of the (one- or higher-dimensional) subspaces $\mathcal{H}_{\text{arr}}^{(m_k)}$, each corresponding to a single real eigenvalue m_k . Thus,

$$\sigma(\hat{M}_{\text{total}}) = \{m_k : k \in \mathcal{I}\}. \quad (1.34)$$

This completes the proof that \hat{M}_{total} is self-adjoint with discrete spectrum $\{m_k\}$. \square

Remark 1.14 (Virological and Physical Context.). In *viral lattice* models, one frequently associates each label m_k with a distinct “mass” or *arrangement state* (e.g., different protein subunits, capsid conformations, or quasiequivalent bonding sites) [2, 5]. Theorem 1.13 thus ensures that these arrangement blocks decouple as orthogonal eigenspaces. In later sections, this spectral decomposition facilitates:

1. *Construction of PDE or semigroup solutions* on each mass sector, allowing separate treatment of wave/phonon dynamics within each arrangement [8].
2. *Embedding into Fock spaces*, where creation/annihilation operators act on these mass-labeled subspaces, capturing viral replication or lattice assembly under resource constraints [21].
3. *Further coupling to Markov transitions and continuum PDE flows*, enabling a full description of hybrid PDE–Markov–Fock operators, which can exhibit non-equilibrium flux loops or break detailed balance [28, 29].

Hence, verifying self-adjointness of \hat{M}_{total} establishes a rigorous foundation for subsequent analyses of viral phonon modes, resource-driven replication processes, and advanced non-self-adjoint perturbations arising in open biological systems.

Definition 1.15 (Mass-Labeled Creation and Annihilation Operators). Let \mathcal{H}_{arr} be a Hilbert space encoding *arrangement* or *internal* states of a viral capsid, with mass-band subspaces indexed by $\{m_k\}_{k \in \mathcal{I}}$. Suppose we wish to describe *indistinguishable particles* (or quasi-particles) that occupy these mass-band subspaces. In an (anti)-symmetric Fock space $\mathcal{F}_{\pm}(\mathcal{H}_{\text{arr}})$ over \mathcal{H}_{arr} , we define operators

$$\hat{b}_{m_k}^{\dagger}, \quad \hat{b}_{m_k}, \quad k \in \mathcal{I}, \quad (1.35)$$

which *create* or *annihilate* a quantum of the mass band m_k . We impose the canonical (anti)-commutation relations:

$$[\hat{b}_{m_i}, \hat{b}_{m_j}^{\dagger}]_{\mp} = \delta_{i,j} I, \quad [\hat{b}_{m_i}, \hat{b}_{m_j}]_{\mp} = 0, \quad [\hat{b}_{m_i}^{\dagger}, \hat{b}_{m_j}^{\dagger}]_{\mp} = 0, \quad (1.36)$$

where the minus sign applies for fermions (anticommutators) and the plus sign for bosons (commutators) [23, 30, 31].

Proposition 1.16 (Number Operators and the Total Mass Operator). *In the bosonic (or fermionic) Fock space built over \mathcal{H}_{arr} , define the number operator for the mass-band m_k by*

$$\hat{N}_{m_k} = \hat{b}_{m_k}^{\dagger} \hat{b}_{m_k}. \quad (1.37)$$

Then the total mass operator \hat{M}_{total} satisfies

$$\hat{M}_{\text{total}} = \sum_{k \in \mathcal{I}} m_k \hat{N}_{m_k}, \quad (1.38)$$

and is self-adjoint. Moreover, each \hat{N}_{m_k} is a nonnegative operator projecting onto subspaces of fixed “mass occupancy” in the Fock space.

Proof. By standard arguments in *second quantization* [23, 30], the operator $\hat{N}_{m_k} = \hat{b}_{m_k}^{\dagger} \hat{b}_{m_k}$ counts the occupancy of mass band m_k . Its spectrum for bosons lies in $\{0, 1, 2, \dots\}$, while for fermions it

is restricted to $\{0, 1\}$. Identifying $P^{(m_k)}$ with the projection $\hat{b}_{m_k}^\dagger \hat{b}_{m_k}$ in the block-diagonal structure of \hat{M}_{total} (as discussed in Theorem 1.13) yields the direct sum decomposition

$$\hat{M}_{\text{total}} = \sum_{k \in \mathcal{I}} m_k (\hat{b}_{m_k}^\dagger \hat{b}_{m_k}) = \sum_{k \in \mathcal{I}} m_k \hat{N}_{m_k}. \quad (1.39)$$

Hence, \hat{M}_{total} is a sum of self-adjoint operators $m_k \hat{N}_{m_k}$, each of which has a nonnegative spectrum (shifted by m_k). The total mass operator is thus self-adjoint and inherits the direct sum spectral structure described in Theorem 1.13. The creation/annihilation operator formalism in (1.35)–(1.36) generalizes finite quantum mechanical models to infinite dimensions, aligning with algebraic quantum field theory [23, 26, 30]. The *mass-band* indices $\{m_k\}_{k \in \mathcal{I}}$ reflect a decomposition of the underlying Hilbert space \mathcal{H}_{arr} , enabling an operator-algebraic perspective on spectral blocks for viral capsid states or arrangement modes. \square

1.1.2 Virological and Biophysical Applications and Interpretations.

In the context of *viral lattices*, each mass band m_k can represent a *discrete* arrangement sector of capsid subunits (proteins) with specified conformations, stoichiometries, or post-translational modifications [2, 5]. The operator $\hat{b}_{m_k}^\dagger$ “creates” a new viral subunit (or quasi-particle) in band m_k , while \hat{b}_{m_k} “annihilates” one, mirroring how the virus may *assemble* new proteins or *disassemble* portions of its lattice. In physical virology terms:

- A “mass-band” might encode a particular shell thickness, glycosylation pattern, or binding state relevant to *capsid stability* [8].
 - Occupation of higher m_k subspaces might correspond to more “massive” or more extensively crosslinked arrangements, possibly requiring greater energy input or ATP from the host [16].
 - The number operator \hat{N}_{m_k} effectively measures how many subunits (or virions) are in arrangement m_k , allowing one to track *replication* or *assembly* levels in each mode.
1. *Mass-Selective Measurements*: Modern virological experiments, such as mass spectrometry of capsid proteins or cryo-EM reconstructions, can reveal distinct mass bands corresponding to partial or fully assembled capsids [2, 5]. The operator \hat{N}_{m_k} then provides a quantum-operator analogue to counting how many subunits occupy each discrete band, potentially guiding analysis of *assembly kinetics* or *subunit stoichiometry*.
 2. *Real-Time Assembly/Disassembly*: In single-molecule fluorescence or FRET experiments, one observes how capsid subunits bind or unbind in real time [7]. Creation/annihilation operators $\hat{b}_{m_k}^\dagger, \hat{b}_{m_k}$ allow a mathematically consistent framework for modeling these transitions as discrete steps in a larger Hilbert space, capturing resource-limited growth or partial lattice disintegration.
 3. *Hybrid PDE–Markov–Fock Models*: When combined with continuum PDE dynamics for viral shell elasticity, or Markov jump processes for conformational flips, the mass-band Fock space yields a powerful *multi-scale* description [8]. One can incorporate *non-self-adjoint* effects (dissipation, external driving) to study how viruses maintain non-equilibrium steady states or form persistent flux loops [28].

From a broader theoretical standpoint, Eqs. (1.37)–(1.38) exemplify how *Fock-space* quantization merges with block-diagonal spectral decompositions to yield self-adjoint mass operators [26,30]. This is reminiscent of the approach in quantum many-body physics or quantum optics, where each \hat{N}_{m_k} counts the number of particles in momentum or energy levels. In viral lattice theory, the “mass band” interpretation expands such ideas to *arrangement states* or *capsid subunit classes*, offering a consistent operator-algebraic structure for analyzing resource-driven assembly, hybrid PDE–Markov processes, and irreversibility in open biological systems.

Overall, this second-quantized formalism, with creation/annihilation operators tied to discrete mass bands, not only ensures a rigorous operator-theoretic foundation but also enriches virological modeling by linking subunit occupancy and arrangement modes to physically measurable “mass” or conformational states. Through advanced imaging and biophysical assays, one can probe these occupancies, thus verifying or refining the proposed quantum-inspired theoretical schemes.

Corollary 1.17 (Direct Sum Structure and (Anti)Symmetrization). *If the quanta follow Bose statistics, the Fock space is the symmetric tensor algebra built over \mathcal{H}_{arr} , whereas for Fermi statistics, it is the antisymmetric (exterior) algebra. In both cases, creation and annihilation operators with label m_k embed as block-diagonal expansions, respecting the direct sum structure*

$$\bigoplus_k \mathcal{H}_{\text{arr}}^{(m_k)}, \quad (1.40)$$

and ensuring that each mass-band subspace is treated consistently [23, 26, 30].

Theorem 1.18 (Many-Lattice Construction with Mass-Band Formalism). *In advanced viral modeling, one frequently considers multiple “lattices” (or lattice sites) representing distinct physical or spatial components of the viral capsid system. From a second-quantized perspective, each lattice may be described as:*

1. **Bosonic-like:** *if multiple capsids or subunits can occupy the same configuration/state without exclusion (classical indistinguishability akin to photons or phonons).*
2. **Fermionic-like:** *if stringent steric or biochemical constraints effectively impose an exclusion principle (only one capsid or subunit per “configuration”), though this scenario seems less common in typical viral assembly unless significant molecular crowding is involved.*

While we adopt the terms “bosons” and “fermions,” we do not assert that virions (or the vibrational quanta mediating their interactions) are fundamental particles in the high-energy physics sense. Instead, we leverage the robust second-quantization formalism—originally developed for elementary particle physics—to capture the motion and excitations of virions and their associated force carriers (“viral phonons”), exploiting well-established quantum-mechanical and operator-theoretic parallels [23, 30, 31].

Theorem 1.19 (Mass-Band Distinctions.). *Such distinctions often surface when lattice sites are categorized by differing genomic content or related macromolecular properties. For example, partially packaged capsids (lower effective mass) vs. fully packaged capsids (higher effective mass) can be labeled by separate mass bands, reflecting distinct internal energies or arrangement states [2, 5, 8].*

Formally, let

$$\mathcal{H}_{\text{arr}} = \bigoplus_{k=1}^N \mathcal{H}_{\text{arr}}^{(m_k)}, \quad (1.41)$$

where each $\mathcal{H}_{\text{arr}}^{(m_k)}$ represents an arrangement Hilbert space for mass band m_k . Subspace $\mathcal{H}_{\text{arr}}^{(m_k)}$ may encode discrete internal configuration states, such as “closed,” “partially open,” etc., along with Markovian transitions or energy landscapes [7, 21]. Denote by

$$\mathcal{H}_{\text{ph}} \tag{1.42}$$

the phonon Hilbert space describing vibrational quanta of the lattice (often elastic or wave-like excitations in the capsid shell [8]). Then the single-lattice Hilbert space can be defined as

$$\mathcal{H}_{\text{lat}} := \bigoplus_{k=1}^N \left(\mathcal{H}_{\text{arr}}^{(m_k)} \otimes \mathcal{H}_{\text{ph}} \right). \tag{1.43}$$

This direct sum and tensor-product structure allows a single-lattice model to accommodate multiple internal states (mass bands) and phonon-type excitations. In multi-lattice or many-particle settings, one extends \mathcal{H}_{lat} to a second-quantized Fock space, thereby capturing large-scale viral assemblies under fluctuating occupancy and resource constraints [16, 26, 28]. By adopting bosonic or fermionic statistics, one can model scenarios from classical indistinguishability (multiple capsids in a shared configuration) to exclusive states (severe steric hindrance). Such flexibility underscores the broad applicability of quantum-mechanical frameworks to biophysical problems in open, non-equilibrium systems. Recent investigations in viral molecular machines [2, 8] suggest that packaging dynamics, capsid conformational shifts, and partial disassembly events can be systematically described via mass-band labels, each corresponding to measurable differences in mass or internal arrangement (for instance, scanning transmission electron microscopy or mass spectrometry could distinguish partially vs. fully packed capsids). The introduction of phonon-like excitations further accounts for nanoscale vibrations or thermal fluctuations in the capsid shell, aligning well with experimental observations of lattice flexibility and transient morphological fluctuations. Ultimately, Theorem 1.18 provides a robust operator-theoretic scheme to unify these physical aspects into a single mathematical construction.

Theorem 1.20 (Fock Construction for Mass-Band Viral Lattices). *Let \mathcal{H}_{lat} be the single-lattice Hilbert space, formed by a direct sum and tensor product of mass-band arrangement subspaces $\{\mathcal{H}_{\text{arr}}^{(m_k)}\}$ and phonon degrees of freedom \mathcal{H}_{ph} (as in Theorem 1.18). To model a system with an indeterminate number $M \in \{0, 1, 2, \dots\}$ of these single-lattice entities (virions or subunits), one constructs the bosonic or fermionic Fock space:*

$$\mathcal{F}_{\pm}(\mathcal{H}_{\text{lat}}) = \bigoplus_{M=0}^{\infty} \left(\mathcal{H}_{\text{lat}}^{\otimes M} \right)_{\pm}, \tag{1.44}$$

where “ \pm ” indicates symmetrization or antisymmetrization in the tensor product, in accordance with bosonic or fermionic statistics [26, 30, 32].

(1) Hilbert-Space Completion and Operator Framework. By endowing (1.44) with the direct-sum norm

$$\|\Psi\|^2 = \sum_{M=0}^{\infty} \|\Psi^{(M)}\|_{\mathcal{H}_{\text{lat}}^{\otimes M}}^2, \tag{1.45}$$

where $\Psi^{(M)}$ denotes the component in the M -particle (or M -lattice) subspace, one obtains a complete Hilbert space $\mathcal{F}_{\pm}(\mathcal{H}_{\text{lat}})$. This *direct-sum completion* ensures a rigorous operator-algebraic

foundation for defining (possibly unbounded) creation/annihilation operators with well-specified domains [26, 30, 32].

(2) Mass-Band, Arrangement, and Phonon Indices. A basis state in $\mathcal{F}_\pm(\mathcal{H}_{\text{lat}})$ can be labeled by:

1. The *mass band* index m_k (identifying which subspace $\mathcal{H}_{\text{arr}}^{(m_k)}$ is occupied),
2. The *arrangement quantum number* $\alpha \in A$ (describing discrete conformations, e.g. “closed,” “partially open,” *etc.*),
3. The *phonon occupation numbers* in \mathcal{H}_{ph} (accounting for vibrational modes or wave-like excitations),
4. The *total number* M of single-lattice objects (capsids or subunits) present.

These indices generate a complete orthonormal system in $\mathcal{F}_\pm(\mathcal{H}_{\text{lat}})$, reflecting the multi-level structure of viral lattices (mass, internal states, vibrational excitations) [5, 8].

(3) Creation/Annihilation Operators in Mass-Band Formalism. Define operators

$$\hat{b}_k^\dagger(\boldsymbol{\psi}) \quad \text{and} \quad \hat{b}_k(\boldsymbol{\psi}), \quad \boldsymbol{\psi} \in \mathcal{H}_{\text{arr}}^{(m_k)} \otimes \mathcal{H}_{\text{ph}}, \quad (1.46)$$

that create (annihilate) a single-lattice excitation in band m_k with internal arrangement/phonon state $\boldsymbol{\psi}$. These operators satisfy canonical (anti)commutation relations

$$[\hat{b}_k(\boldsymbol{\psi}), \hat{b}_\ell^\dagger(\boldsymbol{\chi})]_\pm = \delta_{k,\ell} \langle \boldsymbol{\psi}, \boldsymbol{\chi} \rangle_{\mathcal{H}_{\text{lat}}} \mathbb{I}, \quad \text{and all other (anti)commutators vanish.} \quad (1.47)$$

Here $\langle \cdot, \cdot \rangle_{\mathcal{H}_{\text{lat}}}$ is the product inner product on arrangement and phonon subspaces. By constructing these operators on a dense domain in $\mathcal{F}_\pm(\mathcal{H}_{\text{lat}})$, one ensures standard self-adjointness conditions for the number, mass, and total energy observables [26, 31].

(4) Quasi-Identical Family of Lattices. Despite each lattice possibly differing by mass band m_k or arrangement details, the second-quantized scheme treats them as a “quasi-identical family.” This enables the unification of compositional diversity (e.g. partially versus fully packaged capsids) within the well-established machinery of many-body quantum mechanics and field theory.

1.2 Unified Macro-Arrangement and Continuum-Field Description of a Viral Lattice

Context. We aim to show that each *viral lattice state* can be represented as a combination of:

$$|f\rangle \quad (\text{macro-arrangement label}) \oplus (\mathbf{u}_R, \mathbf{u}_I) \quad (\text{continuum displacement fields}). \quad (1.48)$$

Mathematically, $|f\rangle$ might be chosen from a *discrete* set of macro-states, while $\mathbf{u}_R, \mathbf{u}_I$ lie in a Hilbert space (or Sobolev space) that encodes continuous or finely discretized vibrational modes. The PDE system (which is fully derived in [1]):

$$\mathbf{u}(\mathbf{r}, t) = \mathbf{u}_R(\mathbf{r}, t) + i \mathbf{u}_I(\mathbf{r}, t), \quad (1.49)$$

where:

- $\mathbf{u}_R(\mathbf{r}, t) \in \mathbb{R}^3$ represents the in-phase (real) component of the displacement, associated with the elastic deformation of the viral lattice.

- $\mathbf{u}_I(\mathbf{r}, t) \in \mathbb{R}^3$ denotes the out-of-phase (imaginary) component, encapsulating the dissipative processes such as viscous damping and energy loss mechanisms within the medium.
- i is the imaginary unit, satisfying $i^2 = -1$.

$$\begin{cases} g \frac{\partial^2 \mathbf{u}_R}{\partial t^2} + \eta_R \frac{\partial \mathbf{u}_R}{\partial t} - \nabla \cdot (\boldsymbol{\Lambda}_\Phi \mathbf{u}_R) - \eta_I \frac{\partial \mathbf{u}_I}{\partial t} = \mathbf{W}_{\text{Host}}^R(\mathbf{r}, t) + \tilde{\boldsymbol{\psi}}^R(\mathbf{r}, t), \\ g \frac{\partial^2 \mathbf{u}_I}{\partial t^2} + \eta_R \frac{\partial \mathbf{u}_I}{\partial t} - \nabla \cdot (\boldsymbol{\Lambda}_\Phi \mathbf{u}_I) + \eta_I \frac{\partial \mathbf{u}_R}{\partial t} = \mathbf{W}_{\text{Host}}^I(\mathbf{r}, t) + \tilde{\boldsymbol{\psi}}^I(\mathbf{r}, t), \end{cases} \quad (1.50)$$

governs the real and imaginary displacements $\mathbf{u}_R, \mathbf{u}_I$ in $\Omega \subset \mathbb{R}^3$. Under suitable damping and boundary conditions, one obtains a well-defined semigroup on a product space of states and velocities. Below is a theorem that ties this PDE formulation to an operator-theoretic structure on a Hilbert space \mathcal{H}_{lat} , *plus* the discrete arrangement label $|f\rangle$. Where:

Definition 1.21 (Mass Density Field). Let

$$g : \Omega \longrightarrow \mathbb{R}^+ \quad (1.51)$$

be the **mass density field**, defined by distributing virion masses continuously over the domain Ω . Formally, if each virion has mass m and there are N virions in volume $|\Omega|$, then

$$g(\mathbf{r}) = \lim_{a \rightarrow 0} \frac{m N}{|\Omega|}, \quad (1.52)$$

where a is the lattice spacing. The limit $a \rightarrow 0$ represents passing to the continuum, ensuring that the lattice becomes sufficiently dense.

Definition 1.22 (Displacement Field). Let

$$\mathbf{u} : \Omega \times [0, T] \longrightarrow \mathbb{R}^3 \quad (1.53)$$

be the **displacement field**, where $\mathbf{u}(\mathbf{r}, t)$ describes the deviation of virions from their equilibrium positions at spatial point \mathbf{r} and time t . This field emerges as the continuum analog of the discrete set $\{\mathbf{r}_i(t)\}$ of virion positions.

Definition 1.23 (Complex Damping Coefficient). We incorporate complex viscoelastic damping into the theoretical framework. This extension is crucial for modeling realistic biological environments, which are neither purely elastic nor purely viscous, but instead exhibit a complex rheological response. By introducing a complex damping coefficient, we capture both energy dissipation (through its real part) and energy storage or phase delays (through its imaginary part). Let $\eta : \Omega \times [0, T] \rightarrow \mathbb{C}$ be the **complex damping coefficient**, defined by:

$$\eta(\mathbf{r}, t) = \eta_R(\mathbf{r}, t) + i \eta_I(\mathbf{r}, t), \quad (1.54)$$

where $\eta_R, \eta_I : \Omega \times [0, T] \rightarrow \mathbb{R}$. The real part η_R governs viscous energy dissipation, while the imaginary part η_I encodes elastic energy storage and phase shifts between stress and strain. In a virological context, the presence of $\eta(\mathbf{r}, t)$ reflects the fact that virions move within a complex medium (e.g., intracellular fluids, extracellular matrices) that can temporarily store mechanical energy, induce delays in response, and dissipate energy over time.

Definition 1.24 (Interaction Operator Λ_Φ). Let Λ_Φ be a linear operator acting on vector fields $\mathbf{u}(\mathbf{r}, t)$. It encodes the macroscopic stiffness and elastic properties derived from microscopic inter-virion potentials (e.g., Coulombic, Lennard-Jones). Formally, Λ_Φ is obtained from the Hessian of the interaction energy functional:

$$V(\mathbf{u}) = \frac{1}{2} \int_{\Omega} \int_{\Omega} V_{ij}(r_{ij}) d\mu(i, j), \quad (1.55)$$

where V_{ij} are pairwise potentials and $d\mu(i, j)$ is a measure capturing the continuum limit of a discrete summation. Differentiating twice with respect to \mathbf{u} yields

$$\Lambda_\Phi := \left. \frac{\delta^2 V(\mathbf{u})}{\delta \mathbf{u}^2} \right|_{\mathbf{u}=\mathbf{0}}. \quad (1.56)$$

$$\Phi_{\text{Coulomb}}(a) = \frac{2k_e q_i q_j}{a^3}, \quad \Phi_{\text{LJ}}(a) = 4\epsilon_{ij} \left[156 \frac{\sigma_{ij}^{12}}{a^{14}} - 42 \frac{\sigma_{ij}^6}{a^8} \right]. \quad (1.57)$$

This operator plays the role of a generalized elasticity tensor, relating displacement fields to restoring forces.

Theorem 1.25 (The Viral Lattice Matrix). *For a lattice composed of four “viral cells,” the full dynamical matrix, denoted by Λ_{ij}^Φ , can be structured into sub-matrices representing intra-cell and inter-cell interactions. For example:*

$$\Lambda_{ij}^\Phi = \begin{bmatrix} \mathbf{D}_{11} & \mathbf{D}_{12} \\ \mathbf{D}_{21} & \mathbf{D}_{22} \end{bmatrix}. \quad (1.58)$$

where each sub-matrix is defined as:

$$D_{11} = \begin{bmatrix} \alpha & \beta & \beta & \beta \\ \beta & \alpha & \gamma & \gamma \\ \beta & \gamma & \alpha & \gamma \\ \beta & \gamma & \gamma & \alpha \end{bmatrix}, \quad D_{12} = \begin{bmatrix} \psi & \Omega & \Omega & \Omega \\ \Omega & \psi & \Omega & \Omega \\ \Omega & \Omega & \psi & \Omega \\ \Omega & \Omega & \Omega & \psi \end{bmatrix} \quad (1.59)$$

$$D_{21} = \begin{bmatrix} \psi & \Omega & \Omega & \Omega \\ \Omega & \psi & \Omega & \Omega \\ \Omega & \Omega & \psi & \Omega \\ \Omega & \Omega & \Omega & \psi \end{bmatrix}, \quad D_{22} = \begin{bmatrix} \alpha & \beta & \beta & \beta \\ \beta & \alpha & \gamma & \gamma \\ \beta & \gamma & \alpha & \gamma \\ \beta & \gamma & \gamma & \alpha \end{bmatrix} \quad (1.60)$$

A viral lattice can be viewed as a collection of fundamental units—viral cells—each containing a central virion and its nearby neighbors. To characterize the mechanical and vibrational properties of the entire lattice, one assembles these cells into a global framework represented by the **viral lattice matrix** Λ_{ij}^0 . By summing over intra- and inter-cell interactions, Λ_{ij}^0 serves as a unifying mathematical object for analyzing stability, wave propagation, and collective phenomena in the viral assembly [33–35].

Proposition 1.26 (Virion Positions). *In a simple cubic lattice, the virion positions within a viral cell can be enumerated relative to an origin \mathbf{R}_0 . Using the Cartesian unit vectors $\mathbf{e}_x, \mathbf{e}_y, \mathbf{e}_z$:*

- **Nearest Neighbor Virions (β):**

$$\begin{aligned} \mathbf{R}_1 &= \mathbf{R}_0 + a \mathbf{e}_x, & \mathbf{R}_2 &= \mathbf{R}_0 - a \mathbf{e}_x, \\ \mathbf{R}_3 &= \mathbf{R}_0 + a \mathbf{e}_y, & \mathbf{R}_4 &= \mathbf{R}_0 - a \mathbf{e}_y, \\ \mathbf{R}_5 &= \mathbf{R}_0 + a \mathbf{e}_z, & \mathbf{R}_6 &= \mathbf{R}_0 - a \mathbf{e}_z. \end{aligned} \quad (1.61)$$

- **Local Virions** (γ):

$$\mathbf{R}_j = \mathbf{R}_0 \pm a(\mathbf{e}_i \pm \mathbf{e}_k), \quad i \neq k, \quad j = 7, \dots, 18. \quad (1.62)$$

These correspond to face diagonals, each representing distinct combinations of two lattice directions.

- **Peripheral Virions** (Ω):

$$\mathbf{R}_j = \mathbf{R}_0 \pm a(\mathbf{e}_x \pm \mathbf{e}_y \pm \mathbf{e}_z), \quad j = 19, \dots, 26. \quad (1.63)$$

These represent body diagonals, involving all three coordinate directions simultaneously.

- **Inter-Cellular Peripheral Virions** (ψ): introduced to represent virions at cell boundaries that, once boundaries are conceptually removed, directly interact between adjacent cells. This term ψ encapsulates the interaction potential bridging distinct cells, effectively stitching the lattice together into a cohesive continuum.

Definition 1.27 (Host Work Term). Virions interact with their environment (the host), which can inject or remove energy from the system. Let

$$\mathbf{W}_{\text{Host}} : \Omega \times [0, T] \longrightarrow \mathbb{R}^3 \quad (1.64)$$

be the **host work term**, representing non-conservative forces arising from the host environment. This term generalizes the discrete forcing $\mathbf{W}_{\text{Host},i}$ to the continuum limit:

$$\mathbf{W}_{\text{Host}}(\mathbf{r}, t) = \lim_{N \rightarrow \infty} \sum_{i=1}^N \delta(\mathbf{r} - \mathbf{r}_i) \mathbf{W}_{\text{Host},i}(t), \quad (1.65)$$

where δ is the Dirac delta distribution ensuring a well-defined continuum description. In many practical applications, this limit may be interpreted as a *coarse-graining* of discrete interactions (e.g., molecular collisions or local metabolic actions by the host) into a spatially continuous forcing field.

Definition 1.28 (Complex-Damped Viral Phonon Wave Function). Let $\Gamma(\mathbf{k}) > 0$ denote a wavenumber-dependent decay rate arising from a complex damping coefficient $\eta \in \mathbb{C}$. Define the **complex-damped viral phonon wave function** $\tilde{\psi}_{\text{damped}}$ by

$$\tilde{\psi}_{\text{damped}}(t, \mathbf{R}_i) := \int_{\omega_{\min}}^{\omega_{\max}} A(\mathbf{R}_i) g_{\text{viral}}(\omega) \exp[-i(\omega - i\Gamma(\mathbf{k}))t] \exp[-i\mathbf{k} \cdot \mathbf{R}_i] d\omega, \quad (1.66)$$

where:

- $A(\mathbf{R}_i)$ is an amplitude factor encoding initial or boundary conditions;
- $g_{\text{viral}}(\omega)$ is the viral lattice density of states (DOS);
- The exponential factor $\exp[-i(\omega - i\Gamma(\mathbf{k}))t]$ incorporates both oscillatory behavior (governed by ω) and exponential decay (governed by $\Gamma(\mathbf{k})$).

Remark 1.29. In the undamped limit $\Gamma(\mathbf{k}) \rightarrow 0$, the integral in (1.66) reduces to a typical inverse Fourier transform of the dispersion relation. Introducing a nonzero $\Gamma(\mathbf{k})$ naturally embeds viscoelastic or dissipative processes into the wavefunction, thereby unifying classical partial differential equation analyses of damped oscillations with quantum-inspired (phonon) concepts from solid-state physics.

Theorem 1.30 (Representation of Viral Lattice States as Arrangement Labels + Continuum Fields). *Let $\{|f\rangle\}_{f \in \mathcal{F}}$ be a finite or countably infinite set of macro-arrangement labels describing distinct large-scale capsid conformations in a viral lattice model. Let $\Omega \subset \mathbb{R}^3$ be a spatial domain of interest, and let $(\mathbf{u}_R, \mathbf{u}_I) \in [L^2(\Omega)]^d \times [L^2(\Omega)]^d$ represent displacement fields (with $d \geq 1$) capturing continuum-mechanical degrees of freedom. Define the single-lattice Hilbert space by*

$$\mathcal{H}_{\text{lat}} = \left(\bigoplus_{f \in \mathcal{F}} \mathbb{C} |f\rangle \right) \otimes \left([L^2(\Omega)]^d \times [L^2(\Omega)]^d \right), \quad (1.67)$$

or equivalently

$$|f\rangle \oplus (\mathbf{u}_R, \mathbf{u}_I) \in \mathcal{H}_{\text{arr}} \oplus \mathcal{H}_{\text{disp}}, \quad (1.68)$$

where

$$\mathcal{H}_{\text{arr}} = \text{span}\{|f\rangle : f \in \mathcal{F}\}, \quad \mathcal{H}_{\text{disp}} = [L^2(\Omega)]^{2d}. \quad (1.69)$$

Then, by considering a (generally non-self-adjoint) PDE generator $\hat{\mathcal{G}}$ subject to boundary conditions ensuring dissipativity, the associated strongly continuous semigroup $\{e^{t\hat{\mathcal{G}}}\}_{t \geq 0}$ evolves viral lattice states in \mathcal{H}_{lat} according to

$$(\mathbf{u}_R(\cdot, t), \mathbf{u}_I(\cdot, t)) = e^{t\hat{\mathcal{G}}} (\mathbf{u}_R(\cdot, 0), \mathbf{u}_I(\cdot, 0)). \quad (1.70)$$

Hence each viral lattice configuration is rigorously represented by a vector in this product space, combining macro-arrangement labels with continuum displacement fields.

Proof. Let \mathcal{F} be an index set (finite or countably infinite) whose elements label distinct macro-arrangements, such as major conformational states of a viral capsid [2, 8]. Denote the formal basis vectors by $|f\rangle$, $f \in \mathcal{F}$, and equip

$$\text{span}\{|f\rangle : f \in \mathcal{F}\} \quad (1.71)$$

with the inner product

$$\langle |f\rangle, |f'\rangle \rangle_{\mathcal{H}_{\text{arr}}} = \delta_{f, f'}. \quad (1.72)$$

If \mathcal{F} is finite, this space is finite-dimensional. If \mathcal{F} is countably infinite, one completes the span to form a separable Hilbert space akin to ℓ^2 [23]. Denote the resulting space by

$$\mathcal{H}_{\text{arr}} = \overline{\text{span}\{|f\rangle : f \in \mathcal{F}\}}.$$

This space captures distinct large-scale arrangement modes (e.g. “closed,” “partially open,” or other major conformational states) [5]. Next, let $\Omega \subset \mathbb{R}^3$ be a domain representing the region in which viral lattice displacements occur (e.g. capsid or subunit location). Define

$$\mathcal{H}_{\text{disp}} = [L^2(\Omega)]^{2d} = \left([L^2(\Omega)]^d \right) \times \left([L^2(\Omega)]^d \right), \quad (1.73)$$

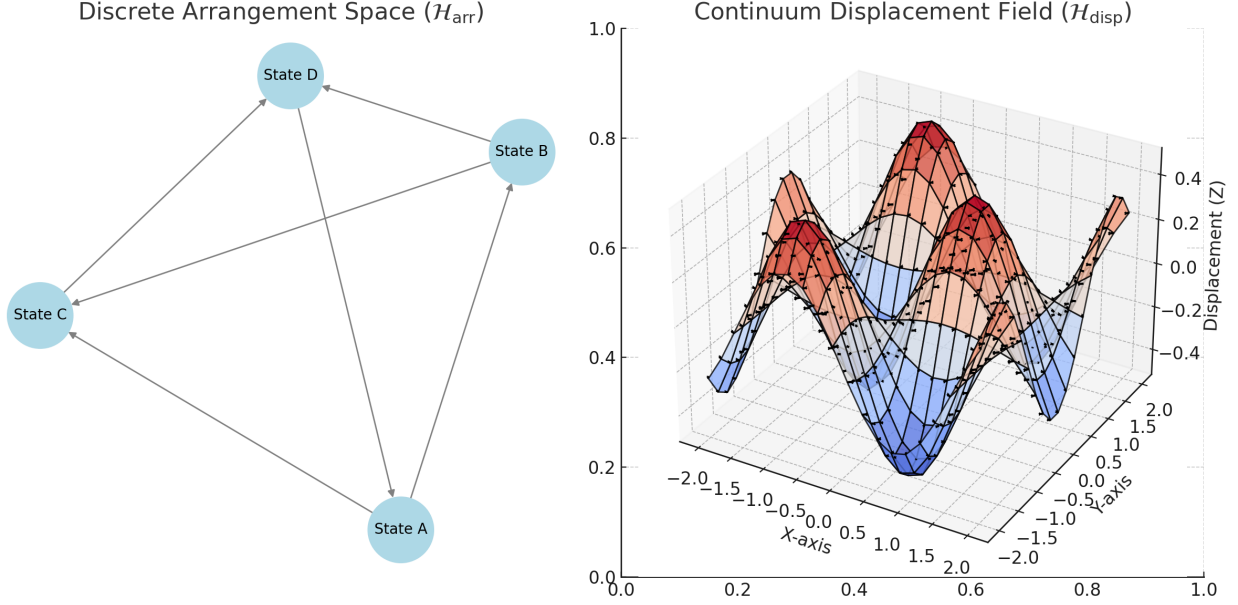


Figure 2: **Discrete Arrangement Space vs. Continuum Displacement Field.** *Left Panel: Discrete Arrangement Space (\mathcal{H}_{arr}).* The network graph depicts macro-arrangement labels $|f\rangle$, each node representing a distinct viral capsid conformation. Edges indicate allowable transitions between these states, illustrating the Markovian character of discrete conformational changes. *Right Panel: Continuum Displacement Field ($\mathcal{H}_{\text{disp}}$).* A 3D surface plot shows the deformation field over a viral capsid-like spatial domain. The superimposed vector field $(\mathbf{u}_R, \mathbf{u}_I)$ reveals how the lattice, and its constituent virions, mechanically deforms under PDE-based dynamics. Together, these panels emphasize the *hybrid* nature of viral lattice theory, combining discrete arrangement jumps with continuum deformations in a unified operator-theoretic framework.

accounting for real and imaginary parts $(\mathbf{u}_R, \mathbf{u}_I)$. The inner product on $\mathcal{H}_{\text{disp}}$ is

$$\langle (\mathbf{u}_R, \mathbf{u}_I), (\mathbf{v}_R, \mathbf{v}_I) \rangle_{\mathcal{H}_{\text{disp}}} = \int_{\Omega} \left(\mathbf{u}_R(\mathbf{x}) \cdot \mathbf{v}_R(\mathbf{x}) + \mathbf{u}_I(\mathbf{x}) \cdot \mathbf{v}_I(\mathbf{x}) \right) d\mathbf{x}, \quad (1.74)$$

reflecting a standard L^2 construction. To link macro-arrangement labels $|f\rangle$ with continuum fields $(\mathbf{u}_R, \mathbf{u}_I)$, one forms a tensor product:

$$\mathcal{H}_{\text{lat}} = \left(\bigoplus_{f \in \mathcal{F}} \mathbb{C} |f\rangle \right) \otimes \mathcal{H}_{\text{disp}}. \quad (1.75)$$

Equivalently, if each arrangement f corresponds to a distinct *sector* for the displacement PDE, one might adopt a direct sum

$$\bigoplus_{f \in \mathcal{F}} \mathcal{H}_{\text{disp}} \simeq \mathcal{H}_{\text{arr}} \oplus \mathcal{H}_{\text{disp}}, \quad (1.76)$$

so that a vector in \mathcal{H}_{lat} stores both the *label* f and the *field* $(\mathbf{u}_R, \mathbf{u}_I)$ [36,37]. Now, consider a PDE (possibly damped or dissipative) for $(\mathbf{u}_R, \mathbf{u}_I)$ in Ω , subject to boundary conditions ensuring $\hat{\mathcal{G}}$ is an m -sectorial or maximal dissipative operator [23]. Formally,

$$\partial_t \begin{pmatrix} \mathbf{u}_R(\mathbf{x}, t) \\ \mathbf{u}_I(\mathbf{x}, t) \end{pmatrix} = \hat{\mathcal{G}} \begin{pmatrix} \mathbf{u}_R(\mathbf{x}, t) \\ \mathbf{u}_I(\mathbf{x}, t) \end{pmatrix}, \quad (1.77)$$

with suitable boundary conditions. By the Lumer–Phillips and Hille–Yosida theorems, $\hat{\mathcal{G}}$ generates a strongly continuous semigroup $e^{t\hat{\mathcal{G}}}$ on $\mathcal{H}_{\text{disp}}$, or on each arrangement sector if f evolves. Thus, for $t \geq 0$,

$$(\mathbf{u}_R(\cdot, t), \mathbf{u}_I(\cdot, t)) = e^{t\hat{\mathcal{G}}}(\mathbf{u}_R(\cdot, 0), \mathbf{u}_I(\cdot, 0)). \quad (1.78)$$

By extension, each macro-arrangement label f can either remain fixed (yielding block-diagonal dynamics) or follow a Markovian transition process among labels $|f'\rangle$, capturing rearrangements or conformational flips of the viral capsid [5]. A viral lattice state vector in \mathcal{H}_{lat} combines:

1. The large-scale arrangement label f , specifying which capsid conformation or macro state is present,
2. The continuum displacement fields $(\mathbf{u}_R, \mathbf{u}_I)$ describing wave-like or elastic deformations at smaller scales [8].

Hence, the PDE evolution implements time-dependent changes in $(\mathbf{u}_R, \mathbf{u}_I)$ while possible transitions in f account for distinct macro states (which can be further incorporated via a block-diagonal or non-self-adjoint coupling operator). This construction provides a rigorous, operator-theoretic representation of *viral lattice states*—one that can be extended to non-equilibrium scenarios if $\hat{\mathcal{G}}$ includes dissipative or driving terms [28, 38].

Combining the macro-arrangement Hilbert space \mathcal{H}_{arr} with the displacement field space $\mathcal{H}_{\text{disp}}$ via (1.75) yields a single-lattice Hilbert space \mathcal{H}_{lat} . The PDE generator $\hat{\mathcal{G}}$ (possibly non-self-adjoint) defines a semigroup that evolves displacement fields in time, and any Markovian or block-diagonal extension can describe changes in f . Thus, every viral lattice configuration—encompassing both arrangement labels and continuum fields—resides in \mathcal{H}_{lat} , ensuring a well-posed and mathematically robust framework for subsequent spectral, dynamical, and non-equilibrium analyses of capsid or subunit deformations in virological contexts. \square

The second-order PDE (1.49) can be reformulated as a first-order system by introducing the vector

$$\mathbf{U}(t) = \begin{pmatrix} \mathbf{u}_R(t) \\ \partial_t \mathbf{u}_R(t) \\ \mathbf{u}_I(t) \\ \partial_t \mathbf{u}_I(t) \end{pmatrix}. \quad (1.79)$$

This transforms the PDE into an abstract ODE of the form

$$\frac{d}{dt} \mathbf{U}(t) = \hat{\mathcal{G}} \mathbf{U}(t) + \Phi, \quad (1.80)$$

where $\hat{\mathcal{G}}$ is a block matrix operator incorporating density g , damping η_R, η_I , stiffness Λ_Φ , and possibly other physical coefficients. The term Φ can represent external forcing or noise. In particular, the operator $\hat{\mathcal{G}}$ acts on vectors

$$\mathbf{U}(t) \in D(\hat{\mathcal{G}}) \subset \left(H^1(\Omega)\right)^{2d} \times \left(L^2(\Omega)\right)^{2d}, \quad (1.81)$$

with boundary conditions (Dirichlet, Neumann, or mixed) encoded in the definition of $D(\hat{\mathcal{G}})$. Under elliptic regularity assumptions on Λ_Φ (e.g., $\text{Re } \Lambda_\Phi \succeq 0$) and positive damping coefficients ($\eta_R, \eta_I > 0$), one can show that $\hat{\mathcal{G}}$ is *m-sectorial* (or maximal dissipative).

To establish *m*-sectoriality, one checks:

$$\text{Re} \langle \hat{\mathcal{G}} \mathbf{U}, \mathbf{U} \rangle_{\mathcal{H}_{\text{disp}}} \leq C \|\mathbf{U}\|_{\mathcal{H}_{\text{disp}}}^2 \quad \text{for some constant } C < \infty, \quad (1.82)$$

demonstrating dissipativity (or sectorial dissipativity if $\eta_R > 0$ and $\eta_I > 0$). By verifying the *range condition* for $I - \hat{\mathcal{G}}$ (or $I + \hat{\mathcal{G}}$), one concludes that $\hat{\mathcal{G}}$ is *maximal* on its domain. Consequently, the Lumer–Phillips Theorem or the Hille–Yosida criteria for non-self-adjoint, linear operators guarantees that $\hat{\mathcal{G}}$ generates a strongly continuous semigroup

$$e^{t\hat{\mathcal{G}}} \quad \text{on} \quad \mathcal{H}_{\text{disp}} = [L^2(\Omega)]^{2d}. \quad (1.83)$$

Hence, for each initial condition $\mathbf{U}(0) = \mathbf{U}_0 \in D(\hat{\mathcal{G}})$, there exists a unique mild or strong solution

$$\mathbf{U}(t) = e^{t\hat{\mathcal{G}}} \mathbf{U}_0, \quad (1.84)$$

continuously depending on the data. This solution satisfies the PDE in a classical or weak sense, depending on the boundary conditions [37]. The vector $\mathbf{U}(t)$ can capture the real (\mathbf{u}_R) and imaginary (\mathbf{u}_I) parts of viral lattice displacements—encompassing mechanical, vibrational, or wave-like deformations in the capsid. For instance, a positive damping $\eta_R, \eta_I > 0$ models frictional or viscous effects (e.g., from host cytoplasm or internal capsid fluid), ensuring the lattice does not oscillate indefinitely. Meanwhile, the stiffness matrix Λ_Φ encodes how strongly subunits resist deformation, such that large displacements demand significant energy input. From a *virological* standpoint, these continuum fields could represent *localized bulges*, partial swelling, or vibrational modes in the capsid lattice [2, 8]. With $\mathbf{U}(t)$ evolving by (1.80), one models how external or internal forces (host metabolism, resource input) drive shape reconfigurations or dampen certain modes, reflecting non-equilibrium processes integral to *capsid assembly and stability* [5].

Finally, one incorporates the *macro-arrangement* label $|f\rangle$ from Theorem 1.30:

- Each label f corresponds to a *major* conformational or morphological state, e.g., “closed capsid,” “partially open,” or “expanded” in response to host factors.
- The PDE dynamics in $\mathbf{u}_R, \mathbf{u}_I$ then apply *within* that arrangement sector, possibly with different boundary conditions or stiffness constants for each f .
- In a fully coupled model, f can transition via discrete Markov jumps, merging PDE wave-like evolutions with arrangement flips [7, 21].

Such *hybrid PDE–Markov* systems with m -sectorial operators can describe how viral capsids break detailed balance and enter persistent flux loops driven by external energy sources [28].

Definition 1.31 (Static vs. Dynamical Macro-Arrangement Labels). In the *simplest* setting, each macro-arrangement label $|f\rangle$ is *static*; i.e., the system does *not* transition from arrangement f to another f' . In this scenario, each macro-arrangement f corresponds to an independent PDE problem with arrangement-dependent parameters $\Lambda_\Phi^{(f)}$, boundary conditions, or damping constants. Concretely,

$$\bigoplus_{f \in \mathcal{F}} \mathcal{H}_{\text{disp}}^{(f)}, \quad (1.85)$$

where each $\mathcal{H}_{\text{disp}}^{(f)}$ is the solution space for a PDE specialized to arrangement f . The total Hilbert space is the orthogonal direct sum of these subspaces, ensuring that each arrangement’s PDE evolves independently, with no coupling operator required [36, 37]. In more *general* models, one allows the arrangement label to transition between states $f \rightarrow f'$, captured by a discrete operator

$$\hat{\mathcal{T}}: \mathcal{H}_{\text{arr}} \rightarrow \mathcal{H}_{\text{arr}}, \quad (1.86)$$

often block-diagonal (or block-off-diagonal) in the basis $\{|f\rangle\}$. In this case, the total single-lattice space

$$\mathcal{H}_{\text{lat}} = \mathcal{H}_{\text{disp}} \otimes \mathcal{H}_{\text{arr}} \quad (1.87)$$

admits a combined generator

$$\hat{\mathcal{G}}_{\text{total}} = \hat{\mathcal{G}} \otimes I_{\mathcal{H}_{\text{arr}}} + I_{\mathcal{H}_{\text{disp}}} \otimes \hat{\mathcal{T}}, \quad (1.88)$$

where $\hat{\mathcal{G}}$ is the (possibly non-self-adjoint) PDE generator describing continuum displacement fields, and $\hat{\mathcal{T}}$ governs the discrete, macro-arrangement transitions [23].

One verifies that $\hat{\mathcal{G}}_{\text{total}}$ is a linear operator on \mathcal{H}_{lat} with domain

$$D(\hat{\mathcal{G}}_{\text{total}}) = \left(D(\hat{\mathcal{G}}) \otimes \mathcal{H}_{\text{arr}} \right) \cap \left(\mathcal{H}_{\text{disp}} \otimes D(\hat{\mathcal{T}}) \right). \quad (1.89)$$

This domain reflects the interplay of PDE-regularity constraints (for $\hat{\mathcal{G}}$) and the discrete domain requirements (for $\hat{\mathcal{T}}$). Under mild assumptions (e.g. positive damping in the PDE, nonnegative transition rates for the macro labels), $\hat{\mathcal{G}}_{\text{total}}$ is m -sectorial or maximal dissipative, thus generating a strongly continuous semigroup $e^{t\hat{\mathcal{G}}_{\text{total}}}$ in \mathcal{H}_{lat} . Given any initial configuration

$$\Psi_{\text{lat}}(0) = \sum_{f \in \mathcal{F}} |f\rangle \otimes (\mathbf{u}_R^{(f)}(\cdot, 0), \mathbf{u}_I^{(f)}(\cdot, 0)) \in D(\hat{\mathcal{G}}_{\text{total}}), \quad (1.90)$$

the semigroup $e^{t\hat{\mathcal{G}}_{\text{total}}}$ yields a unique mild (or strong) solution

$$\Psi_{\text{lat}}(t) = e^{t\hat{\mathcal{G}}_{\text{total}}} \Psi_{\text{lat}}(0), \quad (1.91)$$

continuously depending on the initial data [26, 32]. In this way, each macro-arrangement label f and its associated continuum fields evolve in a coupled—but still rigorously defined—manner:

$$|f\rangle \oplus (\mathbf{u}_R^{(f)}(\mathbf{x}, t), \mathbf{u}_I^{(f)}(\mathbf{x}, t)). \quad (1.92)$$

Virological Interpretation and Biological Relevance.

- *Static Label Case.* If $|f\rangle$ is fixed (*no* transition among macro-arrangements), the model describes a single viral capsid conformation with continuum PDE parameters (stiffness, damping) locked to that arrangement [2, 8]. This is analogous to analyzing vibrations or deformations in a single morphological state (e.g. a “closed” capsid).
- *Dynamical Arrangements.* In realistic viral systems, conformations can switch under various influences (host factors, changes in resource availability, pH levels) [5, 7]. The transition operator $\hat{\mathcal{T}}$ models these discrete jumps—e.g., from a “closed” to a “partially open” arrangement, or from a “packaged” to a “swollen” state. Meanwhile, the PDE generator $\hat{\mathcal{G}}$ captures local elasticity and vibrational phenomena in each arrangement.
- *Assembly Pathways and Non-Equilibrium Flows.* Merging $\hat{\mathcal{G}}$ and $\hat{\mathcal{T}}$ into (1.88) allows for a rich repertoire of *transitions* and *continuum deformations*, reflecting how capsid subunits reorganize under host driving. Non-equilibrium flux loops, resource-driven partial disassembly, or conformational toggling become tractable within a single operator-theoretic scheme [28].

From the standpoint of open-system operator theory, the direct sum $\mathcal{H}_{\text{disp}}^{(f)}$ or the tensor product $\mathcal{H}_{\text{disp}} \otimes \mathcal{H}_{\text{arr}}$ ensures each PDE mode remains integrable and consistent with the Markov-type (or purely discrete) transitions among labels. Standard results in semigroup theory then guarantee a stable evolution in this Hilbert space, thereby establishing *existence, uniqueness, and continuous dependence* on initial data. In other words, the *macro-arrangement labels* are systematically embedded into the continuum PDE description, and the overall viral lattice model is *mathematically well-posed*. Under the direct-sum or tensor-product construction with arrangement labels, each viral lattice state remains well-defined and evolves consistently in \mathcal{H}_{lat} . The PDE portion captures elastic or wave-like displacements, while the discrete operator \hat{T} encodes conformational or macro-arrangement flips. This formalism is sufficiently flexible to handle both *static* (single-conformation) and *dynamic* (multi-conformation) viral capsid models, thereby clarifying the interplay of continuum elasticity with discrete structural changes that underlie many open problems in virology and molecular biology.

Remark 1.32 (Discrete vs. Continuous Phonon Modes). In many physical or numerical settings, the infinite-dimensional space $L^2(\Omega)$ is approximated by a *finite* or *countably infinite* set of modes. This approach arises naturally in *spectral Galerkin* or *finite-element* discretizations, where one retains only a truncated basis of eigenfunctions or mesh functions. From a physical standpoint (see, *e.g.*, [1, 8]), higher-frequency modes may be negligible or lie outside the relevant bandwidth, so a *discrete* truncation of the continuum fields suffices to capture key physics. Concretely, one replaces

$$[L^2(\Omega)]^d \mapsto \text{span}\{\varphi_1, \dots, \varphi_N\} \simeq \mathbb{C}^N, \quad (1.93)$$

where $\{\varphi_j\}_{j=1}^N$ is a set of low-frequency modes or finite elements in $\Omega \subset \mathbb{R}^d$. This drastically reduces complexity while preserving the essential vibrational phenomena. Mathematically, one interprets this as projecting $L^2(\Omega)$ onto a finite-dimensional subspace. As $N \rightarrow \infty$, the truncated solutions converge to the full continuum theory under appropriate norm convergence [20].

Remark 1.33 (Boundary Conditions and m -Sectoriality). If the domain Ω is equipped with damped wave boundary conditions (Dirichlet, Neumann, Robin, or mixed) and the real part of the damping parameter $\eta_R > 0$ enforces energy dissipation, then classical semigroup theory yields a *contractive* C_0 -semigroup on the underlying Hilbert space [36, 37]. Even if $\eta_I \neq 0$ introduces additional *complex* damping or stiffness (thus making the operator non-self-adjoint), the system can remain *m -sectorial*, ensuring unique solvability and continuous dependence on initial data. These results follow from standard PDE and functional-analytic approaches (via Lumer–Phillips or Hille–Yosida theorems); see [32, 37] for extensive treatments. Physically, m -sectoriality guarantees that the damped wave/elastic system generates a strongly continuous semigroup whose growth is controlled by the real part of the spectrum.

Definition 1.34 (Viral Lattice State: Single-Lattice Version). *Viral lattice theory* aims to encode both the *large-scale conformation* of a virion (discrete macro-arrangements or capsid states) and the *fine-scale vibrational dynamics* (PDE or phonon fields). Building on Theorem 1.30, we define a *single viral lattice state* to be any element

$$|\Psi_{\text{lat}}\rangle \in \mathcal{H}_{\text{lat}} = \left(\bigoplus_{f \in \mathcal{F}} \mathbb{C} |f\rangle \right) \otimes \left([L^2(\Omega)]^d \times [L^2(\Omega)]^d \right), \quad (1.94)$$

where:

1. $\{|f\rangle : f \in \mathcal{F}\}$ is an orthonormal basis for the *macro-arrangement space* (possibly finite or countably infinite), representing discrete viral conformations (*e.g.*, folded/unfolded states, capsid expansions, or other large-scale structural variations).

2. $[L^2(\Omega)]^d \times [L^2(\Omega)]^d$ captures the real-imaginary decomposition $(\mathbf{u}_R, \mathbf{u}_I)$ of continuum displacements describing vibrational or phonon-like modes. These fields evolve under a PDE semigroup $\{e^{t\hat{\mathcal{G}}}\}_{t \geq 0}$ stemming from a damped wave or elastic system (potentially non-self-adjoint).
3. The label f may remain *fixed* or transition among $\{|f\rangle\}$ via an operator $\hat{\mathcal{T}}$, reflecting large-scale conformational jumps in the virus.

Together, these ingredients provide a *unified functional-analytic* representation for both discrete viral conformations and continuum phonon-like vibrations within a single lattice model.

Proof of Construction. Consider the set \mathcal{F} of viral *macro-arrangements*. Each $f \in \mathcal{F}$ denotes a particular capsid or genomic conformation. Form the finite or countably infinite span

$$\mathcal{H}_{\text{arr}} = \text{span}\{|f\rangle : f \in \mathcal{F}\}, \quad (1.95)$$

with the inner product $\langle |f\rangle, |f'\rangle \rangle_{\text{arr}} = \delta_{f,f'}$. If \mathcal{F} is infinite, completing this span yields a separable Hilbert space akin to $\ell^2(\mathcal{F})$. Each basis vector $|f\rangle$ identifies one macro-arrangement of the virus. Next, define the continuum-displacement space

$$\mathcal{H}_{\text{disp}} = [L^2(\Omega)]^d \times [L^2(\Omega)]^d, \quad (1.96)$$

whose elements are pairs $(\mathbf{u}_R, \mathbf{u}_I)$ representing real and imaginary parts of the viral displacement field (e.g., in a damped wave or elastic PDE context). An appropriate inner product on $\mathcal{H}_{\text{disp}}$ is

$$\langle (\mathbf{u}_R, \mathbf{u}_I), (\mathbf{v}_R, \mathbf{v}_I) \rangle_{\text{disp}} = \int_{\Omega} [\mathbf{u}_R(\mathbf{x}) \cdot \mathbf{v}_R(\mathbf{x}) + \mathbf{u}_I(\mathbf{x}) \cdot \mathbf{v}_I(\mathbf{x})] d\mathbf{x}. \quad (1.97)$$

Completing this space yields a Hilbert space of vibrational fields [37]. The *single-lattice state space* is then the Hilbert-space tensor product

$$\mathcal{H}_{\text{lat}} = \mathcal{H}_{\text{arr}} \otimes \mathcal{H}_{\text{disp}}, \quad (1.98)$$

whose generic element is a finite or countable sum of simple tensors,

$$\sum_{f \in \mathcal{F}} |f\rangle \otimes (\mathbf{u}_R^{(f)}, \mathbf{u}_I^{(f)}). \quad (1.99)$$

Completeness follows from standard Hilbert-space tensor product theory [23]. This space encodes both the discrete macro-arrangement label f and the continuous fields $(\mathbf{u}_R, \mathbf{u}_I)$ describing phonon-like excitations. If the PDE for $(\mathbf{u}_R, \mathbf{u}_I)$ generates a semigroup $e^{t\hat{\mathcal{G}}}$ on $\mathcal{H}_{\text{disp}}$ and the macro-arrangement f transitions among $\{|f\rangle\}$ via some discrete operator $\hat{\mathcal{T}}$, one defines the *total generator* on \mathcal{H}_{lat} by

$$\hat{\mathcal{G}}_{\text{total}} = \hat{\mathcal{G}} \otimes I_{\text{arr}} + I_{\text{disp}} \otimes \hat{\mathcal{T}}, \quad (1.100)$$

where I_{arr} and I_{disp} are identity operators on the respective spaces. Under mild conditions (e.g., dissipative structure, elliptic regularity, bounded Markov transition rates), $\hat{\mathcal{G}}_{\text{total}}$ is *m-sectorial* or at least generates a strongly continuous semigroup on \mathcal{H}_{lat} . Each initial viral lattice state

$$\Psi_{\text{lat}}(0) = \sum_{f \in \mathcal{F}} |f\rangle \otimes (\mathbf{u}_R^{(f)}(\cdot, 0), \mathbf{u}_I^{(f)}(\cdot, 0)) \quad (1.101)$$

then evolves uniquely in time, reflecting both continuous PDE dynamics and discrete arrangement changes. Thus, \mathcal{H}_{lat} furnishes a *complete* representation of *single viral lattice states* that couples finite or countably many macro-arrangements to the underlying phonon-like vibrational field, culminating in a flexible functional-analytic framework for viral lattice theory. \square

Role of Mass Bands and Microstates. In many viral-lattice formulations, one further subdivides the arrangement space \mathcal{H}_{arr} by introducing *mass bands* (labeled m_k) or other internal parameters. Orthogonal direct sums (or tensor products) are then taken as needed, thereby capturing additional structural detail such as capsid expansions, partial genome packaging, and other intermediate conformational states. Consistent with Remark 1.32, one can reduce computational complexity by truncating the vibrational fields $(\mathbf{u}_R, \mathbf{u}_I)$ to a finite set of “dominant” eigenmodes, with convergence to the full continuum model in the $N \rightarrow \infty$ limit. As noted in Remark 1.33, suitable boundary conditions and positive damping ensure well-posedness and, typically, a contractive or *sectorially* dissipative semigroup evolution. Even if the system is non-self-adjoint (*e.g.*, due to complex damping), the Lumer–Phillips theorem guarantees the existence and uniqueness of solutions.

This unified construction treats the infinite family of lattices on an equal footing as *many-body excitations*, with a mass (band) index k appearing as an internal label. The same second-quantized framework applies to creating or annihilating a lattice in any band. Hence, one may accommodate various internal states (arrangements, phonon modes, mass bands) via direct sums or tensor products, without losing canonical creation/annihilation operators or the usual theorems (see [13, 37]) ensuring a well-defined Fock-space representation. All four steps thereby embed the single-lattice Hilbert space \mathcal{H}_{lat} into a fully functional second-quantized setting. The resulting direct-sum structure and tensor-product formulation keep each mass band distinct, yet allow for an *unbounded* population of lattices in each sector, matching the biological perspective of arbitrarily many viral capsids in diverse structural or vibrational states. Viral capsids frequently occupy different mass or packaging levels (*e.g.*, partially packaged, fully packaged, or disassembled). The second-quantized formalism described here does *not* require all capsids to share the same band or arrangement. Instead, one models transitions among these states dynamically, consistent with observed heterogeneity in viral populations [39].

2 Second Quantization: Many-Lattice Operator on $\mathcal{F}_{\pm}(\mathcal{H}_{\text{lat}})$

In the preceding sections, we introduced a single-lattice operator $\hat{\mathcal{G}}$, which could be non-self-adjoint or m -sectorial, acting on the Hilbert space \mathcal{H}_{lat} . This setting models the continuum fields (and possibly discrete arrangement labels) for *one* viral lattice or capsid. However, viral systems often feature *many* such lattices (or capsids) simultaneously, especially within a single host cell [2, 8]. For instance, multiple virions may co-exist, replicate, or degrade, each described by the single-lattice space \mathcal{H}_{lat} . In real virology contexts, multiple capsids can assemble, disassemble, or co-exist in a cell, with each capsid undergoing local PDE-type motions (elastic/vibrational modes) and discrete arrangement changes. Second quantization offers a powerful means to incorporate *replication* (creation of new virions) or *degradation* (annihilation) if desired, mirroring standard QFT treatments where particle number is not fixed [26]. The resulting many-lattice operator $\hat{\mathcal{G}}_{\text{tot}}$ then describes the collective evolution of an arbitrary number M of viral lattices. This is especially relevant for modeling infection dynamics, capsid–capsid interactions, or the statistical properties of viral populations under host constraints.

To account for an *unbounded number* of viral lattices, we embed $\hat{\mathcal{G}}$ into an operator $\hat{\mathcal{G}}_{\text{tot}}$ on the bosonic or fermionic Fock space

$$\mathcal{F}_{\pm}(\mathcal{H}_{\text{lat}}) = \bigoplus_{M=0}^{\infty} \left(\mathcal{H}_{\text{lat}}^{\otimes M} \right)_{\pm}, \quad (2.1)$$

where “ \pm ” denotes symmetric (bosonic) or antisymmetric (fermionic) tensor product structures.

This approach is analogous to standard many-body quantum mechanics (e.g. describing photons, electrons), but here the “particles” are entire *viral lattices*, each with its own arrangement degrees of freedom, PDE modes, or resource-limited replication processes. Such a second-quantized framework allows us to unify the dynamics of possibly large (or unbounded) numbers of capsids under one operator-theoretic umbrella.

Definition 2.1 ($\hat{\mathcal{G}}_{\text{tot}}$ in Fock Space). Let $M \geq 1$ be an integer denoting the number of lattices (or “particles” in the Fock analogy). The M -lattice sector of the Fock space is

$$\left(\mathcal{H}_{\text{lat}}^{\otimes M}\right)_{\pm}, \quad (2.2)$$

the (\pm) -symmetrized M -fold tensor product of \mathcal{H}_{lat} . On this sector, define

$$\hat{\mathcal{G}}^{(M)} := \sum_{j=1}^M \left(I \otimes \cdots \otimes I \right) \otimes \underbrace{\hat{\mathcal{G}}}_{\text{acts on the } j\text{-th factor}} \otimes \left(I \otimes \cdots \otimes I \right), \quad (2.3)$$

meaning $\hat{\mathcal{G}}$ acts nontrivially on exactly one factor and as the identity on the remaining $M-1$ factors. Summing over j ensures $\hat{\mathcal{G}}$ can act on *any* of the M lattices. For the vacuum sector ($M=0$), we set $\hat{\mathcal{G}}^{(0)} := 0$.

The *second-quantized (many-lattice) operator* is then the direct sum over all M :

$$\hat{\mathcal{G}}_{\text{tot}} = \bigoplus_{M=0}^{\infty} \hat{\mathcal{G}}^{(M)} \quad \text{on } \mathcal{F}_{\pm}(\mathcal{H}_{\text{lat}}). \quad (2.4)$$

By construction, $\hat{\mathcal{G}}_{\text{tot}}$ governs the collective evolution of an *arbitrary* number of lattices, each evolving under the single-lattice operator $\hat{\mathcal{G}}$. If $\hat{\mathcal{G}}$ is m -sectorial or non-self-adjoint, the operator $\hat{\mathcal{G}}_{\text{tot}}$ inherits an analogous sectorial structure (as elaborated below) [26, 30].

Biophysical Extensions and Applications.

- *Multiple Capsids in a Single Cell*: This formalism captures how M distinct viral lattices, each described by continuum PDE fields and arrangement labels, can co-exist. $\hat{\mathcal{G}}^{(M)}$ ensures each lattice is governed by the same single-lattice dynamics, but now we sum over all possible lattices [2, 5].
- *Inter-lattice Interactions*: Although (2.3) describes non-interacting lattices (each factor evolves under $\hat{\mathcal{G}}$ independently), interactions can be introduced via cross-terms in the sum. For instance, adding a potential \hat{V}_{ij} that couples the i th and j th lattices can model capsid–capsid steric effects or cooperative assembly [8].
- *Creation/Annihilation of Lattices*: If one wishes to incorporate replication (creation operators) or degradation (annihilation operators) of viral capsids, one extends the second-quantized operator with additional bosonic or fermionic terms. This allows resource-driven processes to reflect how the total number of virions changes over time, mirroring standard QFT treatments of variable particle number [31].

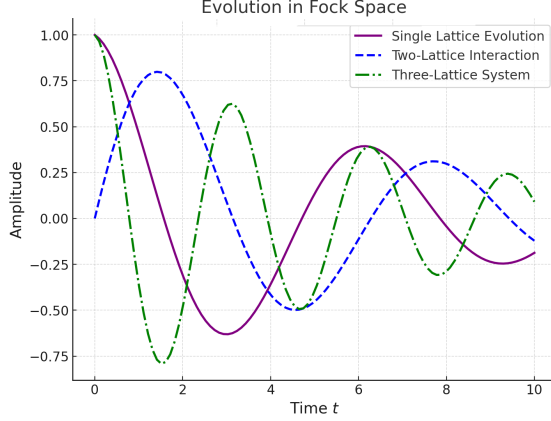


Figure 3: **Multi-Lattice Evolution in Fock Space.** Three example trajectories are shown: a single-lattice PDE solution (solid purple), a two-lattice interacting system (dashed blue), and a three-lattice configuration (dash-dot green). Each curve represents the time evolution of a representative amplitude (e.g., a principal deformation mode), illustrating how additional lattices in the second-quantized framework lead to richer coupled dynamics. In particular, the two- and three-lattice trajectories exhibit phase shifts and amplitude modulation, reflecting inter-lattice interactions and resource competition at the population level. These simulations underscore the unbounded occupancy principle of Fock space, while maintaining m -sectorial properties that ensure physically meaningful boundedness and well-posedness.

Theorem 2.2 (The Many-Lattice Schrödinger-like Equation, and its Inherited Sectorial Structure.). *The resulting many-lattice dynamics satisfy a Schrödinger-type equation (or a more general semigroup evolution if $\hat{\mathcal{G}}$ is dissipative):*

$$\partial_t \Psi_{\text{tot}}(t) = \hat{\mathcal{G}}_{\text{tot}} \Psi_{\text{tot}}(t), \quad \Psi_{\text{tot}}(t) \in \mathcal{F}_{\pm}(\mathcal{H}_{\text{lat}}). \quad (2.5)$$

In the bosonic (symmetric) sector, one can interpret $\Psi_{\text{tot}}(t)$ as an L^2 function of M indistinguishable lattices, each with PDE or arrangement dof (degrees of freedom). In the fermionic (antisymmetric) sector, one imposes an exclusion principle (though less common biologically for viral capsids, it may be formally included if required by steric or biochemical constraints). If the single-lattice operator $\hat{\mathcal{G}}$ is m -sectorial (maximal dissipative), then $\hat{\mathcal{G}}^{(M)}$ is also m -sectorial on the M -lattice sector, and their direct sum $\hat{\mathcal{G}}_{\text{tot}}$ maintains sectorial bounds [26]. As a result, it generates a strongly continuous semigroup $e^{t\hat{\mathcal{G}}_{\text{tot}}}$ on $\mathcal{F}_{\pm}(\mathcal{H}_{\text{lat}})$, guaranteeing well-posedness of the many-lattice evolution.

Proof of Sectorial Extension to Fock Space. Let $\hat{\mathcal{G}}$ be m -sectorial (or maximal dissipative) on \mathcal{H}_{lat} . We claim that the second-quantized operator $\hat{\mathcal{G}}_{\text{tot}}$ (Definition 2.1) is also m -sectorial on

$$\mathcal{F}_{\pm}(\mathcal{H}_{\text{lat}}). \quad (2.6)$$

Consequently, it generates a strongly continuous semigroup

$$\{ e^{-it\hat{\mathcal{G}}_{\text{tot}}} \}_{t \geq 0}, \quad (2.7)$$

which is generally non-unitary due to dissipation.

Step 1: First, we need to show dissipativity on each M -lattice sector. Since $\hat{\mathcal{G}}$ is dissipative on \mathcal{H}_{lat} , there exists a constant $\gamma \geq 0$ such that

$$\text{Re} \langle \hat{\mathcal{G}} \psi, \psi \rangle \leq -\gamma \|\psi\|^2 \quad \text{for all } \psi \in D(\hat{\mathcal{G}}). \quad (2.8)$$

Note: For consistency with standard notational conventions, we reuse certain variables in this proof. Specifically, the parameter (γ) appearing here does not correspond to the interaction potential for local virions. On the M -lattice sector $(\mathcal{H}_{\text{lat}}^{\otimes M})_{\pm}$, the induced operator is

$$\hat{\mathcal{G}}^{(M)} = \sum_{j=1}^M I \otimes \cdots \otimes \hat{\mathcal{G}} \otimes \cdots \otimes I, \quad (2.9)$$

so for any $\Phi \in D(\hat{\mathcal{G}}^{(M)})$,

$$\text{Re} \langle \hat{\mathcal{G}}^{(M)} \Phi, \Phi \rangle = \sum_{j=1}^M \text{Re} \langle \hat{\mathcal{G}} \Phi_j, \Phi_j \rangle, \quad (2.10)$$

where each Φ_j denotes the partial “slice” of Φ in which $\hat{\mathcal{G}}$ acts on the j th factor. Since each inner product satisfies

$$\text{Re} \langle \hat{\mathcal{G}} \Phi_j, \Phi_j \rangle \leq -\gamma \|\Phi_j\|^2, \quad (2.11)$$

summing yields

$$\text{Re} \langle \hat{\mathcal{G}}^{(M)} \Phi, \Phi \rangle \leq -\gamma \sum_{j=1}^M \|\Phi_j\|^2 \leq -\gamma \|\Phi\|^2. \quad (2.12)$$

Thus each $\hat{\mathcal{G}}^{(M)}$ is dissipative on the M -particle sector, and the same inequality extends to the direct-sum Fock space $\bigoplus_{M=0}^{\infty} (\mathcal{H}_{\text{lat}}^{\otimes M})_{\pm}$.

Step 2: Next, we need to show that $\hat{\mathcal{G}}_{\text{tot}} = \bigoplus_{M=0}^{\infty} \hat{\mathcal{G}}^{(M)}$ is *maximal* (or *m-sectorial*), one verifies that $I - \hat{\mathcal{G}}_{\text{tot}}$ has dense range or is surjective in $\mathcal{F}_{\pm}(\mathcal{H}_{\text{lat}})$. Classical results on tensor-product operators (see *e.g.*, [32, Ch. X] or [26, Vol. 2]) guarantee that if $\hat{\mathcal{G}}$ is maximal dissipative on \mathcal{H}_{lat} , then $\hat{\mathcal{G}}_{\text{tot}}$ is maximal dissipative on the direct sum of symmetrized M -fold tensor products. In essence, one solves

$$(I - \hat{\mathcal{G}}_{\text{tot}}) \Phi = \Theta \quad (2.13)$$

sector by sector (for each M) using the resolvent $(I - \hat{\mathcal{G}})^{-1}$ on the single-lattice factor.

Step 3: By the Lumer–Phillips theorem, any *m-sectorial* operator on a Hilbert space generates a strongly continuous semigroup of contractions (or quasi-contractions). Therefore, $\hat{\mathcal{G}}_{\text{tot}}$ generates

$$e^{-it\hat{\mathcal{G}}_{\text{tot}}} \quad (t \geq 0), \quad (2.14)$$

which is in general *non-unitary* if $\text{Re} \langle \hat{\mathcal{G}}\psi, \psi \rangle < 0$. Thus the *m-sectorial* extension to Fock space ensures well-posed *many-lattice* dynamics. $\mathcal{F}_{\pm}(\mathcal{H}_{\text{lat}})$ encodes an *arbitrary* number of viral capsids (lattices), each with PDE-type displacement fields and possibly discrete arrangement labels. The operator $\hat{\mathcal{G}}$ describes the elastic/damped evolution of a single capsid (plus conformation states). In many-capsid infections, replication or degradation processes might cause the number of capsids to vary over time. An *m-sectorial* operator typically reflects resource dissipation, boundary damping, or other physical constraints ensuring that the evolution does not blow up in finite time but instead remains stable [2, 8]. This sectorial extension to Fock space then captures *non-equilibrium* viral ensembles where multiple capsids coexist and undergo PDE-based shape fluctuations, Markov transitions, or interactions, each factor evolving under the same single-lattice rules.

Therefore, $\hat{\mathcal{G}}_{\text{tot}}$ is *m-sectorial* on $\mathcal{F}_{\pm}(\mathcal{H}_{\text{lat}})$ and generates a strongly continuous semigroup $\{e^{-it\hat{\mathcal{G}}_{\text{tot}}}\}_{t \geq 0}$. A many-lattice state

$$|\Psi(t)\rangle \in \mathcal{F}_{\pm}(\mathcal{H}_{\text{lat}}) \quad (2.15)$$

thus evolves via the (non-unitary) semigroup, reflecting dissipative or driven dynamics for an unbounded number of viral capsids. The overall model—rooted in PDE elasticity, arrangement labels, and sectorial operator theory—can describe diverse virological phenomena where multiple viral lattices replicate, degrade, or interact under resource-limited, host-mediated conditions. \square

Theorem 2.3 (Well-Posedness in Many-Lattice Fock Space). *Let $\hat{\mathcal{G}}_{\text{tot}}$ be m -sectorial on $\mathcal{F}_{\pm}(\mathcal{H}_{\text{lat}})$. For each initial condition $|\Psi_0\rangle \in D(\hat{\mathcal{G}}_{\text{tot}})$ and each forcing $|\Phi(t)\rangle$ in a suitable Bochner-integrable class, there is a unique mild solution*

$$|\Psi(t)\rangle = e^{-it\hat{\mathcal{G}}_{\text{tot}}} |\Psi_0\rangle + \int_0^t e^{-i(t-s)\hat{\mathcal{G}}_{\text{tot}}} |\Phi(s)\rangle ds, \quad (2.16)$$

such that $|\Psi(t)\rangle \in \mathcal{F}_{\pm}(\mathcal{H}_{\text{lat}})$ for all $t \geq 0$. Moreover, if $|\Phi\rangle \equiv 0$ (i.e. no external forcing) and the dissipativity constant of $\hat{\mathcal{G}}_{\text{tot}}$ is strictly positive ($\gamma > 0$), then $\|\Psi(t)\|$ is non-increasing in time, reflecting the decay or “leakage” typical of dissipative processes.

Sketch of Proof. By the Lumer–Phillips theorem (or Hille–Yosida criteria for m -sectorial operators), an m -sectorial operator on a Hilbert space generates a strongly continuous contraction (or quasi-contraction) semigroup [32, 37]. Thus,

$$e^{-it\hat{\mathcal{G}}_{\text{tot}}} \quad (t \geq 0) \quad (2.17)$$

is well-defined on $\mathcal{F}_{\pm}(\mathcal{H}_{\text{lat}})$, and satisfies the usual properties of existence, uniqueness, and continuous dependence on initial data in the mild solution sense (2.16). If $\hat{\Phi}(t)$ is Bochner-integrable, one incorporates it through the standard variation of parameters formula, ensuring a unique solution in $C([0, T], \mathcal{F}_{\pm}(\mathcal{H}_{\text{lat}}))$.

When $\gamma > 0$, the semigroup is strictly contractive in norm. In particular,

$$\text{Re} \langle \hat{\mathcal{G}}_{\text{tot}} \Psi, \Psi \rangle \leq -\gamma \|\Psi\|^2, \quad (2.18)$$

guaranteeing that $\|\Psi(t)\|^2$ decays in time. Physically, this enforces damped or resource-limited dynamics among an unbounded number of viral lattices, ensuring stability and no finite-time blow-up. Thus the system is well-posed and remains bounded, capturing the dissipative character of real non-equilibrium processes in which viral capsids may gradually lose energy or degrade in the host environment [2, 8]. \square

Remark 2.4 (Creation and Annihilation of Viral Lattices). In more *generalized* viral replication models, one augments $\hat{\mathcal{G}}_{\text{tot}}$ with *creation* and *annihilation* operators ($\hat{a}^\dagger(\alpha)$, $\hat{a}(\alpha)$) that couple the M -lattice and $(M \pm 1)$ -lattice subspaces of $\mathcal{F}_{\pm}(\mathcal{H}_{\text{lat}})$. Physically:

- $\hat{a}^\dagger(\alpha)$ might model *viral replication*, creating a new lattice (labeled by “internal” quantum data α , e.g., conformation, mass band, or arrangement state).
- $\hat{a}(\alpha)$ might model *viral decay or release*, removing a lattice from the system (e.g. upon degradation or exit).

The total generator $\hat{\mathcal{G}}_{\text{tot}}$ then acquires off-diagonal block terms coupling the M -particle to $(M \pm 1)$ -particle Fock sectors, capturing *birth/death* processes for viral capsids [16, 26]. In such cases, one can still verify m -sectoriality using standard second-quantization criteria [32], as long as the transition rates align with dissipativity bounds (e.g. ensuring no explosive replication in finite time under resource limitations). Consequently, the semigroup remains well-posed and describes how the number of viral lattices dynamically changes through replication or clearance in a biophysically realistic manner.

Theorem 2.5 (Guaranteeing Well-Posedness). *The well-posedness theorem guarantees that, given any initial population of viral lattices and continuum fields, the many-body dynamics under $\hat{\mathcal{G}}_{\text{tot}}$ evolve uniquely over time. This covers a range of realistic scenarios:*

1. Multiple Capsid Assemblies in a Cell: *Each lattice may have distinct PDE wave modes, arrangement states, or resource constraints, yet remain governed by the same fundamental operator $\hat{\mathcal{G}}$. The m -sectorial property enforces damped or stable evolution of each subunit's vibration, paralleling experimental observations of partial disassembly or post-translational modifications [8, 40].*
2. Viral Replication and Clearance: *Creation/annihilation extensions capture how new capsids form (when viral polymerase and host resources allow) and how existing capsids degrade or exit the cell. Mathematically, this ensures the total system remains finite or well-controlled, reflecting biological constraints of finite resource availability [16].*
3. Energy Dissipation and Non-Equilibrium Steady States: *Positive damping constants ($\gamma > 0$) imply that each lattice's amplitude cannot grow unboundedly without external energy input. This aligns with the classical picture of viruses requiring host ATP or nutrients for large-scale rearrangements or replication, reinforcing the notion of non-equilibrium flux loops in resource-driven settings [28].*

Thus, the well-posedness result in Theorem 2.3 provides a mathematically rigorous basis for exploring multi-capsid, PDE–Markov–Fock models of viral dynamics, anchoring them in established operator theory while connecting to real virological phenomena observed in advanced imaging and biochemical assays [2, 21].

2.1 Purely Formal Model vs. Resource Constraints: An Operator-Theoretic Resolution

Is There a Mathematical Limit to the Number of Viral Lattices?

As noted above, the *formal* Fock-space construction can, in principle, accommodate infinitely many viral lattices, much like an unbounded photon or phonon population in quantum optics [13,14]. However, real virological systems typically exhibit *finite* replication capacity due to resource constraints, immune responses, and other biological feedback mechanisms [10,41]. The following section refines the operator-theoretic model to reconcile unbounded mathematical occupancy with physical resource limitations. In an unconstrained Fock-space approach to viral replication, one might write the total generator (or Hamiltonian) in a fashion analogous to standard many-body quantum theory:

$$\hat{\mathcal{H}}_{\text{tot}} = \hat{\mathcal{H}}_{\text{free}} + \hat{\mathcal{H}}_{\text{int}}, \quad (2.19)$$

where linear or bilinear creation operators appear, for example:

$$\Gamma(\hat{a}^\dagger(y)\hat{a}^\dagger(z)), \quad (2.20)$$

mirroring bosonic field interactions in quantum many-body theory [13,14]. Such a bare-bones formulation omits the crucial *biological fact* that resources are finite in real infections. Without additional constraints, purely linear or bilinear creation terms allow, in principle, *unbounded* increases in virion number ($M \rightarrow \infty$). To reconcile this with experimental reality, one introduces an *effective resource function* to damp creation at large occupancy. This yields a more biologically grounded, yet mathematically coherent, second-quantized model [10,41].

Theorem 2.6 (A Resource Function in Fock Space). Let \hat{N} be the number operator on the Fock space $\mathcal{F}_\pm(\mathcal{H}_{\text{lat}})$,

$$\hat{N} = \sum_{M=0}^{\infty} M \mathbf{P}_M, \quad (2.21)$$

where \mathbf{P}_M projects onto the M -lattice subspace. Suppose $\mathcal{R}: \mathbb{R}_{\geq 0} \rightarrow \mathbb{R}_{\geq 0}$ is a nonincreasing function satisfying $\lim_{x \rightarrow \infty} \mathcal{R}(x) = 0$ and $\mathcal{R}(0) > 0$. Define the modified creation operator

$$\hat{\Gamma}_+(y) = \hat{a}^\dagger(y) \mathcal{R}(\hat{N}), \quad (2.22)$$

using functional calculus; for instance, one may take

$$\mathcal{R}(\hat{N}) = \frac{1}{1 + \mu \hat{N}}, \quad \mu > 0, \quad (2.23)$$

so as to penalize replication at large \hat{N} . Then, under standard m -sectorial or dissipative conditions on the total generator, the expected lattice number $\langle \hat{N} \rangle$ remains finite for all finite t , precluding unbounded growth in the particle population. The operator \hat{N} counts the total viral lattice occupancy in Fock space, while $\mathcal{R}(\hat{N})$ is a decreasing function that saturates to zero as $\hat{N} \rightarrow \infty$. This modification ensures that creation processes slow or even halt when M becomes large, thereby reflecting the finite pools of capsid proteins, nucleotides, and other host factors available during infection [41]. Standard arguments in second-quantization theory [26, 32] then show that the damped creation operators $\hat{\Gamma}_+(y)$ cannot lead to exponential proliferation of \hat{N} , as the effective replication amplitude diminishes with occupancy. The combined effect of m -sectorial PDE dynamics and saturable creation terms preserves both well-posedness and boundedness of $\langle \hat{N} \rangle$.

Remark 2.7 (Virological Interpretation). In biological systems, saturable creation operators capture the phenomenon of resource depletion: as a viral load increases, the limited availability of capsid proteins, nucleotides, and host machinery imposes a natural cap on replication [2]. Additionally, immune clearance further restricts viral expansion. Thus, while the formal Fock-space construction admits the possibility of infinite replication, the introduction of a resource function $\mathcal{R}(\hat{N})$ introduces negative feedback that ensures a realistic, finite virion population. This aligns with experimental observations where viral replication saturates due to host limitations, even if mathematically unbounded growth is permitted in an idealized model. Nonlinear or saturable modifications to the creation operator capture the essential *negative feedback* required to reflect finite resource constraints in real infections. These refinements reconcile the formal mathematical possibility of infinite lattice occupancy in Fock space with the experimentally verified phenomenon of saturable viral replication. The resulting framework provides a robust foundation for multi-scale PDE–Fock models of viral dynamics, demonstrating how non-equilibrium replication, limited host resources, and immune responses merge into a comprehensive operator-algebraic description.

Proof of Resource-Constrained Creation. By the spectral theorem for self-adjoint operators [14, 23], the number operator \hat{N} on the Fock space $\mathcal{F}_\pm(\mathcal{H}_{\text{lat}})$ has discrete spectrum $\{0, 1, 2, \dots\}$ on each M -particle subspace. A continuous, nonincreasing function $\mathcal{R}: \mathbb{R}_{\geq 0} \rightarrow \mathbb{R}_{\geq 0}$ with $\lim_{x \rightarrow \infty} \mathcal{R}(x) = 0$ and $\mathcal{R}(0) > 0$ induces a bounded operator

$$\mathcal{R}(\hat{N}) = \sum_{M=0}^{\infty} \mathcal{R}(M) \mathbf{P}_M, \quad (2.24)$$

where \mathbf{P}_M is the projection onto the M -lattice sector. Since $\mathcal{R}(x)$ achieves its maximum at $x = 0$ (with $\mathcal{R}(0) > 0$) and tends to 0 at large x , $\|\mathcal{R}(\hat{N})\| \leq C$ for some $C > 0$. Thus, the modified creation operator

$$\hat{\Gamma}_+(y) = \hat{a}^\dagger(y) \mathcal{R}(\hat{N}) \quad (2.25)$$

is well-defined on a dense domain in $\mathcal{F}_\pm(\mathcal{H}_{\text{lat}})$, since $\|\hat{a}^\dagger(y) \mathcal{R}(\hat{N})\| \leq C \|\hat{a}^\dagger(y)\|$.

Let $\hat{\mathcal{G}}_{\text{free}}$ be the baseline generator (which may include dissipative PDE terms, damping, etc.) for the single-lattice viral system. Assume $\hat{\mathcal{G}}_{\text{free}}$ is m -sectorial on $\mathcal{F}_\pm(\mathcal{H}_{\text{lat}})$ [14, 42]. We then form a total generator

$$\hat{\mathcal{G}}_{\text{tot}} = \hat{\mathcal{G}}_{\text{free}} + \hat{\Gamma}_+(y) + \hat{\Gamma}_-(z), \quad (2.26)$$

where $\hat{\Gamma}_-(z)$ may represent annihilation or other interaction processes. Since $\|\hat{\Gamma}_+(y)\| \leq \|\hat{a}^\dagger(y)\| \cdot C$, the operator sum of $\hat{\Gamma}_+(y)$ with $\hat{\mathcal{G}}_{\text{free}}$ preserves sectorial bounds, ensuring that $\hat{\mathcal{G}}_{\text{tot}}$ remains m -sectorial if the coupling is sufficiently small (or quasi-accretive) [10, 14].

Because \hat{N} is diagonalizable with eigenvalues $M = 0, 1, 2, \dots$, it follows that

$$\mathcal{R}(M) \longrightarrow 0 \quad \text{as } M \rightarrow \infty. \quad (2.27)$$

Hence, for large M , the creation amplitude $\hat{\Gamma}_+(y)$ becomes arbitrarily small, imposing a *de facto* cap on replication. One formal proof approach is to *truncate* the Fock space to $M \leq M_{\text{max}}$, show that the truncated generator is m -sectorial with bounded population, and then let $M_{\text{max}} \rightarrow \infty$ to recover the full space while preserving well-posedness of the limiting semigroup [32].

In the Heisenberg picture, the number operator evolves according to

$$\frac{d}{dt} \hat{N}(t) = [\hat{N}, \hat{\mathcal{G}}_{\text{tot}}] + (\partial_t \hat{N})_{\text{explicit}}, \quad (2.28)$$

with $\hat{\mathcal{G}}_{\text{tot}} = \hat{\mathcal{G}}_{\text{free}} + \hat{\Gamma}_+(y) + \dots$. Since

$$[\hat{N}, \hat{\Gamma}_+(y)] = [\hat{N}, \hat{a}^\dagger(y) \mathcal{R}(\hat{N})] \quad (2.29)$$

is bounded above by terms proportional to $\mathcal{R}(\hat{N})$ (which vanishes as $M \rightarrow \infty$), one concludes that $\langle \hat{N}(t) \rangle$ cannot explode to infinity in finite time. Thus, the system evades unbounded exponential proliferation of viral lattices.

The resource-constrained creation mechanism (2.22) encapsulates a central tenet of viral biophysics: although the abstract Fock-space formalism permits an unbounded number of viral lattices (analogous to the unlimited photon or phonon populations in quantum optics [13, 14]), real viral replication is inherently limited by finite host resources. In vivo, viral propagation is curtailed by restricted availability of capsid proteins, nucleotides, and metabolic energy, as well as by active immune clearance. As the number of virions increases, replication saturates in a manner reminiscent of logistic growth or Michaelis–Menten kinetics [43, 44], and the effective creation amplitude diminishes.

In our theoretical biophysics framework, the operator $\mathcal{R}(\hat{N})$ —a nonincreasing function with $\lim_{x \rightarrow \infty} \mathcal{R}(x) = 0$ —is introduced to modulate the creation operator. This modification enforces a negative feedback loop at high occupancy levels, thereby ensuring that the expected viral lattice number $\langle \hat{N} \rangle$ remains finite for all finite times. Such saturable behavior is crucial not only for mathematical well-posedness but also for faithfully representing the biological limitations imposed by host cell resources and immune responses [2, 8].

Moreover, the model allows further refinement: spatial heterogeneity in resource availability, immune-mediated clearance, and latent phases can be integrated by letting the resource function depend on additional variables (e.g., space or time) or by incorporating additional damping operators. In this way, the operator-theoretic framework captures both the idealized quantum-mechanical limits and the rich, nonlinear feedback mechanisms observed in viral replication dynamics. This synthesis of operator theory with modern virological insights lays the groundwork for multi-scale PDE–Fock models that accurately describe non-equilibrium viral replication and the dynamic interplay between viral propagation and host-imposed resource limitations. \square

1. **Host Resource Modeling via $\mathcal{R}(\hat{N})$.** Let \hat{N} be the number operator on the Fock space $\mathcal{F}_{\pm}(\mathcal{H}_{\text{lat}})$. By the spectral theorem for self-adjoint operators, its spectrum in each M -lattice sector is $\text{Spec}(\hat{N}) = \{0, 1, 2, \dots\}$. A nonincreasing function $\mathcal{R}: \mathbb{R}_{\geq 0} \rightarrow \mathbb{R}_{\geq 0}$ then lifts to an operator $\mathcal{R}(\hat{N})$ via

$$\mathcal{R}(\hat{N}) \Psi = \sum_{M=0}^{\infty} \mathcal{R}(M) \Psi^{(M)}, \quad (2.30)$$

where $\Psi^{(M)}$ denotes the M -particle (or M -lattice) component of $\Psi \in \mathcal{F}_{\pm}(\mathcal{H}_{\text{lat}})$. This construction ensures that, as the occupancy increases, the operator $\mathcal{R}(\hat{N})$ dampens the effective creation amplitude, thus enforcing a reduced capacity for further replication.

Two prototypical forms for $\mathcal{R}(x)$ are:

- *Rational (Michaelis–Menten) Type:*

$$\mathcal{R}(x) = \frac{1}{1 + \mu x}, \quad \mu > 0, \quad (2.31)$$

which mimics saturable enzyme kinetics [43] and represents a first-order depletion process. As $x \rightarrow \infty$, $\mathcal{R}(x) \rightarrow 0$, thereby preventing unbounded replication rates.

- *Power-Law (Hill-Type):*

$$\mathcal{R}(x) = \frac{1}{1 + (\mu x)^k}, \quad k > 1, \quad (2.32)$$

which exhibits a sharper threshold at high occupancy, reflecting cooperative or multi-step constraints on resource usage.

Inserting $\mathcal{R}(\hat{N})$ into the creation operator modifies it as

$$\hat{\Gamma}_+(\varphi) = \hat{a}^\dagger(\varphi) \mathcal{R}(\hat{N}). \quad (2.33)$$

Within the M -lattice subspace, $\hat{\Gamma}_+(\varphi)$ maps states to the $(M + 1)$ -lattice subspace with an amplitude weighted by $\mathcal{R}(M)$. Thus, the probability of creating new virions diminishes as the current occupancy increases, effectively modeling a saturable, resource-limited replication mechanism.

2. **Dynamical Interpretation and Operator Semigroup Evolution.** Let $\hat{\mathcal{G}}_{\text{free}}$ denote the baseline generator describing the intrinsic dynamics (e.g., single-lattice motion, damping, and elasticity) in \mathcal{H}_{lat} . When the resource feedback creation operator $\hat{\Gamma}_+(\varphi)$ is incorporated, the total operator becomes

$$\hat{\mathcal{G}}_{\text{tot}} = \hat{\mathcal{G}}_{\text{free}} + \hat{\Gamma}_+(\varphi). \quad (2.34)$$

Under standard m -sectorial conditions [10, 14], $\hat{\mathcal{G}}_{\text{tot}}$ generates a strongly continuous semigroup $e^{t\hat{\mathcal{G}}_{\text{tot}}}$ on the Fock space. This semigroup governs the time evolution of the viral population state vector $\Psi(t)$, incorporating both the intrinsic lattice dynamics and the resource-limited replication processes.

Boundedness of the Mean Number Operator. Due to the presence of the resource function $\mathcal{R}(x)$, the expectation $\langle \hat{N}(t) \rangle$ remains bounded or grows at most subexponentially over time, in stark contrast with the potential blow-up caused by unconstrained creation operators. This mathematically rigorous control reflects the biological reality in which viral replication is curtailed by limited supplies of essential host factors such as capsid proteins, nucleotides, ATP, and other resources [45]. Consequently, the operator-level feedback mechanism ensures that while the formalism allows for unbounded occupancy, the effective viral population remains finite.

3. **Logistic-Type Population Saturation in the Viral Fock Space** Consider the Heisenberg equation for the total number operator \hat{N} :

$$\frac{d}{dt} \hat{N} = [\hat{N}, \hat{\mathcal{G}}_{\text{tot}}]_- + \left(\frac{\partial \hat{N}}{\partial t} \right)_{\text{explicit}}, \quad (2.35)$$

where $\hat{\mathcal{G}}_{\text{tot}}$ denotes the full generator of the dynamics—encompassing creation, annihilation, and damping terms—in the many-lattice Fock space. In an idealized, resource-unlimited scenario, the average virion count $\langle \hat{N} \rangle$ may grow without bound.

However, realistic models must incorporate finite host resources (such as available capsid proteins, nucleotides, and ATP), which limit replication. To capture this, one introduces a *resource-limited* creation operator:

$$\hat{\Gamma}_+(\psi) = \hat{a}^\dagger(\psi) \mathcal{R}(\hat{N}), \quad (2.36)$$

where $\mathcal{R}(\hat{N})$ is a saturation function that attenuates the creation amplitude as the population increases.

In mean-field treatments, higher-order correlations are often approximated (e.g., $\langle \hat{N}^2 \rangle \approx \langle \hat{N} \rangle^2$), reducing the dynamics of $\langle \hat{N} \rangle$ to a logistic-type ODE:

$$\frac{d}{dt} \langle \hat{N} \rangle \approx \alpha_1 \langle \hat{N} \rangle - \alpha_2 \langle \hat{N}^2 \rangle, \quad (2.37)$$

where α_1, α_2 arise from expansions of the resource-limited creation amplitude $\mathcal{R}(\hat{N})$ and from damping contributions. The saturation (or “plateau”) of $\langle \hat{N} \rangle$ in such models mirrors the empirically observed *viral load saturation* in infections [41]. If \mathcal{R} is a bounded, monotone-decreasing function—diminishing the creation rate as \hat{N} grows—then the modified generator $\hat{\mathcal{G}}_{\text{tot}}$ remains dissipative. By classical semigroup theorems (Hille–Yosida, Lumer–Phillips), one obtains global existence of the time evolution for all $t \geq 0$ [10, 37]. Biologically, this reflects viral replication being unrestrained at low population levels yet self-limiting at high occupancies, preventing unphysical runaway growth.

Definition 2.8 (Density-Dependent Decay Operators.). Immune responses or clearance mechanisms, which strengthen with increasing virion counts, can be captured by a *nonlinear* annihilation operator:

$$\hat{\Gamma}_-(y) = \hat{a}(y) \mathcal{C}(\hat{N}), \quad (2.38)$$

where \mathcal{C} is an increasing function (e.g., $\mathcal{C}(x) = bx$, $b > 0$). Hence, net changes in \hat{N} reflect a balance between resource-limited creation and density-enhanced decay. Operator-theoretically, the commutators

$$[\hat{N}, \hat{\Gamma}_+(y)]_-, \quad [\hat{N}, \hat{\Gamma}_-(y)]_- \quad (2.39)$$

now include extra \hat{N} -dependent terms. The system is driven toward equilibrium (or bounded oscillations in $\langle \hat{N} \rangle$), consistent with the biological observation that high virion loads activate immune responses, removing excess virions. One can implement \mathcal{R} and \mathcal{C} as step functions or smooth monotone functions while maintaining dissipativity in the total generator $\hat{\mathcal{G}}_{\text{tot}}$, ensuring a bounded steady state for $\langle \hat{N} \rangle$.

Proof of the Total Generator's Well-Posedness. We propose a generator of the form

$$\hat{\mathcal{G}} = -\delta \hat{N} + \hat{\Gamma}_+ + \hat{\mathcal{D}}, \quad (2.40)$$

acting on a dense domain

$$D(\hat{\mathcal{G}}) \subset \mathcal{F}_{\pm}(\mathcal{H}_{\text{lat}}), \quad (2.41)$$

where:

1. $\mathcal{F}_{\pm}(\mathcal{H}_{\text{lat}})$ is the (bosonic or fermionic) Fock space built over the single-lattice space \mathcal{H}_{lat} . The operator \hat{N} is the *number operator*, counting total viral-lattice excitations in all modes.
2. $-\delta \hat{N}$ (with $\delta > 0$) serves as a negative contribution to the generator, producing direct linear decay. Large \hat{N} thus experiences more robust damping, preventing unbounded growth of virion counts [41].
3. $\hat{\Gamma}_+ = \hat{a}^\dagger(\phi) \mathcal{R}(\hat{N})$ introduces *nonlinear* birth/creation, where:
 - $\hat{a}^\dagger(\phi)$ is shorthand for creating a lattice in mode ϕ ,
 - $\mathcal{R}(\hat{N})$ is a real-valued function of \hat{N} that $\rightarrow 0$ as $\hat{N} \rightarrow \infty$. Typical examples are $\mathcal{R}(x) = 1/(1 + \alpha x)$ or Michaelis–Menten–type saturable forms.
4. $\hat{\mathcal{D}}$: Collects any additional damping, diffusion, or interaction operators ensuring that $\hat{\mathcal{G}}$ is *m*-sectorial (generates a contraction semigroup in a suitable norm). Formally, $\hat{\mathcal{D}}$ must not induce unbounded growth in $\langle \hat{N} \rangle$.

By checking dissipativity and maximality (Lumer–Phillips or Hille–Yosida), one confirms $\hat{\mathcal{G}}$ generates a strongly continuous semigroup $\{e^{t\hat{\mathcal{G}}}\}_{t \geq 0}$ on $\mathcal{F}_{\pm}(\mathcal{H}_{\text{lat}})$. Hence, for any initial state $|\Psi_0\rangle \in D(\hat{\mathcal{G}})$, there is a unique mild solution $|\Psi(t)\rangle$ to

$$\frac{d}{dt} |\Psi(t)\rangle = \hat{\mathcal{G}} |\Psi(t)\rangle, \quad |\Psi(0)\rangle = |\Psi_0\rangle. \quad (2.42)$$

Defining the Heisenberg-picture operator

$$\hat{N}(t) = e^{t\hat{\mathcal{G}}} \hat{N} e^{-t\hat{\mathcal{G}}} \quad (2.43)$$

and letting $\langle \hat{N}(t) \rangle = \langle \Psi(t), \hat{N} \Psi(t) \rangle$, one computes

$$\frac{d}{dt} \langle \hat{N}(t) \rangle = \langle \Psi(t), [\hat{\mathcal{G}}, \hat{N}]_- \Psi(t) \rangle. \quad (2.44)$$

Observing that:

$$[-\delta \hat{N}, \hat{N}]_- = 0 \quad \text{and} \quad [\hat{\Gamma}_+, \hat{N}]_- = 0 \quad (\text{since } \hat{N} \text{ commutes with } \mathcal{R}(\hat{N})), \quad (2.45)$$

the main negative feedback arises from $-\delta \hat{N}$ and any additional damping in $\hat{\mathcal{D}}$. Thus,

$$\frac{d}{dt} \langle \hat{N}(t) \rangle \leq -\delta \langle \hat{N}(t) \rangle + [\text{terms from } \hat{\mathcal{D}}], \quad (2.46)$$

indicating a logistic-type cap on $\langle \hat{N}(t) \rangle$. Because $\mathcal{R}(\hat{N})$ vanishes at large \hat{N} , creation is suppressed for high occupancy, preventing unbounded exponential replication. Consequently, $\langle \hat{N}(t) \rangle$ remains finite $\forall t$, fulfilling a resource-limited, biologically realistic dynamic in the many-lattice (second-quantized) setting. \square

Viral Dynamics with Finite Resources and Immunological Clearance: Real infections face limitations (proteins, nucleotides, host machinery) that saturate at high virion loads. The negative feedback of $\mathcal{R}(\hat{N})$ prevents runaway replication, matching empirical data on viral load plateaus [2, 41]. Density-dependent removal operators $\hat{\Gamma}_-(\psi) = \hat{a}(\psi) \mathcal{C}(\hat{N})$ reflect the intensification of immune responses at higher viral titers, driving down \hat{N} [8]. These saturable or density-dependent processes ensure that $\hat{\mathcal{G}}$ remains m -sectorial, generating a stable semigroup whose trajectories stay confined to finite-mean subspaces of Fock space, validating the well-posedness of PDE–Markov–Fock models in virology [10]. To see that $\hat{\mathcal{G}}$ indeed generates a well-defined, strongly continuous semigroup without blow-up in the many-lattice Fock space, one checks the following:

1. Since the resource-limited creation operator $\hat{\Gamma}_+$ is *not* unboundedly amplifying (it behaves “sublinearly” in \hat{N} for large \hat{N}), its real part cannot drive the spectrum of $\hat{\mathcal{G}}$ to large positive values. The linear damping term $-\delta \hat{N}$ and any negative contributions in $\hat{\mathcal{D}}$ dominate for high \hat{N} , ensuring no runaway replication [10, 41].
2. One verifies that the resolvent $(\hat{\mathcal{G}} - \lambda I)^{-1}$ exists and is bounded for sufficiently large $\text{Re}(\lambda)$ (or within a suitable sector). Hence, $\hat{\mathcal{G}}$ is m -sectorial, generating a C_0 -semigroup in the Fock space [26, 32].
3. From the logistic-like ODE analogy, the expectation $\langle \hat{N}(t) \rangle$ remains finite. Higher moments similarly remain bounded provided $\hat{\Gamma}_+$ is sufficiently regular (*e.g.*, polynomial or rational forms of $\mathcal{R}(\hat{N})$). Thus, no blow-up occurs in finite time.

Although the Fock space itself allows infinitely many virions (lattices), the dynamics $|\Psi(t)\rangle$ do *not* explosively populate high-occupancy ($N \gg 1$) states. Instead, typical trajectories approach or oscillate around finite-occupancy regions, consistent with resource constraints and the biological intuition that viral replication saturates [2, 46].

To summarize:

- The *Resource function* $\mathcal{R}(\hat{N})$ ensures that the creation rate vanishes at large \hat{N} , preventing unbounded particle (virion) growth.

- The *Damping operator* $-\delta \hat{N}$ plus the dissipative parts in \hat{D} yield negative real parts at high occupancy, enforcing stability.
- No unbounded positive growth modes remain, reproducing at the operator level a logistic or Lotka–Volterra-type population cap.

Hence, the total generator \hat{G} produces a unique mild solution $|\Psi(t)\rangle$ for all $t \geq 0$, maintaining $\langle \hat{N}(t) \rangle < \infty$. In equilibrium or the long-time limit, a steady-state distribution emerges, balancing resource-limited creation and damping and providing a biologically plausible second-quantized model of viral replication.

2.2 Hybrid PDE–Markov–Noise Model with Second Quantization

The following theorem and discussion extend the prior remark’s multi-scale perspective, which encompasses non-self-adjoint PDEs, Markov jump processes, and second-quantized replication mechanisms. We now incorporate *multiplicative noise* at the PDE level and show how one can still achieve a well-posed, m -sectorial description of viral lattices in an open, resource-limited system. This perspective accommodates complex dynamics (e.g. partial damping or localized gains) and discrete conformational switches, all embedded in a rigorous operator-algebraic framework, suitable for modeling *non-equilibrium* viral processes.

Theorem 2.9 (Hybrid PDE–Markov–Noise Model with Second Quantization). Consider a family of PDEs, one per arrangement label $y \in \{y_1, y_2, \dots\}$, coupled by Markov jump rates $\lambda_{y \rightarrow z}$ (for $y \neq z$), and subject to *multiplicative* stochastic forcing. Concretely, let $\mathbf{U}_y(t)$ evolve via

$$d\mathbf{U}_y(t) = \mathcal{G}_y \mathbf{U}_y(t) dt + \hat{N}_y(\mathbf{U}_y(t)) \circ d\mathbf{W}_t, \quad (2.47)$$

where

- \mathcal{G}_y is a (generally non-self-adjoint) operator capturing damped or driven elastic modes relevant to viral capsid distortions [2, 8].
- $\hat{N}_y(\mathbf{U}_y)$ is a (possibly nonlinear) *multiplicative noise* coefficient, representing state-dependent stochastic forcing. Biologically, it can reflect fluctuations in resource availability, pH, or temperature [2, 8, 16].
- \mathbf{W}_t is an infinite-dimensional Wiener process (cylindrical Brownian motion) in the sense of Da Prato–Zabczyk [47], driving the PDE dynamics in a Stratonovich (or Itô) formulation.
- The jumps among arrangement states $y \rightarrow z$ are captured by a block-off-diagonal (finite-state) generator \widehat{M} , indicating Markovian conformational changes in the viral capsid.

Define the total Hilbert space $\tilde{\mathcal{H}}_{\text{lat}}$ as a direct sum (or tensor product) over arrangement sectors, each hosting an m -sectorial PDE operator plus noise. Under the local Lipschitz and linear growth hypotheses of Da Prato–Zabczyk theory [47], the combined PDE + Markov + Noise system remains m -sectorial on $\tilde{\mathcal{H}}_{\text{lat}}$. Second-quantizing this single-lattice model to a Fock space $\mathcal{F}_{\pm}(\tilde{\mathcal{H}}_{\text{lat}})$ yields a unique mild solution (or semigroup evolution) for an *unbounded number* of such viral lattices, with well-posedness guaranteed by m -sectoriality. *The state variable for each arrangement (or conformational) label y solves (2.47). The Markov jump operator \widehat{M} then acts on the discrete arrangement index y . When combined into a single (unbounded) generator $\hat{G}_{+\infty}$, the block structure*

$$\hat{G}_{+\infty} = \left(\bigoplus_y (\mathcal{G}_y + \hat{N}_y) \right) + \widehat{M} \quad (2.48)$$

emerges on the “hybrid” Hilbert space $\tilde{\mathcal{H}}_{\text{lat}} = \bigoplus_y \mathcal{H}_y$. The off-diagonal entries of \widehat{M} (i.e. the jump rates $\lambda_{y \rightarrow z}$) couple different arrangement subspaces in a way that respects the overall m -sectorial property. In particular, one typically checks dissipativity by verifying inequalities of the form

$$\operatorname{Re} \langle (\mathcal{G}_y + \widehat{M})u, u \rangle \leq -\alpha \|u\|^2 \quad \text{for some } \alpha > 0, \forall u \in \operatorname{dom}(\mathcal{G}_y) \subset \mathcal{H}_y, \quad (2.49)$$

with suitable operator domain restrictions, and similarly for the noise terms by classical Da Prato–Zabczyk criteria [47].

In many physical or biological scenarios, we do not track a single viral lattice but rather *multiple* copies of identical lattices. By moving from the single-virion Hilbert space $\tilde{\mathcal{H}}_{\text{lat}}$ to the Fock space $\mathcal{F}_{\pm}(\tilde{\mathcal{H}}_{\text{lat}})$, we enable a variable number of virions. The associated second-quantized operator $d\Gamma(\widehat{\mathcal{G}}_{+\infty})$ is defined on the many-particle subspace and inherits m -sectoriality if the single-particle generator $\widehat{\mathcal{G}}_{+\infty}$ is m -sectorial [26]. Formally,

$$d\Gamma(\widehat{\mathcal{G}}_{+\infty}) = \bigoplus_{n=0}^{\infty} \left(\underbrace{\widehat{\mathcal{G}}_{+\infty} \otimes I \otimes \cdots \otimes I}_{n \text{ times}} + \cdots \right) \quad (2.50)$$

depending on whether the lattice degrees of freedom are effectively bosonic or fermionic. Biologically, viral assemblies are typically bosonic in nature, but the functional approach only requires a consistent Fock representation. Creation/annihilation operators $\widehat{a}^\dagger, \widehat{a}$ can then be incorporated to capture replication or immune clearance events. Provided these processes obey *energy-like bounds* (e.g. saturable replication rates, polynomial or exponential bounds on creation intensities), the entire second-quantized operator remains quasi-accretive/ m -sectorial, guaranteeing a global semigroup solution.

A central tenet of the m -sectorial framework is that, once the relevant dissipativity conditions are verified, the *Hille–Yosida theorem* (or its non-self-adjoint generalizations) secures the existence and uniqueness of a strongly continuous semigroup $\{e^{t\widehat{\mathcal{G}}_{+\infty}}\}_{t \geq 0}$. That semigroup fully characterizes the time evolution of the PDE-with-jumps system and, after second quantization, the evolution of a potentially infinite virion population. The formal statements typically rely on inequalities of the form

$$\|(\widehat{\mathcal{G}}_{+\infty} + \omega I)^{-1}\| \leq \frac{1}{\operatorname{Re} \omega - c} \quad \text{for } \operatorname{Re} \omega > c, \quad (2.51)$$

for some real constant c , ensuring resolvent bounds within a sector of the complex plane. Such a resolvent estimate implies the generation of a *quasi-contractive* semigroup on the Hilbert space, preserving positivity and ruling out finite-time blow-up.

2.2.1 Multiplicative Noise and Host Fluctuations.

Definition 2.10 (Stochastic PDE Block Structure with Multiplicative Noise and Virological Context). In the context of viral capsids, the *multiplicative noise* operator $\widehat{N}_y(\mathbf{U}_y)$ may represent local fluctuations in host factor concentrations, pH variations, or temperature shifts [2, 16]. Mathematically, this noise is modeled by operator-valued functions that scale with the state vector \mathbf{U}_y , in contrast to *additive* noise that imparts a uniform random forcing. Empirically, viral assembly and polymerization rates often strongly depend on microenvironmental conditions, which justifies using state-dependent (multiplicative) terms. Such feedback can bolster or suppress deformations based on the current amplitude of $\|\mathbf{U}_y\|$, mirroring the self-regulatory dynamics of many biological processes. Multiplicative noise can be interpreted as:

- *State-Dependent Variability*: Multiplicative terms grow or shrink with $\|U_y\|$, leading to unequal perturbations across different regions of phase space. This asymmetry aligns with empirical observations that certain capsid states are more “fragile” or susceptible to large fluctuations [2].
- *Confinement Due to Damping*: If \mathcal{G}_y is dissipative (negative real parts in its spectrum), trajectories cannot wander indefinitely; the system is repeatedly “pulled back” into a bounded region, even under chaotic noise.
- *Ergodicity and Stationary Distributions*: Over prolonged timescales, many such stochastic PDE systems settle into an invariant measure in phase space, indicating that, despite local randomness, the viral lattice states cluster around a “preferred” region in \mathcal{H}_y [41, 47].

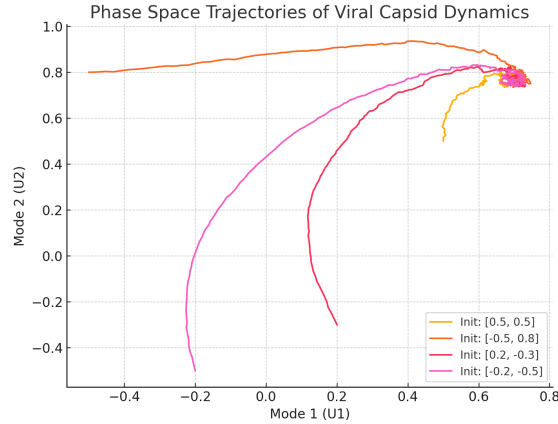


Figure 4: **Phase Space Trajectories of Viral Capsid Deformations in a Reduced Mode Space.** Each colored curve represents a distinct realization of the system starting from different initial displacements, (U_1, U_2) . The *multiplicative noise* drives state-dependent fluctuations, yielding chaotic yet confined trajectories. Damping within \mathcal{G}_y ensures that solutions do not diverge to infinity; instead, they wander unpredictably within a bounded region of phase space. Such behavior reflects the balance of noise-induced perturbations and the dissipative pull of the PDE operator, mirroring how real viral capsids experience dynamic but ultimately contained deformations under host microenvironmental fluctuations.

One can view this phenomenon as akin to a *stochastic pendulum* in a fluctuating fluid environment: while noise complicates the pendulum’s trajectory, damping (friction) prevents it from escaping to infinity, and the system typically hovers around certain equilibrium regions. Analogously, for viral capsids, state-dependent perturbations (via \hat{N}_y) can intensify or diminish random forcing based on the current deformation amplitude, effectively *self-regulating* the capsid’s motion in the host environment. So, just as the pendulum’s amplitude stays bounded despite fluctuating external forces, a viral capsid’s deformation remains confined under multiplicative noise, combining adaptive flexibility with intrinsic dissipative effects. This balance of random perturbations and damping captures how capsid stability persists within biological microenvironments, resonating with the intuitive notion that viruses exploit stochastic but ultimately self-regulating dynamics in host cells.

Under standard Da Prato–Zabczyk conditions (local Lipschitz continuity and linear growth bounds of \hat{N}_y), one obtains well-posedness in the mild sense for the PDE block. Moreover, each \mathcal{G}_y is constructed to be *dissipative* in the appropriate sense (often requiring physically motivated

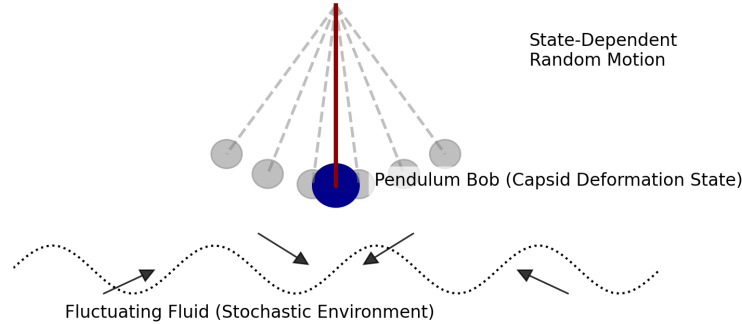


Figure 5: **Stochastic Pendulum Analogy for Viral Capsid Dynamics.** This schematic compares viral capsid deformation (under multiplicative noise) to a pendulum oscillating in a fluctuating fluid environment. The dark red arm signifies the system’s equilibrium alignment, whereas the dark blue bob represents the capsid’s deformation state. Gray, dashed pendulum arms and faded bobs depict random perturbations driven by state-dependent noise, altering the trajectory based on the pendulum’s current position. At the bottom, the dotted black wave symbolizes environmental factors (pH, temperature, ATP concentration) that inject stochastic fluctuations into the system. Black arrows illustrate how these host-dependent variations feed back into the motion.

boundary conditions and damping terms), and hence, together with suitable coercivity assumptions on the noise term, the operator in the PDE block remains *m-sectorial* in the infinite-dimensional stochastic analysis framework. Recall that a (possibly unbounded) linear operator A on a Hilbert space is *m-sectorial* if it is closed, densely defined, and its resolvent $(A + \lambda I)^{-1}$ is bounded and holomorphic in a sector of the complex plane [14]. Viral lattices can abruptly transition between discrete arrangements or “conformational states” (e.g., partial channel openings, subunit rotations, protonation events). We model these jumps by a discrete Markov operator \widehat{M} acting on the arrangement space (indexed by y), with off-diagonal rates $\lambda_{y \rightarrow z} \geq 0$. In standard notation, for a function $f : \{\text{arrangements}\} \rightarrow \mathbb{R}$,

$$(\widehat{M}f)(y) = \sum_{z \neq y} \lambda_{z \rightarrow y} f(z) - \left(\sum_{z \neq y} \lambda_{y \rightarrow z} \right) f(y). \quad (2.52)$$

Such an operator \widehat{M} is typically negative semidefinite (the diagonal entries are negative, summing the exit rates), and it is the generator of a continuous-time Markov chain on the discrete arrangement space [48]. When this jump operator \widehat{M} is coupled with the PDE blocks $\{\mathcal{G}_y\}_y$, one obtains a hybrid operator that describes both the continuous SPDE evolution *within* each arrangement sector, and the Markov jumps *between* different arrangements. Under suitable conditions ensuring that each block \mathcal{G}_y remains dissipative and that \widehat{M} has no positive eigenvalues, one verifies that the overall generator (block-diagonal for the PDE part, plus off-diagonal jumps) stays *m-sectorial* by standard perturbation arguments [47].

In many biological contexts, viruses are not found as a single lattice but rather multiple copies (virions) that can replicate or degrade. To accommodate an *unbounded number* of such lattices, we

second-quantize the single-lattice Hilbert space $\tilde{\mathcal{H}}_{\text{lat}} \cong \bigoplus_y \mathcal{H}_y$ into the Fock space $\mathcal{F}_{\pm}(\tilde{\mathcal{H}}_{\text{lat}})$. This allows each arrangement label y and its corresponding PDE–noise block to act as a *one-particle* operator, which is then lifted to *many-particle* (many-virion) dynamics by the usual second-quantization procedure [26, 32, 49]. If we include creation/annihilation operators to reflect replication, infection bursts, or immune-mediated clearance of virions, these can be structured to preserve *m-sectoriality* under physically sensible rate constraints (e.g., saturable replication rates). Such constraints prevent blow-up in finite time and ensure a well-posed many-body description of the viral population [41]. By combining:

1. Each individual PDE + noise operator $\mathcal{G}_y + \hat{N}_y$ from (2.47),
2. The discrete jump operator \widehat{M} encoding transitions among arrangement states (cf. typical form in Markov chains [48]), and
3. The second-quantized (creation/annihilation) extensions for unbounded lattice populations,

we obtain a single unbounded operator

$$d\Gamma(\widehat{\mathcal{G}}_{+\infty}) \quad \text{on} \quad \mathcal{F}_{\pm}(\tilde{\mathcal{H}}_{\text{lat}}), \quad (2.53)$$

where $\widehat{\mathcal{G}}_{+\infty}$ is, at the single-virion (single-lattice) level,

$$\widehat{\mathcal{G}}_{+\infty} = \left(\bigoplus_y [\mathcal{G}_y + \hat{N}_y] \right) + \widehat{M}. \quad (2.54)$$

Under classical results in operator theory (notably Kato’s theorem [14], Da Prato–Zabczyk [47], and quantum many-body theory [26]), an *m-sectorial* generator $d\Gamma(\widehat{\mathcal{G}}_{+\infty})$ produces a strongly continuous *quasi-contractive* semigroup. Concretely, this means there exists a unique, global (in time) evolution operator

$$e^{t d\Gamma(\widehat{\mathcal{G}}_{+\infty})} : \mathcal{F}_{\pm}(\tilde{\mathcal{H}}_{\text{lat}}) \longrightarrow \mathcal{F}_{\pm}(\tilde{\mathcal{H}}_{\text{lat}}), \quad (2.55)$$

which (in a mild or strong sense, depending on boundary domain technicalities) solves the underlying PDE-plus-jump-plus-creation/annihilation system. This semigroup property encodes the Markovian structure of both the continuous (SPDE) and discrete (jump) dynamics while ensuring uniqueness of trajectories and prohibiting finite-time blow-up.

Novel Aspects of the SPDE and Operator Framework.

1. **Non-Self-Adjoint Sectoriality.** In many quantum or wave-like systems, self-adjointness is assumed to leverage strong spectral theorems. In this work, however, the operator \mathcal{G}_y can be non-self-adjoint, representing damped or driven oscillatory modes with boundary dissipation or external forcing [23, 37]. Such an operator may possess complex eigenvalues indicating energy-loss (negative real parts) or partial amplification (positive real parts). The *sectorial* framework accommodates this complexity by imposing dissipativity bounds on the real part of the spectrum, ensuring that energy-type inequalities remain valid and preventing uncontrolled runaway solutions [47].
2. **Discrete–Continuous Hybridization.** The transition operator \widehat{M} handles *discrete* jumps (e.g. subunit rotations, gating events, or conformational flips), typically via a block-off-diagonal structure that couples arrangement states $y \rightarrow z$ at some rate $\lambda_{y \rightarrow z}$. Meanwhile, each PDE block $\mathcal{G}_y + \hat{N}_y$ encodes *continuous* motion (elastic modes, vibrational displacements,

etc.) in an infinite-dimensional function space [8, 48]. This yields a *piecewise-continuous* and *piecewise-random* dynamic, akin to piecewise-deterministic Markov processes in finite dimensions, but now lifted to a continuum of capsid modes. The interplay of discrete rearrangements and continuous PDE evolution accurately reflects how viral capsids undergo abrupt conformational shifts on top of ongoing elastic deformations.

3. **Second Quantization for Unbounded Populations.** A single-lattice operator, $\widehat{\mathcal{G}}_{+\infty}$, may be second-quantized to allow an *unbounded number* of viral lattices (capsids) within a host [26]. Each lattice evolves under the same PDE + Markov + noise operator at the single-capsid level, but creation/annihilation operators facilitate replication or clearance events at the population level. Provided the growth rates for replication satisfy dissipativity constraints (e.g. saturable resource usage [21]), the global second-quantized operator, denoted $d\Gamma(\widehat{\mathcal{G}}_{+\infty})$, remains m -sectorial. This unification of continuum PDE mechanics with Markov population dynamics is especially *novel* and allows modeling of large-scale viral outbreaks while retaining physically realistic saturation limits.
4. **Quasi-Contractive Semigroup and Prevention of Blow-Up.** Sectorial resolvent estimates on $d\Gamma(\widehat{\mathcal{G}}_{+\infty})$ yield a quasi-contractive semigroup on the Fock space. In classical PDE settings, contractivity often implies L^2 -damping or exponential decay. Here, partial dissipativity in each arrangement block (non-self-adjoint PDE plus noise) and Lipschitz-type conditions on replication or Markov jumps ensure *global* well-posedness [10]. Practically, this means that despite random forces and an unbounded virion population, the state of the system does *not* blow up in finite time. Instead, resource constraints and dissipation combine to yield physically meaningful saturation, mirroring the limited replication observed in real infections where host-imposed boundaries (immune responses, metabolic limits) prevent infinite virion proliferation [2].

Physics and Biology Context. From a *physical* standpoint, the freedom to handle non-Hermitian operators allows for energy loss or gain—key to open systems and realistic damping phenomena [28, 47]. Simultaneously, the *discrete-continuous* hybrid structure accommodates abrupt conformational jumps in viral subunits (e.g. domain flips, partial unfolding). Biologically, second quantization introduces a robust population-scale perspective: each lattice evolves under the same PDE, but unlimited lattices (virions) may coexist, replicating subject to resource limitations [41]. Ultimately, the resulting quasi-contractive semigroup ensures well-posedness and boundedness, preventing unrealistic blow-up and reflecting the finite environment in which viruses actually replicate. We can further interpret these results as:

- *Host-driven fluctuations* (e.g. temperature, pH, immune factors) appear as multiplicative noise terms $\widehat{N}_y(\mathbf{U}_y(t))$, allowing for variability in capsid elasticity or subunit attachment rates [2]. From a mechanistic perspective, these fluctuations may correspond to local changes in ATP levels, ionic strength, or interfering molecules that modulate the viral shell’s stability.
- *Conformational leaps* among discrete arrangement states capture sudden structural rearrangements during replication or assembly [5, 21]. Such jumps may reflect protonation-triggered channel openings, or large-scale reorientations of capsid subunits, realistically modeled by rate-based Markov transitions. This synergy of discrete/continuous dynamics is central to many biological processes where a continuum surface structure undergoes discrete gating events.

- *Potential replication or clearance* arises via creation/annihilation operators in the second-quantized Fock space, modeling how multiple virions co-exist, interfere, and compete under resource limitations [16, 41]. This is especially relevant for studying large populations of viruses within a single host cell environment, where repeated infection cycles or immune responses dynamically shift virion counts.
- *Global well-posedness* follows from m -sectoriality: each virion’s conformational PDE + noise remains well-defined under abrupt arrangement jumps and unbounded population expansions, enabling rigorous analyses of emergent capsid patterns, large-deviation events, or even synergy with branching processes [28, 48].

In summary, the combination of *non-self-adjoint PDE operators*, *Markov jump processes*, *multiplicative noise*, and *second-quantized replication* provides a comprehensive open-system framework for viral biology. The m -sectorial approach ensures well-defined, unique evolutionary trajectories, thus paving the way for a mathematically rigorous study of viral evolution, structural transformations, and population-level competition effects. This framework is *novel* in its level of detail and unification, offering both fine-scale continuum modeling at the single-virion level and large-scale population dynamics in a single operator-theoretic setting.

3 Flux Integrals, Cycle Summations, and Markovian Jumps in Finite and Infinite Dimensions

In what follows, we refine the standard picture of probability-flux loops by incorporating a *Markovian jump* perspective in both finite and infinite-dimensional settings. Our goal is to formalize how flux loops can generate infinitely many solutions (or “paths”) in configuration space, each carrying statistical weight and reflecting the most likely transitions among various parameters (arrangements, mass bands, particle-number sectors, *etc.*). Below, we develop precise definitions and propositions to illuminate the role of Markovian cycles, then conclude by discussing their physical (virological) interpretations and mathematical implications for operator theory and non-equilibrium dynamics.

Definition 3.1 (Infinite-Dimensional Configuration Space). Let \mathcal{M} be an infinite-dimensional manifold of possible configurations. For example, \mathcal{M} may consist of solutions

$$\varphi(\mathbf{x}, t) \quad \text{to a PDE or continuum field equation,} \quad (3.1)$$

where \mathbf{x} denotes a spatial variable in some domain $D \subset \mathbb{R}^d$. A *closed loop* \mathcal{C} in \mathcal{M} is a continuous path

$$\mathcal{C} : [0, 1] \rightarrow \mathcal{M} \quad \text{with} \quad \mathcal{C}(0) = \mathcal{C}(1). \quad (3.2)$$

Definition 3.2 (Probability-Current Functional). Let $\check{N}(d\varphi)$ be a (possibly time-dependent) probability measure on \mathcal{M} . Define the *probability-current functional* $\mathbf{J}(\varphi)$ to be a vector-valued mapping

$$\mathbf{J} : \mathcal{M} \longrightarrow T\mathcal{M}, \quad (3.3)$$

where $T\mathcal{M}$ denotes the (formal) tangent bundle over \mathcal{M} . Intuitively, $\mathbf{J}(\varphi)$ captures the local flow of probability in the configuration space \mathcal{M} .

Definition 3.3 (Flux Integral in Infinite Dimensions). For a closed loop $\mathcal{C} \subset \mathcal{M}$, the *flux integral* of \mathbf{J} along \mathcal{C} is

$$\oint_{\mathcal{C}} \mathbf{J}(\varphi) \cdot d\varphi, \quad (3.4)$$

where $d\varphi$ denotes an infinitesimal displacement along \mathcal{C} . In formal analogy with finite-dimensional line integrals, this quantity measures the net circulation of probability along the loop \mathcal{C} .

Proposition 3.4 (Steady States with Nonzero Circulation). *Suppose the probability density $\check{N}(\varphi, t)$ satisfies the continuity-type equation*

$$\partial_t \check{N}(\varphi, t) + \nabla_{\varphi} \cdot \mathbf{J}(\varphi) = 0, \quad (3.5)$$

where $\nabla_{\varphi} \cdot$ denotes a suitable functional divergence on \mathcal{M} . If \check{N} is time-invariant (i.e., $\partial_t \check{N} = 0$) but $\mathbf{J}(\varphi)$ is nonzero, then there exist closed loops $\mathcal{C} \subset \mathcal{M}$ for which

$$\oint_{\mathcal{C}} \mathbf{J}(\varphi) \cdot d\varphi \neq 0. \quad (3.6)$$

Such a system is said to be in a non-equilibrium steady state (NESS) with persistent probability flux loops.

Proof. The condition $\partial_t \check{N} = 0$ in (3.5) implies a balance of probability flux at every point $\varphi \in \mathcal{M}$. However, if $\mathbf{J}(\varphi)$ does not globally vanish, Stokes' Theorem (extended to infinite-dimensional manifolds; see, e.g., [50,51]) allows for nonzero circulation around certain closed paths. Hence, there must exist loops \mathcal{C} for which the flux integral (3.4) is nonzero, indicating persistent circulation of probability. \square

3.0.1 Markovian Jumps in Fock Space

In many physical models, one moves to a second-quantized description by embedding a single-lattice Hilbert space \mathcal{H}_{lat} into a Fock space

$$\mathcal{F}(\mathcal{H}_{\text{lat}}) = \bigoplus_{n=0}^{\infty} (\mathcal{H}_{\text{lat}}^{\otimes n})_{\text{sym/asym}}, \quad (3.7)$$

where symmetrization or antisymmetrization depends on the statistics of the particles (bosons, fermions, *etc.*) which constitute the lattice. The number operator \hat{N} counts the total number of “viral-lattice quanta,” and

$$p_n = \mathbb{P}(\hat{N} = n) \quad (3.8)$$

gives the occupation probability of the n -particle subspace in steady state.

Definition 3.5 (Markovian Jump Rates). Let $\nu_{n \rightarrow n+1}$ and $\nu_{n+1 \rightarrow n}$ denote the net transition rates between adjacent number sectors n and $n+1$. The associated *flux* from n to $n+1$ is

$$J_{(n \rightarrow n+1)} = p_n \nu_{n \rightarrow n+1} - p_{n+1} \nu_{n+1 \rightarrow n}. \quad (3.9)$$

A nonzero value of $J_{(n \rightarrow n+1)}$ indicates persistent circulation among number sectors in the steady state.

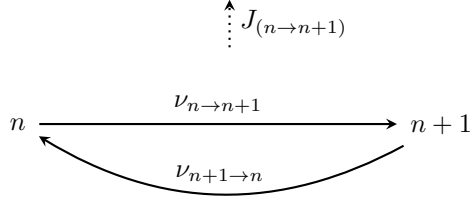


Figure 6: A schematic of the Markovian jump rates between adjacent lattice-number sectors. A system in sector n can transition to $n + 1$ at rate $\nu_{n \rightarrow n+1}$, or in the reverse direction at rate $\nu_{n+1 \rightarrow n}$. The *flux* $J_{(n \rightarrow n+1)}$ accounts for the net probability current flowing from n to $n + 1$, defined by $p_n \nu_{n \rightarrow n+1} - p_{n+1} \nu_{n+1 \rightarrow n}$. In steady-state, a nonzero $J_{(n \rightarrow n+1)}$ indicates persistent circulation among these number sectors.

Definition 3.6 (Closed Loops in Fock-Space Configurations). Consider more general transitions among arrangement states labeled by $f \in \{f_1, f_2, \dots\}$ and integer lattice sectors $\{n_1, n_2, \dots\}$. A *closed loop* in the Fock-space configuration is a sequence

$$(f_1, n_1) \rightarrow (f_2, n_1) \rightarrow (f_2, n_2) \rightarrow \dots \rightarrow (f_1, n_1), \quad (3.10)$$

whose net flux contribution combines creation, annihilation, and arrangement transitions. In an *infinite* Fock space, there are infinitely many such loops, each forming a *Markovian cycle*.

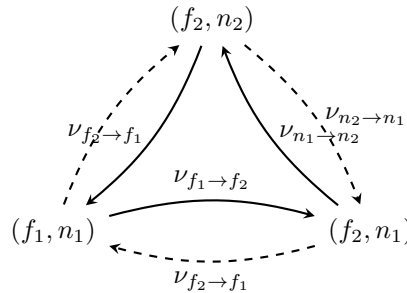


Figure 7: A sample *closed loop* in the Fock space. Here, (f_1, n_1) transitions to (f_2, n_1) (an arrangement change at fixed lattice number), then to (f_2, n_2) (a creation or annihilation event), and eventually returns to (f_1, n_1) . Such loops contribute a *net flux* in steady state, indicating a nonzero probability circulation among these Fock-space sectors.

Remark 3.7 (Cycle Expansion of Steady States). When the configuration space is countably (or uncountably) infinite, one obtains an unbounded set of possible closed cycles, each of which contributes to the overall non-equilibrium flow in the steady-state distribution \check{N} . Summing over these loops (or enumerating them in a path integral or cycle expansion) yields the full steady-state measure \check{N} [29, 48, 52, 53].

Energy/Resource Considerations and Non-Self-Adjoint Generators

Each nontrivial flux loop often corresponds to net free-energy consumption or production. For instance, a chemical potential $\Delta\mu$ or continuous resource input can drive creation processes, while partial annihilation or damping channels balance the system at a NESS. The generator \hat{G} governing these processes is typically *non-self-adjoint*, thereby violating detailed balance and permitting circulation in state space.

Definition 3.8 (Entropy Functional and Irreversibility). Let \tilde{N} be a density operator (or probability distribution) in the Fock space. An *entropy functional* $S(\tilde{N})$ can be associated to \tilde{N} , measuring the disorder or uncertainty in the system [54]. If there exist ongoing flux loops at steady state, the rate of entropy production is generally positive, reflecting the irreversibility of the underlying Markovian dynamics.

Theorem 3.9 (Existence of Persistent Flux Loops in Non-Self-Adjoint Systems). Let $\hat{\mathcal{G}}$ be a non-self-adjoint generator of a Markovian jump process on a Fock-space configuration. Suppose the system attains a unique steady state \tilde{N} . If detailed balance is not satisfied, then there must be at least one nontrivial closed loop in configuration space along which the steady probability flux is nonzero.

The absence of detailed balance implies that for some pairs of states (i, j) , the ratio of forward to backward rates does not match the equilibrium ratio required by the standard detailed-balance criterion [48, 55]. Equivalently, the generator $\hat{\mathcal{G}}$ has no real eigenvalue decomposition that can be used to write the stationary distribution in a purely “gradient-flow” form. By standard cycle decomposition arguments in Markov chain theory [29, 52], at least one cyclic path exhibits a net positive (or negative) flux. Hence, persistent circulation arises in that cycle, contradicting the possibility of global detailed balance.

Remark 3.10 (Physical Consequences). Nonzero loop integrals in such systems indicate ongoing energy/resource turnover; *i.e.*, the system is not at a Boltzmann-type equilibrium. Instead, the steady distribution \tilde{N} describes a *dynamically active* state, wherein probability mass continually circulates among various modes or particle-number sectors. These flux loops are intimately related to entropy production and the irreversibility of the underlying Markovian dynamics [28, 29].

Definition 3.11 (Viral/Molecular Biophysics Context). In a biological setting, one may interpret each state in the configuration space \mathcal{M} as describing a particular *viral* or *molecular* arrangement. For instance, $\varphi(\mathbf{x}, t)$ could represent the concentration of viral proteins or nucleic acids across spatial coordinates \mathbf{x} , while α, n might represent distinct replication or assembly states in a coarse-grained lattice (Fock-space) model. In this picture,

- *Creation processes* correspond to production of new virions or assembly intermediates (driven by cellular resources or a chemical potential),
- *Annihilation processes* capture degradation or loss of viral components,
- *Reconfiguration processes* encode conformational changes, protein binding, or transport phenomena relevant to viral replication.

Far from thermodynamic equilibrium, these reactions and transitions can form persistent cycles (*flux loops*) that reflect active consumption of metabolic energy/resources [5].

Definition 3.12 (Configuration Manifold). Let \mathcal{M} be a Banach (or Hilbert) manifold parametrizing PDE configurations, or equivalently, the discrete (n, α) sectors in a Fock-space decomposition. A generic point $\varphi \in \mathcal{M}$ may be:

- A function $\varphi(\mathbf{x})$ (continuum PDE setting), or
- A vector of occupation numbers $\{\varphi_n, \varphi_\alpha\}$ (second-quantized or lattice-based setting).

Definition 3.13 (Master Equation / Continuity Equation). A measure $\tilde{N}(d\varphi)$ (or a density matrix in an operator formulation) evolves according to the general form

$$\partial_t \tilde{N} = \hat{\mathcal{G}}^\dagger \tilde{N}, \quad (3.11)$$

where $\hat{\mathcal{G}}$ is an (in general) non-self-adjoint operator encoding all Markovian jumps, PDE drift/diffusion, creation/annihilation mechanisms, and other processes.

Definition 3.14 (Non-Equilibrium Steady State (NESS)). A *non-equilibrium steady state* arises when $\partial_t \tilde{N} = 0$. In other words,

$$\hat{\mathcal{G}}^\dagger \tilde{N} = 0, \quad (3.12)$$

yet the corresponding probability-current functional $\mathbf{J}(\varphi)$ need not vanish. Thus, even though the global measure \tilde{N} is time-invariant, one can still observe nontrivial flux loops across different state sectors in \mathcal{M} .

Definition 3.15 (Line Integrals and Circulation in \mathcal{M}). Consider a closed path $\mathcal{C} : [0, 1] \rightarrow \mathcal{M}$ with $\mathcal{C}(0) = \mathcal{C}(1)$. Define the *flux integral* of the probability-current functional \mathbf{J} as

$$\oint_{\mathcal{C}} \mathbf{J}(\varphi) \cdot d\varphi = \int_0^1 \left\langle \mathbf{J}(\mathcal{C}(s)), \mathcal{C}'(s) \right\rangle_{\mathcal{T}_{\mathcal{C}(s)}\mathcal{M}} ds. \quad (3.13)$$

A nonzero value of (3.13) indicates a net probability current circulating around the loop \mathcal{C} . In a Fock-space viewpoint, one similarly defines *cycle flux sums* over discrete transitions to capture persistent Markovian loops among integer-valued sectors.

Remark 3.16 (Infinite Families of Flux Loops). In both continuum PDE manifolds and second-quantized Fock-space representations, *closed loops* in state space, together with nonvanishing probability currents, yield an infinite family of possible “flux-loop” solutions consistent with a steady-state measure \tilde{N} . Each loop represents a Markovian cycle—either continuous in \mathcal{M} or discrete among integer-valued sectors—exhibiting ongoing creation, annihilation, and reconfiguration.

The net circulation around these loops demonstrates a fundamentally non-equilibrium character, entailing continuous resource consumption and positive entropy production. From a modeling standpoint, this provides a powerful framework for identifying the *most likely dynamical pathways* (the loops with greatest net flux) and for quantifying how rarely the system explores subdominant paths in a high-dimensional parameter landscape. Such mathematical formulations thereby elucidate *viral replication processes*, emergent pattern formation, and broader classes of *open* dissipative systems far from equilibrium.

3.0.2 Implications for Virus Particle Motion and Non-Equilibrium Biology

The above homological and Hodge-theoretic notions illuminate *viral lattice theory* and non-equilibrium biological processes. By treating the PDE solution space for lattice displacements or internal modes as a manifold \mathcal{M} , any *nonzero flux loop* implies:

Definition 3.17 (Ongoing Reconfiguration in Viral Lattices). A flux loop $\mathcal{C} \subset \mathcal{M}$ with

$$\oint_{\mathcal{C}} \mathbf{J}(\varphi) \cdot d\varphi \neq 0 \quad (3.14)$$

represents an *ongoing reconfiguration* of the viral lattice or capsid state. Biologically, such shape fluctuations are fueled by ATP hydrolysis, pH gradients, or mechanical factors from the host environment [2]. This prevents the system from collapsing into a single stable “equilibrium” geometry.

Probability-Current Functional on Configuration Space

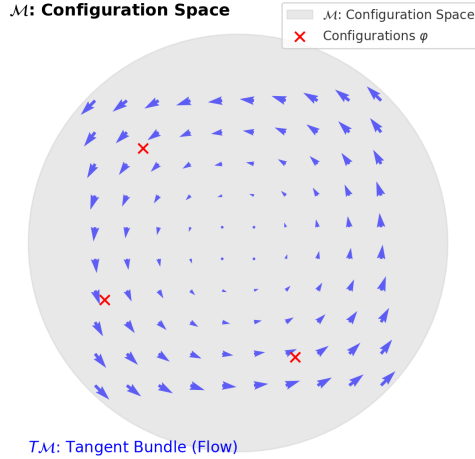


Figure 8: **Probability-Current Functional on Configuration Space.** A schematic of the infinite-dimensional manifold \mathcal{M} (shown here as a representative 2D projection) with several sample configurations (red crosses). The blue arrows illustrate the local probability-current vector field $\mathbf{J}(\varphi)$, capturing how probability flows in the vicinity of each configuration φ . Geometrically, this field resides in the tangent bundle $T\mathcal{M}$, reflecting the dynamical tendency of the viral system to move through \mathcal{M} under both deterministic and stochastic forces. Nonzero loops of this current signal broken detailed balance, where probability circulates indefinitely among configurations rather than settling to a single equilibrium.

Remark 3.18 (Second-Quantized Population Wavefunction). In the second-quantized setting, each point $\Phi \in \mathcal{F}(\mathcal{H}_{\text{lat}})$ represents a population-level wavefunction describing multiple virions and their arrangement states. A non-zero loop integral around a closed trajectory indicates the population does *not* settle into a static distribution but continually cycles through replication and annihilation stages. From a virological standpoint, this parallels ongoing infection cycles where virions are neither fully cleared nor frozen at a stable count [5, 7].

Definition 3.19 (Energy Consumption and Dissipation in Viral Systems). A “closed” probability circulation typically signals *continuous energy consumption or dissipation*. Each traversal of $\mathcal{C} \subset \mathcal{M}$ invests or releases free energy into the environment, as viruses hijack host metabolic pathways to sustain these loops. Mathematically, the *nonzero flux integral* encodes this topologically manifest dissipation and reflects the virus’s capacity to remain in an active, out-of-equilibrium state [2, 29].

Remark 3.20 (Biological Mechanisms of Persistent Cycling). Seeing flux integrals as line integrals of differential forms in infinite-dimensional geometries not only refines the theoretical lens—demonstrating the topological essence of “persistent loops”—but also highlights concrete biological mechanisms of viral survival, adaptation, and replication. Specifically, these loops reflect how viruses continually explore microstates or population sizes, powered by finite resources from the host, thereby *evading any single equilibrium configuration* [5].

Definition 3.21 (Fock-Space Operators in Viral Replication). In a viral lattice context, let $\hat{\Gamma}_+(\varphi) = \hat{a}^\dagger(\varphi) \mathcal{R}(\hat{N})$ represent creation (replication) operators that saturate for large \hat{N} (finite resources). Similarly, annihilation or degradation operators $\hat{\Gamma}_-(\varphi) = \hat{a}(\varphi) \mathcal{C}(\hat{N})$ describe loss of virions. Hence, no *a priori* cap on \hat{N} is imposed, allowing transitions among $n \in \{0, 1, 2, \dots\}$ particulate states [2, 21].

Remark 3.22 (Mathematical Consequences). Crucially, the generator (incorporating PDE dynamics, Markov jumps, and creation/annihilation) is often m -sectorial on $\mathcal{F}(\mathcal{H}_{\text{lat}})$, ensuring semigroup well-posedness and boundedness of mean occupancy in resource-limited settings. The key topological aspect is that in the presence of flux loops (non-exact 1-forms), one cannot simply write the probability current as $\mathbf{J} = \nabla\Phi$. Instead, the Hodge-like decomposition reveals a *cohomologically non-trivial* component reflecting irreversibility and sustained energy turnover [56].

Proposition 3.23 (Persistent Loops and Non-Equilibrium Dynamics). *Suppose the probability current $\mathbf{J}(\varphi)$ on the infinite-dimensional manifold \mathcal{M} satisfies:*

$$\exists \mathcal{C} \subset \mathcal{M} \quad \text{with} \quad \oint_{\mathcal{C}} \mathbf{J}(\varphi) \cdot d\varphi \neq 0. \quad (3.15)$$

Then the steady state of the system is non-equilibrium, exhibiting a persistent loop in (α, n) sectors or PDE modes. Biophysically, this loop corresponds to ongoing replication or shape reconfiguration, driven by resource inputs and offset by damping or clearance. Hence, no global free-energy potential Φ can capture the full dynamics [5, 28].

Proof. If \mathbf{J} were globally a gradient field, one would have $\oint_{\mathcal{C}} \mathbf{J} \cdot d\varphi = 0$ for every closed loop \mathcal{C} , implying detailed balance and equilibrium. The nonzero integral breaks this possibility, so the dynamics remain irreversibly active. Formally, \mathbf{J} must belong to a nontrivial cohomology class in $H_{\text{dR}}^1(\mathcal{M})$ [56], guaranteeing a steady flux around \mathcal{C} . \square

Remark 3.24 (Geometrical and Topological Insights). The lens of de Rham–Hodge-type geometry clarifies *why* flux loops (in PDE configuration or Fock space) signal topological obstructions to equilibrium. From a global perspective, such loops encode non-exact probability currents (1-forms) that cannot be written as $d\Psi$, ensuring persistent circulation in the system. This reveals a deep interface between differential geometry, operator theory, and non-equilibrium dynamics, bearing considerable significance for modeling complex biological systems (such as viral capsids) and purely mathematical studies of infinite-dimensional dissipative systems [57].

Proposition 3.25 (Bridge Between PDE/Semigroup Methods and Topology). *The results herein form a novel, flexible framework uniting:*

- Advanced PDE/semigroup *techniques for m -sectorial operators on Banach/Hilbert spaces [37], and*
- Topological methods *in infinite-dimensional differential geometry (de Rham/homological approaches to flux loops).*

This bridge facilitates deeper insights into irreversibility, resource consumption, and persistent dynamical loops far from equilibrium, surpassing classical ODE or near-equilibrium approximations [5, 21, 39].

Remark 3.26 (Limitations of Classical Viral Models). Classical models of viral infection and capsid mechanics often rely on relatively simple ordinary differential equations (ODEs) or low-dimensional continuum approximations. Such frameworks capture broad trends but can oversimplify the intricate structural rearrangements and stochastic processes inherent to viral life cycles [2, 7].

Definition 3.27 (m -Sectorial PDE Models). In contrast to low-dimensional ODEs, we adopt an *m -sectorial PDE model* wherein large assemblies of capsomeres, nucleocapsids, or viral shell units are treated as a continuous medium. The PDE may possess:

- *Elastic constants and damping mechanisms* to encode how structural proteins shift or deform in response to mechanical stress,
- *Forcing terms* arising from host-induced mechanical forces or boundary shearing, and
- *Non-self-adjoint components* to capture dissipation, driving, or resource inflows [36, 37].

Thermal fluctuations (Brownian motion) can be modeled via stochastic perturbations that still preserve well-posedness under suitable conditions.

Remark 3.28 (Discrete Markov Generators Within PDE Operators). Viral capsids and their protein subunits exhibit *discrete* switching events, such as bond formation/breakage or folded vs. partially unfolded states. Embedding a *finite-state Markov generator* into the PDE operator unifies smooth (elastic) deformations with abrupt conformational transitions [5, 39]. Such hybrid modeling allows the PDE flow to incorporate local energy thresholds or chemical potentials that trigger Markovian state changes, mirroring real biochemical pathways (e.g. capsid maturation/uncoating).

Definition 3.29 (Second-Quantization and Mass Labeling). To capture heterogeneous viral populations, one extends the single-lattice Hilbert space \mathcal{H}_{lat} to include mass or composition labels. A second-quantized Fock space $\mathcal{F}(\mathcal{H}_{\text{lat}})$ is then formed, where each “particle species” (capsid variant) evolves under identical dynamical rules but distinct initial conditions or structural parameters [7, 21]. This allows simultaneous simulation of diverse viral subpopulations under uniform physical laws, capturing realistic heterogeneity in size, glycoproteins, or encapsidated material.

Remark 3.30 (Noise and Resource Constraints). Biophysical processes often involve low copy numbers, random collisions, and fluctuations in energy availability. Incorporating noise into an m -sectorial framework ensures the theoretical guarantees (existence, uniqueness, long-term stability) remain valid while embedding operator-valued stochastic terms. Host cell factors, such as nucleotide pools or immune effectors, can be modeled as random processes coupling into the generator, yielding robust simulations of viral replication under realistic intracellular volatility [2, 29].

Proposition 3.31 (Well-Posedness and Quasi-Contractive Dynamics). *When viral replication or capsid deformation processes are resource-limited or damped, m -sectoriality imparts a quasi-contractive structure that precludes blow-up in finite time (e.g. unbounded virion counts or infinite lattice amplitude). As a result, the mild solutions [36, 37] of the combined PDE–Markov–Fock operator reflect genuine viral evolution under continuous deformations and discrete jumps, without pathologies like infinite occupancy.*

Proof. By definition, an m -sectorial operator generates a well-posed contraction (or quasi-contraction) semigroup on a Banach (or Hilbert) space. Imposing resource-limited coefficients in the creation terms and suitable dissipative conditions in the PDE part ensures the semigroup norms remain bounded. Hence, the viral state (capsid configuration + Markov chain + particle number) grows only to levels allowed by resource availability. Detailed proofs can be found in [37], extended to quantum or second-quantized systems in [38]. \square

Remark 3.32 (Cohomological Classification of Non-Equilibrium Processes). These cohomological considerations provide a powerful lens for classifying *types* of non-equilibrium processes by examining the loop (cycle) structure of the probability current \mathbf{J} . In more rigorous mathematical terms:

- The relevant loops in the configuration manifold \mathcal{M} (or in the Fock-space representation) can be viewed as elements of the first homology group $H_1(\mathcal{M})$.

- The probability current \mathbf{J} is a 1-form whose cohomology class $[\mathbf{J}] \in H_{\text{dR}}^1(\mathcal{M})$ determines whether these loops carry net flux.

When $[\mathbf{J}] \neq 0$, there exist closed cycles \mathcal{C} with $\oint_{\mathcal{C}} \mathbf{J}(\varphi) \cdot d\varphi \neq 0$, indicating persistent, non-equilibrium loops. Below, we add further mathematical detail on each classification aspect and discuss how these loops reflect physically irreversible processes such as viral replication and capsid reconfiguration [2, 5].

4 Homology, Cohomology, and Flux Classification

In this section, we delve deeper into the interplay between *infinite-dimensional geometry* (such as manifolds of PDE solutions or Fock-state representations) and virological applications (e.g. capsid conformations, Markov transitions, second-quantized replication). Our goal is to show how the classification of loops in homology $H_1(\mathcal{M})$ and their associated probability-current 1-forms in the de Rham cohomology $H_{\text{dR}}^1(\mathcal{M})$ sheds new light on key features of viral dynamics: *persistent replication cycles*, structural rearrangements, and *broken detailed balance* in open systems.

Background on Homology and Cohomology

In pure mathematics, *homology* and *cohomology* are topological invariants that capture global properties of spaces. We summarize the essentials:

Definition 4.1 (Homology Groups). Let \mathcal{M} be a (topological) manifold, which may be infinite-dimensional in our application (e.g. a manifold of PDE solutions, Markov states, or Fock configurations). *Singular homology* identifies equivalence classes of k -cycles under boundary operations:

$$H_k(\mathcal{M}) = \frac{\ker(\partial : C_k(\mathcal{M}) \rightarrow C_{k-1}(\mathcal{M}))}{\text{im}(\partial : C_{k+1}(\mathcal{M}) \rightarrow C_k(\mathcal{M}))}, \quad (4.1)$$

where $C_k(\mathcal{M})$ is the free abelian group generated by continuous maps from the k -simplex to \mathcal{M} , and ∂ is the boundary operator. A *loop* (or 1-cycle) in \mathcal{M} contributes an element to $H_1(\mathcal{M})$. For rigorous treatments, see [56, 58].

Definition 4.2 (de Rham Cohomology Groups). If \mathcal{M} is sufficiently smooth (e.g. a manifold of differentiable structures), *de Rham cohomology* is defined using differential forms. The k -th cohomology group is

$$H_{\text{dR}}^k(\mathcal{M}) = \frac{\ker(d : \Omega^k(\mathcal{M}) \rightarrow \Omega^{k+1}(\mathcal{M}))}{\text{im}(d : \Omega^{k-1}(\mathcal{M}) \rightarrow \Omega^k(\mathcal{M}))}, \quad (4.2)$$

where $\Omega^k(\mathcal{M})$ denotes the space of k -forms and d is the exterior derivative. In physical applications, a 1-form in $H_{\text{dR}}^1(\mathcal{M})$ often represents a *probability current* or *flux* that cannot globally be written as a gradient of a potential [56].

Key Idea (Flux Loops): A loop $\mathcal{C} \subset \mathcal{M}$ that yields a nonzero integral of a 1-form $\omega \in H_{\text{dR}}^1(\mathcal{M})$ signals *non-gradient* or *cyclic* behavior. In stochastic or virological settings, such cycles typically reflect persistent, energy-driven processes (i.e. broken detailed balance).

4.1 Homology Loops and Their Virological Significance

Definition 4.3 (Homology Loops in \mathcal{M}). Let \mathcal{M} be the infinite-dimensional manifold describing PDE solutions, Markov chains, or second-quantized Fock states (Section 2.1, [8,21]). A *loop* $\mathcal{C} \subset \mathcal{M}$ with $\mathcal{C}(0) = \mathcal{C}(1)$ determines a 1-cycle in the singular chain complex of \mathcal{M} . Its *homology class* $[\mathcal{C}]$ lies in $H_1(\mathcal{M})$, capturing topological information about closed orbits in this configuration space [56,58].

Remark 4.4 (Virological Context). In viral lattice models, the manifold \mathcal{M} may represent:

1. *Continuum capsid configurations* governed by PDEs describing elastic or wave-like deformations of the capsid shell [2,8].
2. *Discrete Markov transitions* among conformational states of a protein subunit (folded/unfolded, bound/unbound, etc.).
3. *Second-quantized Fock states* encoding varying particle numbers (virions), each with an internal configuration [21].

A closed loop \mathcal{C} then represents a full cycle of state changes (e.g. from partially assembled to fully assembled, or from creation to annihilation of virions) that returns to an original configuration. Its homology class reflects the *global* topological nature of that cycle.

4.1.1 Loop Classifications and Hierarchies

Definition 4.5 (Hierarchy of Flux Classes). One may classify flux loops by their *hierarchy* in the first homology group $H_1(\mathcal{M})$:

1. *Primary Loops*: Generators of $H_1(\mathcal{M})$ that carry a net flux (i.e. cannot be decomposed into simpler homologically trivial loops).
2. *Composite Loops*: Formed by integer (or integral) combinations of primary loops; some may yield net flux, while others may be exact cancellations of fluxes.

In biophysical models, primary loops often represent the most *energetically dominant* or persistent cycles, while composite loops describe secondary or rarer pathways [28,29].

Remark 4.6 (Loop Classification in Viral Dynamics). In virological contexts, distinct loops $\mathcal{C}_1, \mathcal{C}_2 \subset \mathcal{M}$ may represent different cycles of capsid protein rearrangements, receptor binding/unbinding events, or replication–annihilation balances. Homologically distinct loops yield *independent* non-equilibrium cycles, each contributing to the total resource consumption and entropy production [2,5,8,21]. Possible physical manifestations include:

1. *Large-scale* reorganizations of a viral capsid (e.g. dome-to-sphere transitions driven by pH changes),
2. *Discrete* flips from pre-assembled to post-assembled subunits,
3. *Population fluxes* in second-quantized models where virion creation or annihilation occurs.

Such cycles typically rely on continuous energy input (e.g. ATP, GTP) and therefore cannot be captured by a single equilibrium distribution.

4.2 Cohomological Currents and Dynamical Phenotypes

Remark 4.7 (Cohomological Invariants and Dynamical Phenotypes). Beyond revealing broken detailed balance, the cohomology class $[\mathbf{J}] \in H_{\text{dR}}^1(\mathcal{M})$ of a *probability-current 1-form* \mathbf{J} serves as a *dynamical invariant* distinguishing *non-equilibrium phenotypes*. For viral models, such phenotypes might include:

1. *Steady cycling* between partially folded and fully assembled capsid states,
2. *Wave-like replication fronts* (in PDE formulations) transporting probability density across different lattice sites or compartments,
3. *Mixed particle-number sectors* in Fock-space formalisms, describing bursts of virion production followed by damping or immune-mediated clearance.

Tracking which cohomological classes (i.e. flux loops) persist under perturbations (*e.g.*, changed resource levels, immune pressure, or mutation rates) can reveal *robust strategies* of viral adaptation [5, 44].

4.3 Connecting Homology & Cohomology to Viral Open-System Dynamics

1. Defining the Viral Configuration Manifold.

- **Continuum + Markov + Fock Picture.** To capture *all* relevant viral processes, we merge:
 1. *Continuum PDEs* for elasticity or vibrational modes of the capsid shell,
 2. *Markov jump processes* for subunit state transitions,
 3. *Fock-space formalism* for population-level replication or clearance events (creation/annihilation operators).

The resulting infinite-dimensional space \mathcal{M} can be endowed with a measure or a probability-current framework. Non-equilibrium loops in $H_1(\mathcal{M})$ then represent irreversible cycles fueled by host resources [16, 59].

2. Flux Loops and Broken Detailed Balance.

- **Cohomological Signature of Open Systems.** Nonzero loop integrals of a current 1-form \mathbf{J} indicate that no scalar potential Φ exists such that $\mathbf{J} = d\Phi$. In simpler terms, one cannot account for these fluxes by a single equilibrium *free-energy landscape*, implying persistent driving [28]. In viral lattice models, this is directly tied to the energy input required for capsid reconfiguration and replication.
- **Informational and Energetic Runoff.** In extended manifolds \widehat{X} (virus + host cell environment), the host supplies the flux balancing these loops. From the virus's viewpoint, persistent fluxes are manifested as ongoing replication (*e.g.* encapsidation of nucleic acids) or structural rearrangements. From the host's perspective, net energy consumption is reflected in increased entropy production and resource depletion [8].

In summary:

1. **Homology Classes** in $H_1(\mathcal{M})$ classify the global topological structure of viral configuration loops (e.g. cycles of assembly/disassembly, gating events), underscoring *which* cyclic processes are fundamentally distinct.
2. **Cohomology Classes** in $H_{\text{dR}}^1(\mathcal{M})$ detect fluxes that cannot be captured by any equilibrium potential. Viral replication cycles often reside in these nontrivial cohomology classes, inherently requiring an external resource input.
3. **Link to Non-Equilibrium Phenotypes.** The interplay of homology and cohomology clarifies how viruses sustain persistent subunit rearrangements, population expansions, and adaptation in hostile or variable environments. This is critical for modeling viral evolution, immune evasion, and the design of antiviral interventions.

Overall, the homological and cohomological classification of flux loops in \mathcal{M} provides a rigorous mathematical lens for understanding *persistent* and *energy-driven* dynamics in viral systems. By explicitly capturing structural rearrangements, replication events, and Markovian gating, one gains a unified picture of how viruses operate far from equilibrium, leveraging host resources to navigate a high-dimensional landscape of possible states.

4.4 Theoretical Implications for Viral Fitness and Pathogenesis

In this section, we connect the homology/cohomology framework and non-equilibrium loops to key *biological* insights about viral replication and pathogenesis. The primary goal is to illustrate how persistent fluxes in the viral configuration space imply continuous *entropy export* to the host environment, helping to explain the energetic and functional demands of infection.

Definition 4.8 (Continuous Entropy Export). Consider an open stochastic system (e.g. a viral lattice with PDE + Markov + Fock dynamics) that remains out of equilibrium by cycling through configurations in \mathcal{M} . Let $p(\mathbf{x}, t)$ denote the probability density over \mathcal{M} at time t , and let $\mathbf{J}(\mathbf{x}, t)$ represent the associated probability-current (or flux) of states. In many formulations of non-equilibrium thermodynamics [28, 29], the *total entropy production rate* \dot{S}_{tot} can be decomposed into two parts:

$$\dot{S}_{\text{tot}} = \frac{d}{dt} S_{\text{sys}}(t) + \dot{S}_{\text{env}}(t), \quad (4.3)$$

where $S_{\text{sys}}(t)$ is the system’s internal entropy (e.g. the Gibbs–Shannon entropy of $p(\mathbf{x}, t)$), and $\dot{S}_{\text{env}}(t)$ is the rate of *entropy export* to the environment.

When a system reaches a *non-equilibrium steady state* with persistent flux loops ($\oint_{\mathcal{C}} \mathbf{J} \neq 0$), one often has $\frac{d}{dt} S_{\text{sys}}(t) \approx 0$ on average, but $\dot{S}_{\text{env}}(t) \neq 0$. In other words, the system’s *internal* distribution $p(\mathbf{x}, t)$ may appear steady, yet it continuously *exports* entropy to external reservoirs. This reservoir is effectively the host cell’s energy/metabolic pool. From the *virus* perspective, the loop flux $\oint_{\mathcal{C}} \mathbf{J} \neq 0$ implies ongoing transformations of capsid or genome states. Because the overall virus–host system is open, the viral subsystem does not settle to a static equilibrium; rather, the *host* continuously provides resources (energy, substrates). From the host perspective, this manifests as *cellular stress*, depletion of ATP pools, and immune activation [16, 40].

3.1. Non-Equilibrium Steady States in Viral Replication Cycles.

Many viruses exhibit replicative phases in which partial assembly/disassembly states persist, often guided by cellular chaperones or specific compartments [2]. From a topological viewpoint, persistent flux loops in \mathcal{M} characterize the fact that even if the *macro-observed* phenotype appears

unchanged (i.e. a “steady state” infection), the *micro-level* probability flux of viral configurations remains nonzero. Equivalently, the system does not approach global equilibrium but rather a *non-equilibrium steady state* supported by a continuous influx of host energy [59].

Because viruses depend on the host for replication factors (e.g., ATP, nuclear import signals), each cycle of assembly or partial disassembly involves the *expenditure* of resources. Persistent loops with nonzero integral ($\oint_{\mathcal{C}} \mathbf{J} \neq 0$) quantify that net resource turnover. In the language of Markov processes, the system never “detailed balances”; in PDE–Fock terms, wave-like or creation/annihilation events keep transferring probability among states. This situation mirrors other actively driven processes (e.g. muscle contractions, bacterial metabolism), where a steady outward flux of entropy is required to sustain ordered structures or cyclical behavior [28].

3.2. Entropy Export & Cellular Stress.

Although global flux conservation implies no net flow *in the combined virus–host supersystem*, local analysis reveals continuous *entropy export* from the viral subsystem to the host. Mathematically, when $dS_{\text{sys}}/dt \approx 0$ (because the virus is in a steady-cycle regime) but $dS_{\text{tot}}/dt > 0$, the remainder dS_{env}/dt is borne by the host cell environment [28].

- **Proteostasis Overload.** Empirically, viruses can overload cellular quality-control machinery: proteasomes, chaperones (Hsp70, Hsp90), ER stress pathways, etc. The topological loops in \mathcal{M} reflect repeated subunit folding/unfolding or binding/unbinding cycles, each requiring free energy and generating misfolded proteins or aggregated byproducts [40].
- **Immune Activation.** Continuous flux of viral proteins or RNAs into distinct cellular compartments (e.g. nucleus, ER, Golgi) can trigger stress or immune sensors (PKR, RIG-I, TLRs). These pathways detect abnormal protein or RNA flux, increasing cytokine production and cell-autonomous defenses [8].

3.3. Implications for Antiviral Strategies.

Identifying the loops in \mathcal{M} that sustain a virus’s replication cycle provides clear therapeutic targets. Disrupting or *capping* these fluxes effectively prevents the virus from completing essential conformational or population-level transitions.

- **Resource Influx Interference.** Since flux loops depend on external free-energy supply, small-molecule drugs or metabolic interventions that reduce ATP or chaperone availability can stall viral replication [8]. Analogous approaches are seen in antimicrobial or anticancer therapies, where *resource limitation* cripples actively dividing or assembling cells.
- **Locking Key Conformational States.** If a viral protein subunit has two (or more) conformations essential for capsid assembly, an inhibitor that *locks* the protein in a low-affinity state can block the flux around the loop \mathcal{C} . Mathematically, such inhibition can be seen as raising the *barrier* or removing the link in the topological path [21, 40]. In so doing, the virus can no longer complete the cycle, halting virion production.
- **Synergistic Blockade of Multiple Loops.** Composite loops (Definition 4.5) may rely on multiple sub-cycles. Targeting only one sub-cycle may allow the virus to bypass the blockade by rerouting along another. Hence, *combination therapies* that simultaneously block different loop generators in $H_1(\mathcal{M})$ have better chances at completely halting replication [41].

Summary of Section 4.4: Persistent *non-equilibrium* loops in the viral configuration manifold \mathcal{M} lead to a continuous, steady-state entropy export to the host environment. This reflects the

fundamental resource consumption and continuous activity required for effective viral replication and pathogenesis. From a therapeutic standpoint, identifying and disrupting these loops offers a powerful avenue to limit infection, aligning with broader principles of targeting active (energy-reliant) processes in biological systems.

Conclusion and Future Directions

By unifying partial differential equation (PDE) drift, discrete Markov transitions, and second-quantized creation/annihilation operators, *viral lattice theory* adopts an m -sectorial framework [37] that offers a comprehensive mathematical representation of capsid dynamics, resource-driven replication, and open-system interactions. Nonzero loop integrals in the associated 1-form (probability flux) correspond to cohomologically nontrivial flows in configuration space, indicating *broken detailed balance* (i.e. no global free-energy potential). This analytical detection of persistent circulation emphasizes the fundamentally non-equilibrium character of viral processes.

Novel Theoretical Contributions.

- *Operator-Theoretic Rigor*: By employing m -sectorial operators on infinite-dimensional spaces (PDE + Markov + Fock), we ensure well-posedness despite unbounded population growth or abrupt conformational jumps. This framework incorporates continuum elasticity, subunit switching, and replication/clearance within a single operator-algebraic setting.
- *Homology and Cohomology of Flux Loops*: Introducing homology loops in $H_1(\mathcal{M})$ and cohomological fluxes in $H_{\text{DR}}^1(\mathcal{M})$ reveals new perspectives on viral *replication cycles* and *structural rearrangements*. Nonzero loop integrals highlight the net circulation driven by host resources, quantifying the continuous *entropy export* sustaining viral activity.
- *Entropy Export and Resource Dependence*: At non-equilibrium steady states, viruses effectively channel host metabolic and energetic resources. Our model clarifies how partial assembly/disassembly cycles and repeated subunit binding/unbinding persist through ongoing flux loops, translating into continuous entropy generation and cellular stress.

Bridging Theory and Experiment. Recent advances in *cryo-electron microscopy* and *single-molecule fluorescence* enable near real-time observation of individual capsid components [2]. These datasets can validate flux loops or cyclical conformational transitions predicted by the model, offering empirical evidence for (or against) the presence of nonzero homology loops in the viral configuration space. Furthermore, *proteomic* and *transcriptomic* methods can track the dynamic turnover of proteins and RNA in host cells, correlating with the net resource consumption and continuous entropy export central to our formalism. Experimental confirmations of PDE–Markov–Fock simulations would strengthen the operator-theoretic approach as a *predictive tool* in virology, and could also illuminate infection mechanisms in bacteriophages, prions, or intracellular bacteria.

Therapeutic and Biological Implications.

- *Targeting Persistent Flux Loops*: Because nonzero flux loops represent critical highways for viral assembly or replication, interventions that *lock* capsid proteins into single conformations (or limit host ATP availability) can effectively “cap” such loops [8], impeding key pathways in the viral life cycle.

- *Designing Combination Therapies:* Viruses often possess *multiple* major flux loops (primary homology generators), each providing an alternative replication or assembly route [41]. Combination treatments that inhibit multiple loops simultaneously stand a better chance of eradicating infection without leaving fallback pathways.
- *Generalization to Other Pathogens:* Though our illustrations focus on viruses, the same operator-theoretic viewpoint can describe replication in bacteriophages, prions, or intracellular bacteria reliant on host resources [16]. PDE–Markov–Fock models thus have broader utility for understanding varied infection strategies under finite host constraints.

Limitations and Future Directions. Although this framework integrates continuum elasticity, discrete subunit transitions, and population-scale replication, it remains predominantly *theoretical*. Future enhancements might involve:

1. *Refined PDE Models:* Incorporating higher-fidelity structural data (cryo-EM, X-ray crystallography) to capture subunit geometry and detailed intramolecular forces,
2. *Coupling Immune Interactions:* Incorporating immune dynamics (e.g. cytokine responses, antibody binding) into the PDE–Markov–Fock architecture, elucidating how immune pressures alter or disrupt viral flux loops,
3. *High-Throughput Assays:* Tracking subunit arrangements *in vivo* through real-time imaging, then comparing observed transition rates with model predictions to confirm or refute major flux loops,
4. *Multi-Scale Simulations:* Merging agent-based or PDE continuum methods with second-quantized operator techniques for tissue-level or patient-level modeling, capturing epidemiological scales while retaining molecular accuracy.

Overall, *viral lattice theory* demonstrates how infinite-dimensional, combinatorial–analytic topology and operator semigroup methods apply to realistic biological processes. Nonzero flux loops in PDE–Markov–Fock space encapsulate critical *irreversible* cycles driving viral replication and pathogenesis. By uniting this mathematical insight with advanced experimental techniques, we open pathways toward both *fundamental* discoveries in non-equilibrium dynamics and *practical* antiviral strategies that disrupt resource-driven loops sustaining viral fitness.

Concluding Remarks. Nonzero flux loops in PDE–Markov–Fock space highlight the *irreversible*, resource-dependent cycles that drive viral replication. Identifying, characterizing, and then disrupting these cycles opens new perspectives for antiviral therapy, parallel to how resource-limiting strategies have been adopted in anticancer and antibacterial treatments. Through ongoing collaboration between theorists and experimentalists, we anticipate that these operator-theoretic models will continue to mature, providing fresh insights into viral pathogenesis and unveiling novel targets for intervention.

References

- [1] L. St. Kleess. Viral Lattice Theory: A Biophysical Model for Virion Motion. *arXiv e-prints*, 2501.05459 [physics.bio-ph], 2025. <https://doi.org/10.48550/arXiv.2501.05459>.
- [2] D. M. Knipe and P. M. Howley (Eds.). *Fields Virology*. 7th ed., Wolters Kluwer, 2020.

- [3] R. L. Atmar, D. S. Opekun, B. M. Gilger, A. R. Estes, S. P. Crawford, L. Neal, D. J. Neill, and R. S. Graham. Determination of the 50% human infectious dose for norwalk virus. *Journal of Infectious Diseases*, 209(7):1016–1022, 2014.
- [4] R. Wölfel, V. Corman, W. Guggemos, M. Seilmaier, S. Zange, M. M. Müller, D. N. Niemeyer, T. Jones, P. V. Vollmar, C. Rothe, M. Hoelscher, and C. Drosten. Virological assessment of hospitalized patients with COVID-2019. *Nature*, 581(7809):465–469, 2020.
- [5] S. J. Flint, V. R. Racaniello, G. F. Rall, and A. M. Skalka. *Principles of Virology*, 4th edition. ASM Press, 2015.
- [6] A. J. Cann. *Principles of Molecular Virology*, 6th edition. Academic Press, 2015.
- [7] R. M. Zucker, J. J. Mateus, and J. D. Murray. Mathematical approaches to medical virology. In *Handbook of Mathematical Biology*, volume II, pages
- [8] S. C. Harvey and M. G. Orton (Eds.). *Viral Molecular Machines*. Springer, 2019.
- [9] S. C. Harvey. The hidden structure of viral capsids. *Annual Review of Virology*, 6(1):73–92, 2019.
- [10] G. Da Prato and J. Zabczyk. *Stochastic Equations in Infinite Dimensions*. Cambridge University Press, 2nd edition, 2014.
- [11] J. L. Van Etten. *Viruses of Microorganisms*. Caister Academic Press, 2019.
- [12] K. Grünewald, P. Desai, D. C. Winkler, B. S. Heymann, W. Baumeister, A. C. Steven, and H. G. Trus. Three-dimensional structure of herpes simplex virus from cryo-electron tomography. *Science*, 302(5649):1396–1398, 2003.
- [13] A. L. Fetter and J. D. Walecka. *Quantum Theory of Many-Particle Systems*. McGraw–Hill, 1971.
- [14] T. Kato. *Perturbation Theory for Linear Operators*. Springer, 1980.
- [15] C. Florence, M. H. Johnson, Y. Cheng, and B. He. Viral population dynamics and the role of defective interfering particles in persistent infections. *PLOS Pathogens*, 13(12):e1006789, 2017.
- [16] E. O. Freed. HIV-1 assembly, release and maturation. *Nature Reviews Microbiology*, 13(8):484–496, 2015.
- [17] C. Wang, D. Liu, Y. Zhang, S. Feng, and J. Hu. Single-particle tracking uncovers dynamic assembly processes of viral capsids. *Journal of Virology*, 96(12):e00567–22, 2022.
- [18] M. Lewenstein, A. Sanpera, and V. Ahufinger. *Ultracold Atoms in Optical Lattices: Simulating Quantum Many-Body Systems*. Oxford University Press, 2012.
- [19] M. Greiner, O. Mandel, T. Esslinger, T. W. Hänsch, and I. Bloch. Quantum phase transition from a superfluid to a Mott insulator in a gas of ultracold atoms. *Nature*, 415:39–44, 2002.
- [20] L. C. Evans. *Partial Differential Equations*. Graduate Studies in Mathematics, Vol. 19, American Mathematical Society, 2nd edition, 2010.

- [21] A. J. Cann. *Principles of Molecular Virology*, 6th edition. Academic Press, 2015.
- [22] J. B. Conway. *A Course in Functional Analysis*. Springer, New York, 1990.
- [23] M. Reed and B. Simon. *Methods of Modern Mathematical Physics, Vol. I–IV*. Academic Press, 1972–1979.
- [24] V. G. Chinchar, A. Hyatt, T. Miyazaki, and T. Williams. Family Iridoviridae: poor viral relations no longer. In *Iridoviruses*, Springer, 2009. DOI: 10.1007/978-3-540-68618-7_4.
- [25] F. A. Berezin, ed. *The Method of Second Quantization*. Moscow State University, Moscow, U.S.S.R., Vol. 24, pp. 1–228, 1966.
- [26] O. Bratteli and D. W. Robinson. *Operator Algebras and Quantum Statistical Mechanics 1 & 2*. Springer, 2nd edition, 1987.
- [27] O. Bratteli and D. W. Robinson. *Operator Algebras and Quantum Statistical Mechanics: Volume 1: C*- and W*-Algebras. Symmetry Groups. Decomposition of States*. Springer, 2012.
- [28] U. Seifert. Stochastic thermodynamics, fluctuation theorems, and molecular machines. *Reports on Progress in Physics*, 75(12):126001, 2012.
- [29] N. G. Van Kampen. *Stochastic Processes in Physics and Chemistry*. North-Holland (Elsevier), 3rd edition, 2007.
- [30] S. Weinberg. *The Quantum Theory of Fields: Volume 2, Modern Applications*. Cambridge University Press, 1996.
- [31] M. E. Peskin and D. V. Schroeder. *An Introduction to Quantum Field Theory*. Cambridge University Press, 1995.
- [32] M. Reed and B. Simon. *Methods of Modern Mathematical Physics II: Fourier Analysis, Self-Adjointness*. Academic Press, 1975.
- [33] Kittel, C. (2005). *Introduction to Solid State Physics* (8th ed.). Wiley.
- [34] Born, M., & Huang, K. (1998). *Dynamical Theory of Crystal Lattices*. Oxford University Press.
- [35] Landau, L. D., & Lifshitz, E. M. (1986). *Theory of Elasticity* (3rd ed.). Butterworth-Heinemann. ISBN: 978-0750626330.
- [36] J.-L. Lions and E. Magenes. *Non-Homogeneous Boundary Value Problems and Applications. Vol. I*. Springer-Verlag, New York, 1972.
- [37] A. Pazy. *Semigroups of Linear Operators and Applications to Partial Differential Equations*. Springer-Verlag, New York, 1983.
- [38] R. Alicki and K. Lendi. *Quantum Dynamical Semigroups and Applications*. Lecture Notes in Physics, Vol. 717. Springer, Berlin Heidelberg, 2007.
- [39] D. M. Knipe and P. M. Howley (Eds.). *Fields Virology*. 6th ed., Wolters Kluwer Health, 2013.
- [40] S. J. Flint, V. R. Racaniello, G. F. Rall, A. M. Skalka, and L. W. Enquist. *Principles of Virology*. ASM Press, 5th edition, 2020.

- [41] M. A. Nowak and R. M. May. *Virus Dynamics: Mathematical Principles of Immunology and Virology*. Oxford University Press, 2000.
- [42] D. Henry. *Geometric Theory of Semilinear Parabolic Equations*. Lecture Notes in Math. 840, Springer, 1981.
- [43] I. H. Segel. *Enzymatic Kinetics: Behavior and Analysis of Rapid Equilibrium and Steady-State Enzyme Systems*. Wiley, 1993.
- [44] J. D. Murray. *Mathematical Biology: I. An Introduction*, 3rd ed. Springer, 2002.
- [45] B. Hérs, D. J. Smith, and R. P. Simmonds. Feedback mechanisms in viral replication: limiting resources and immune pressure. *Trends in Microbiology*, 26(8):635–647, 2018.
- [46] S. C. Harvey. The hidden structure of viral capsids. *Annual Review of Virology*, 6(1):73–92, 2019.
- [47] G. Da Prato and J. Zabczyk. *Stochastic Equations in Infinite Dimensions*. Cambridge University Press, 1st edition, 1992.
- [48] T. M. Liggett. *Interacting Particle Systems*. Springer, 1985.
- [49] W. Thirring. *A Course in Mathematical Physics: Quantum Mechanics of Large Systems*. Springer, 1983.
- [50] B. K. Driver. *Analysis Tools with Applications*. Springer, 2003.
- [51] S. Albeverio, F. Gesztesy, R. Hoegh-Krohn, and H. Holden. *Solvable Models in Quantum Mechanics*. AMS Chelsea Publishing, 2012 (reprint of the 1988 edition).
- [52] C. W. Gardiner. *Stochastic Methods: A Handbook for the Natural and Social Sciences*. Springer, 4th edition, 2009.
- [53] J. Kurchan. Fluctuation theorem for stochastic dynamics. *Journal of Physics A: Mathematical and General*, 31(16):3719, 1998.
- [54] C. W. Gardiner. *Handbook of Stochastic Methods*. Springer, 1985.
- [55] F. P. Kelly. *Reversibility and Stochastic Networks*. Wiley, 1979.
- [56] R. Bott and L. Tu. *Differential Forms in Algebraic Topology*. Springer, 1982.
- [57] P. W. Michor. *Topics in Differential Geometry*. Graduate Studies in Mathematics, Vol. 93, American Mathematical Society, 2008.
- [58] E. H. Spanier. *Algebraic Topology*. Corr. 3rd ed., Springer, 1994.
- [59] D. Baltimore. Expression of animal virus genomes. *Bacteriological Reviews*, 35(3):235–241, 1971.